ELECTRONIC SUPPORTING INOFRMATION
Construction of Spirooxindole Analogues Engrafted with Indole and Pyrazole Scaffolds as Acetylcholinesterase Inhibitors

Mohammad Shahidul Islam,[¶,a,b] Abdullah Mohammed Al-Majid,[a] Mohammad Azam,[a] Ved Prakash Verma,[b,*] Assem Barakat,[¶,a,c,*] Matti Haukka,[d] Abdullah A. Elgazar,[e] Amira Mira,[f] Farid A. Badria[f]

[a] Department of Chemistry, College of Science, King Saud University, P.O. Box 2455, Riyadh 11451, Saudi Arabia.
[b] Department of Chemistry, Banasthali Vidyapith, Banasthali-304022, Rajasthan, India.
[c] Department of Chemistry, Faculty of Science, Alexandria University, P.O. Box 426, Ibrahimia, Alexandria 21321, Egypt.
[d] Department of Chemistry, University of Jyväskylä, P.O. Box 35, FI-40014 Jyväskylä, Finland.
[e] Department of Pharmacognosy, Faculty of Pharmacy, Kafrelsheikh University, Kafrelsheikh 33516, Egypt.
[f] Department of Pharmacognosy, Faculty of Pharmacy, Mansoura University, Mansoura 35516 Egypt.
* Corresponding authors: Ved Prakash Verma (vedprakash079@gmail.com); Assem Barakat (ambarakat@ksu.edu.sa)

Table of Contents

Acetylcholine Esterase (AChE) Inhibitory Assay (AChEI)

AChE from *Electrophorus electricus* (electriceel), 500 U/mg, and 5,5-dithiobis[2-nitrobenzoic acid] (DTNB) were purchased from Sigma (St. Louis, MO, USA). Acetylthiocholine iodide (ACTI) was purchased from Tokyo Chemical Industry (Tokyo, Japan).

AChEI activity was measured using Ellman's method as previously described[1-3]. Briefly, in a 96-well plate, 25 µL of 15 mM ACTI, 125 µL of 3 mM DTNB in buffer B (50 mM Tris HCl, pH = 8, 0.1 M NaCl, 0.02 M $MgCl_2 \cdot 6H_2O$), 50 µL of buffer A (50 mM Tris-HCl, PH 8, 0.1% BSA) and 25 µL of tested compounds at five different final concentrations 6.25, 12.5, 25, 50 and 100 µM or galanthamine as a positive control (dissolved in 25% DMSO) were mixed, and the absorbance was measured using a microplate reader (Biotek, Winooski, VT, USA) at 405 nm every 16 s ten times. Then, 25 µL of AChE (0.25 U/mL in buffer A) was added and the absorbance was measured ten times every 16 s. A solution of 25% DMSO was used as a negative control. Absorbance was plotted against time and enzyme activity was calculated from the slope of the line so obtained and expressed as a percentage compared to an assay using a buffer without any inhibitor. The absorbance before addition of the enzyme was subtracted from the absorbance after adding the enzyme to avoid any increase in absorbance due to the color of the compounds or spontaneous hydrolysis of the substrate. Compounds with IC_{50} >100 µM were considered inactive [1-3].

Molecular docking study protocol

To investigate the binding mode of the synthesized compounds the chemical structure of the compounds **8i**, **8h** and **8i** were drawn using Chemoffice software[4] and saved as SDF file, which was exported MOE software[5] for 3D structure generation and energy minimization using MMFF94x forcefield and the file was saved as mol2 file.

The 3D structure of human acetylcholinesterase (hACHE) was downloaded from Protein data bank PDB: 4EY7 where water molecules were removed, bond orders was assigned, hydrogens were added, hydrogen bonds were optimized, charges were corrected, the protein complex was minimized and saved as PDB. The optimized PDB was loaded in protein preparation module integrated in IGEMDOCK software[6], where the active site was defined as sphere with radius 8 A around the co-crystallized ligand.

The software was validated by redocking the co-crystallized ligand and calculating RMSD between the produced and experimental pose. The compounds were loaded to the IGEMDOCK preparation module and were docked to the active site. The docking parameters were set as Population size 300, Generations 80, and number of solutions were 3. Post docking analysis was done to determine best poses and types of interaction between the compound and the binding site. Finally, Poses were visualized using Discovery studio ligand interaction visualizer[7].

NMR Spectra

Figure S1. ^{1}H-NMR and ^{13}C-NMR of acetylpyrazole-**3**

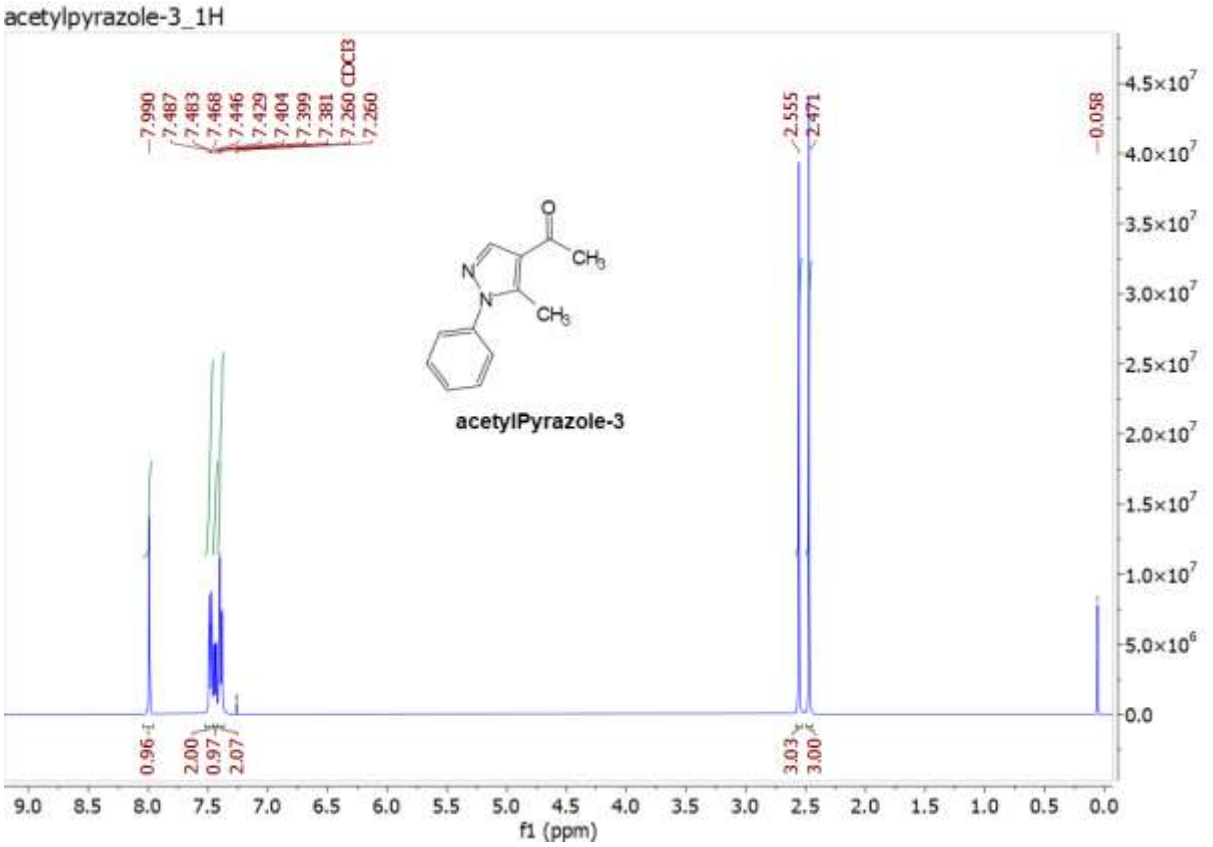

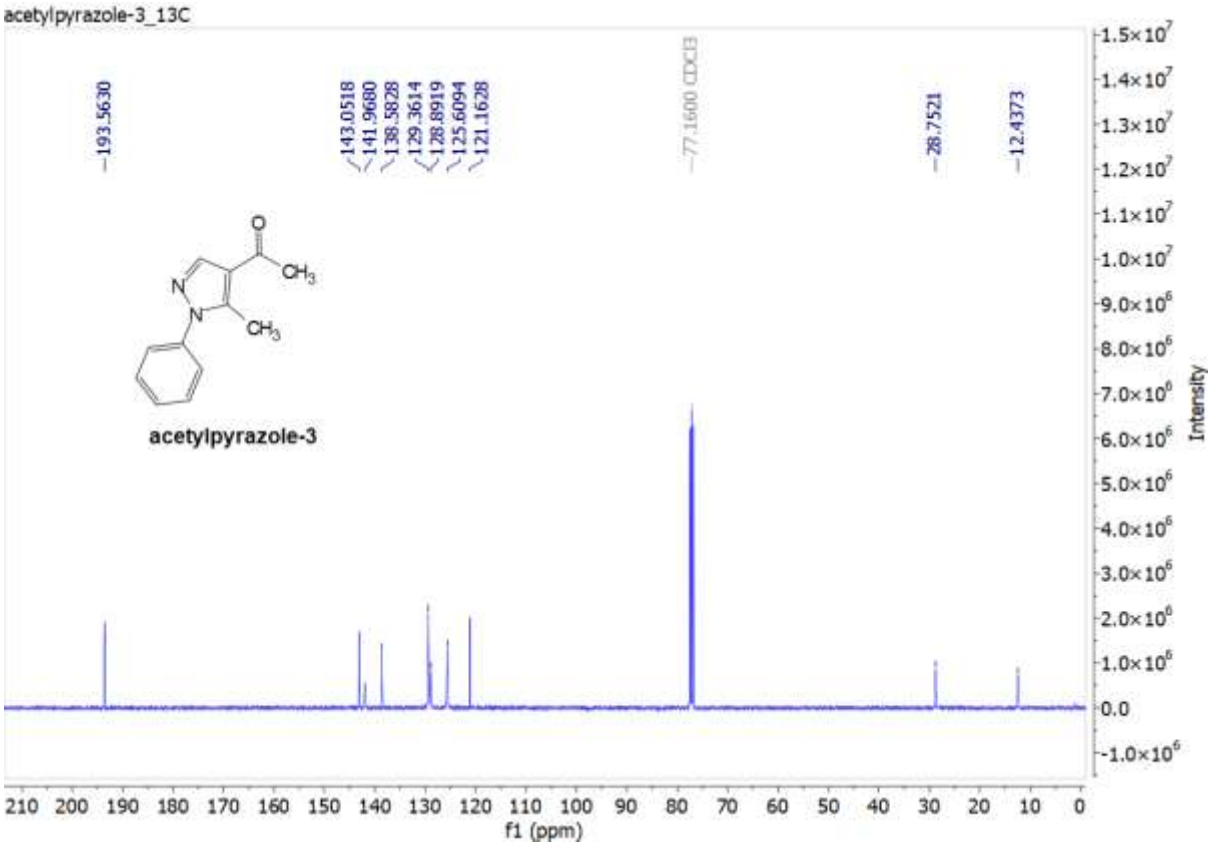

Figure S2. ^{1}H-NMR and ^{13}C-NMR for chalcone-**5a**

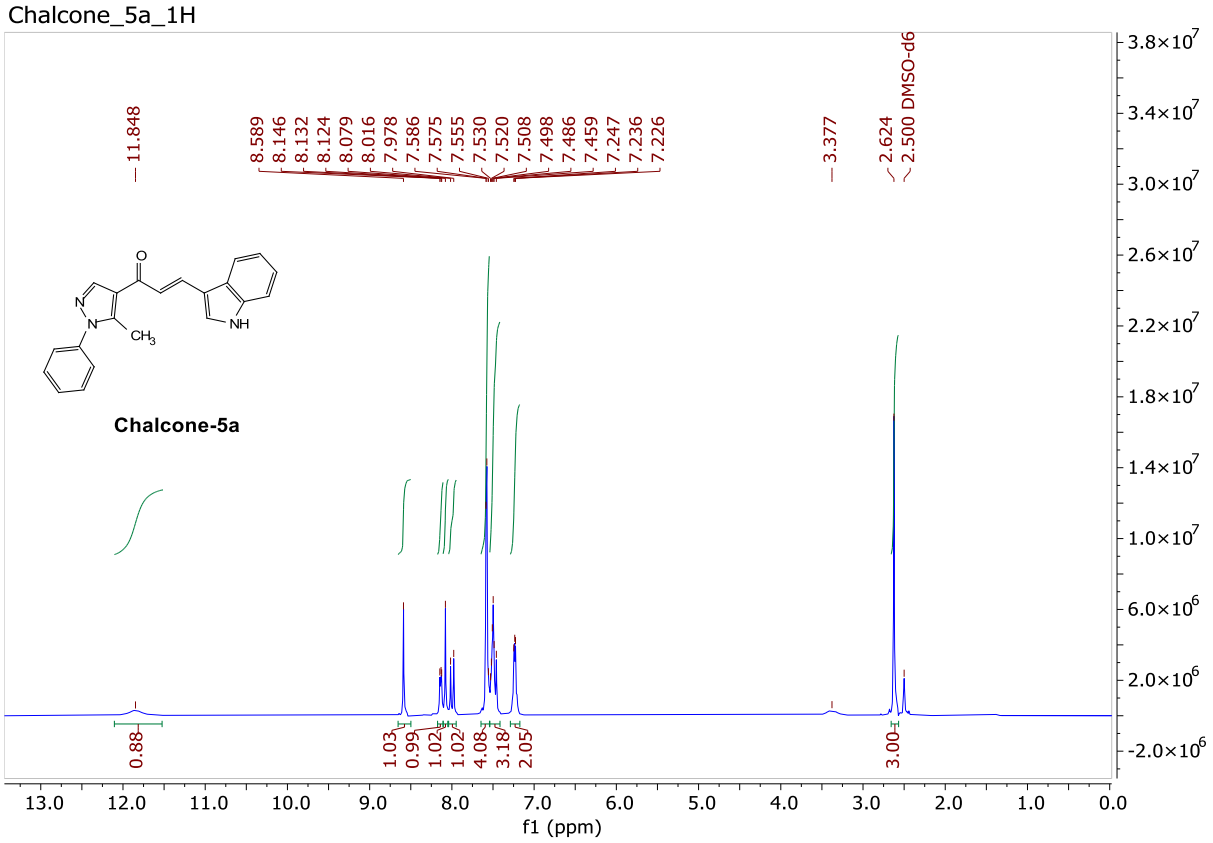

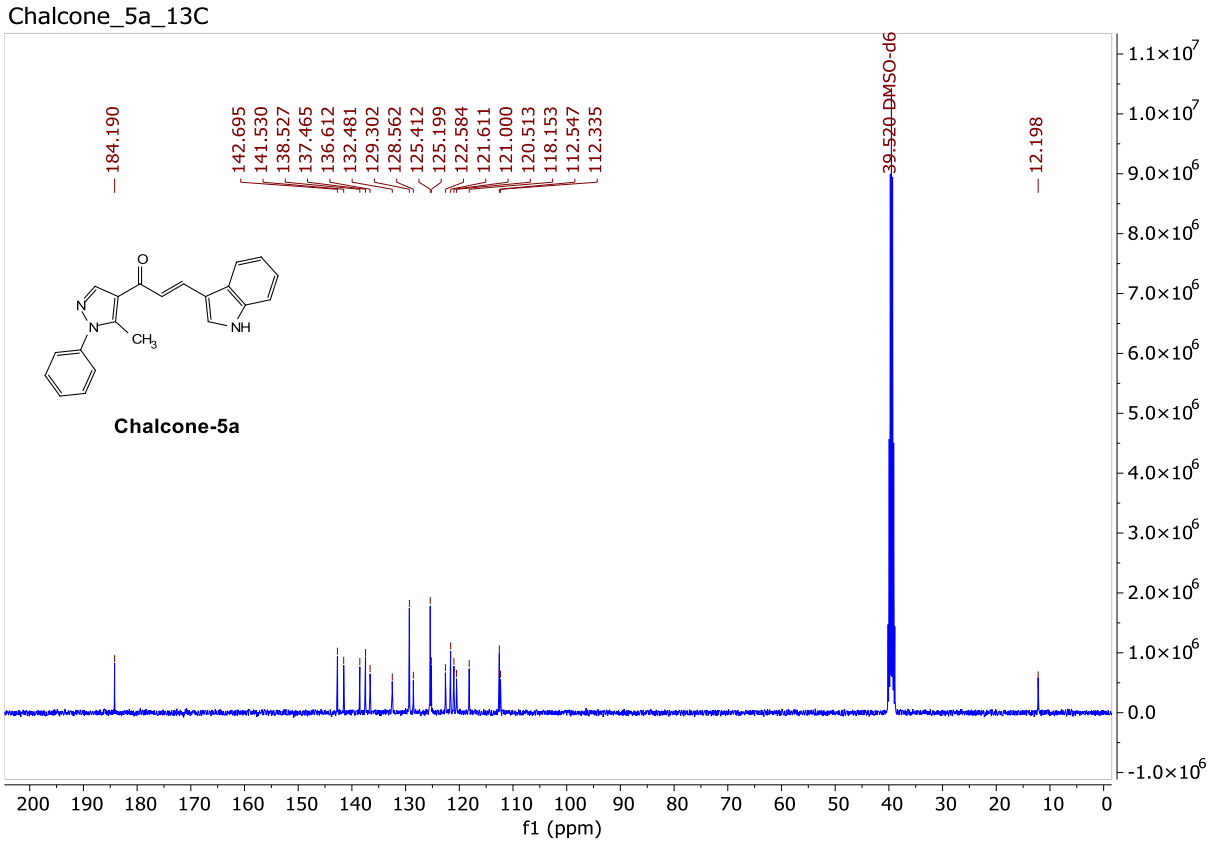

Figure S3. ^{1}H-NMR and ^{13}C-NMR for chalcone-**5b**

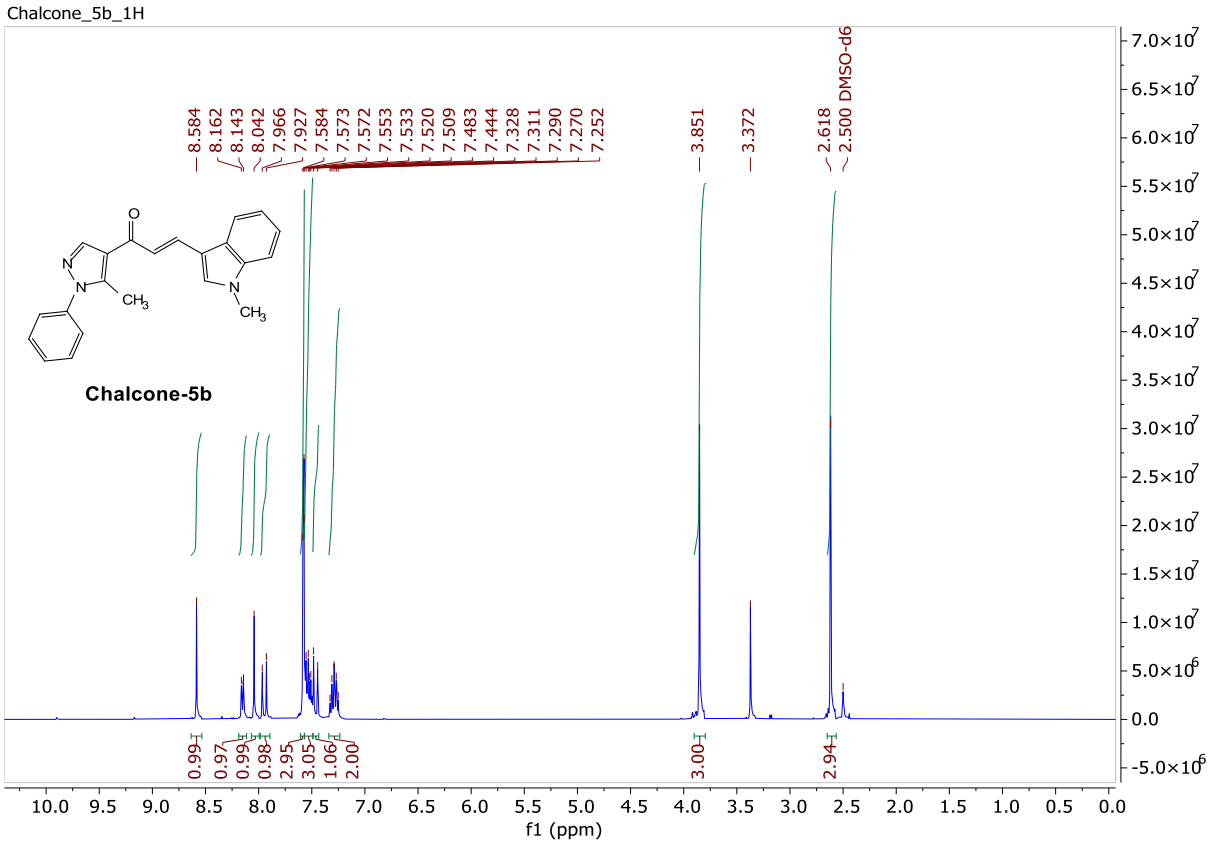

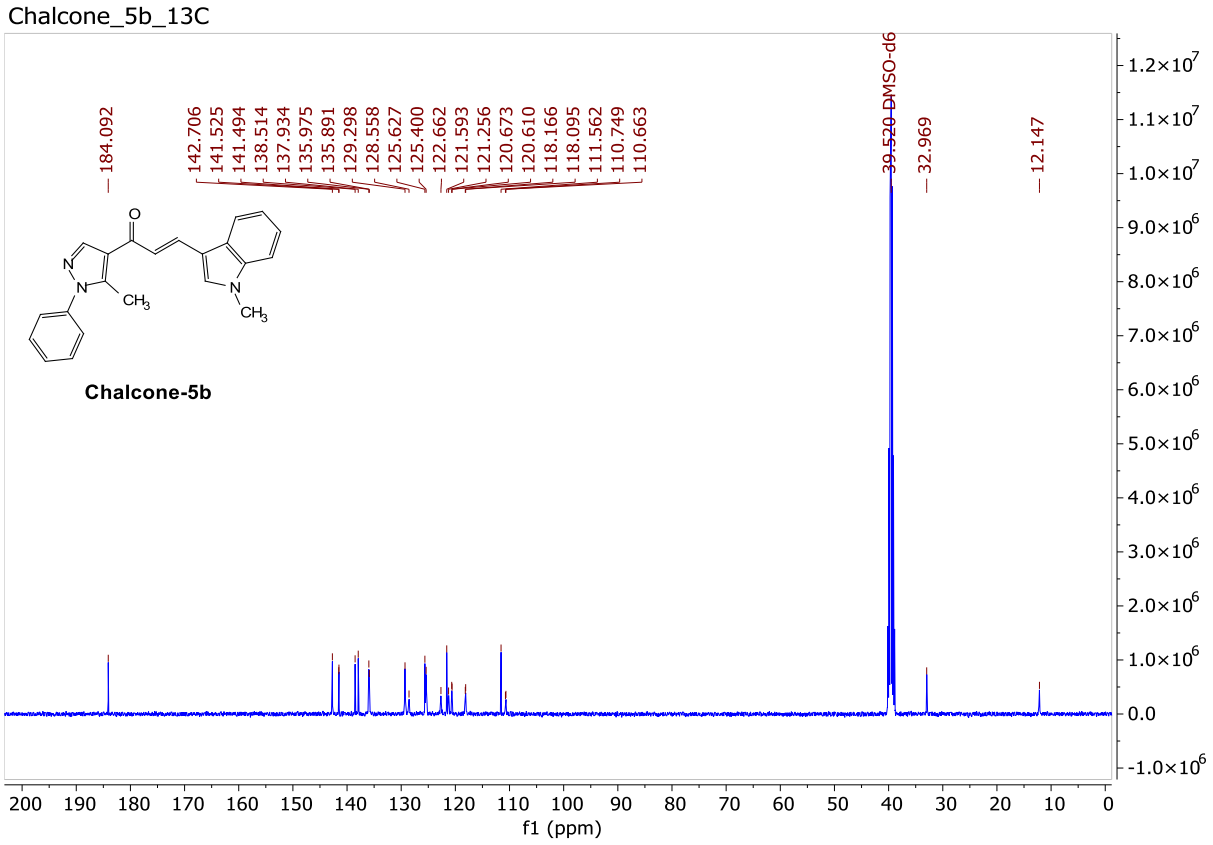

Figure S4. ^{1}H-NMR and ^{13}C-NMR for chalcone-**5c**

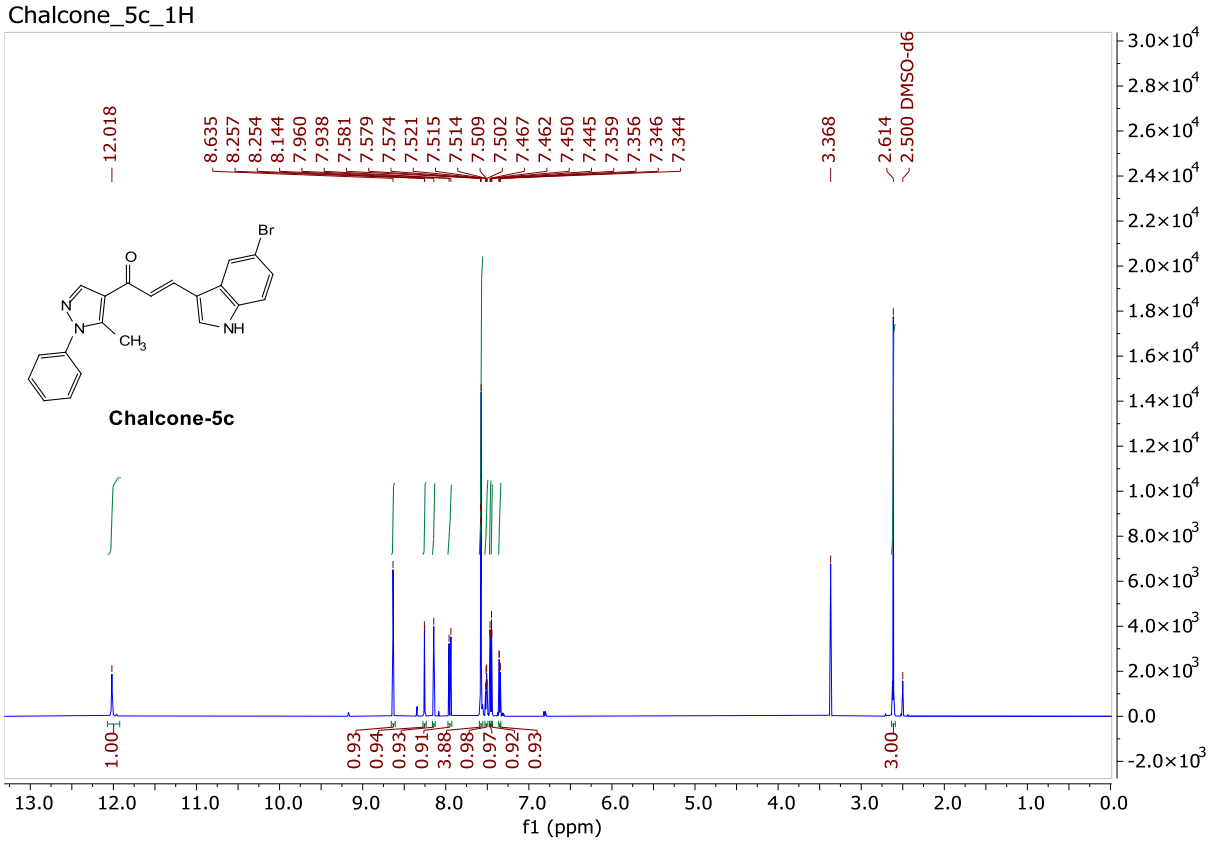

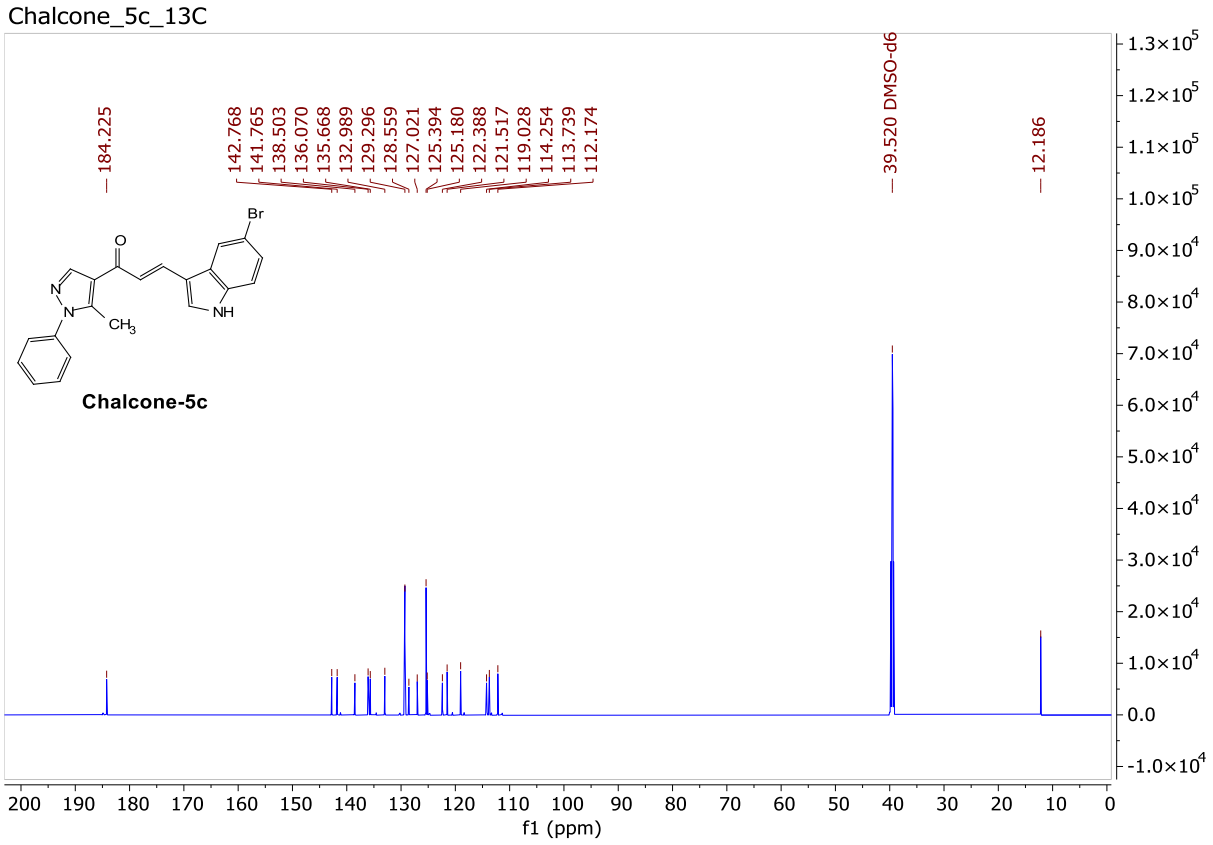

Figure S5. ^{1}H-NMR and ^{13}C-NMR for chalcone-**5d**

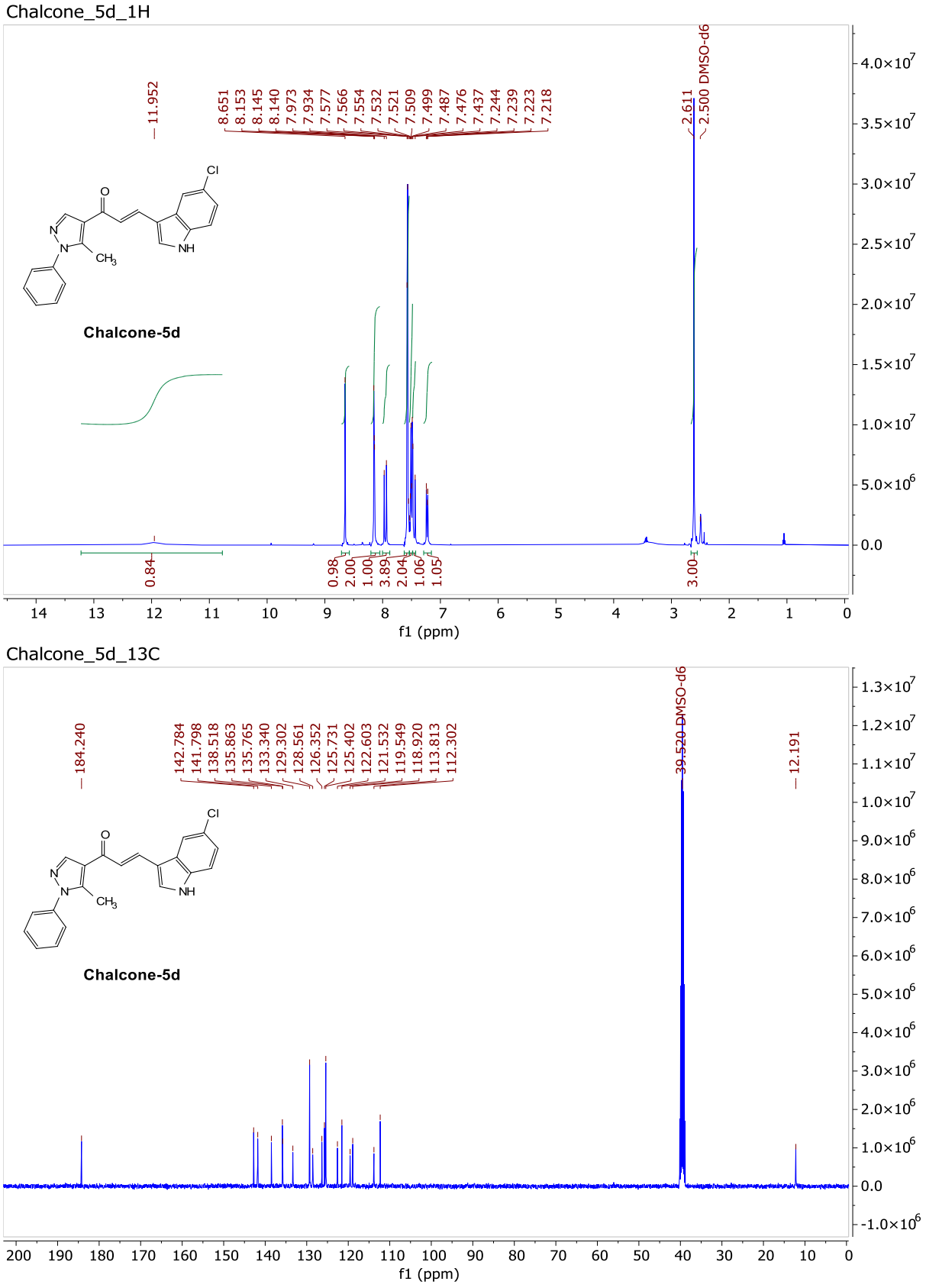

Figure S6. ^{1}H-NMR and ^{13}C-NMR for compound-**8a**

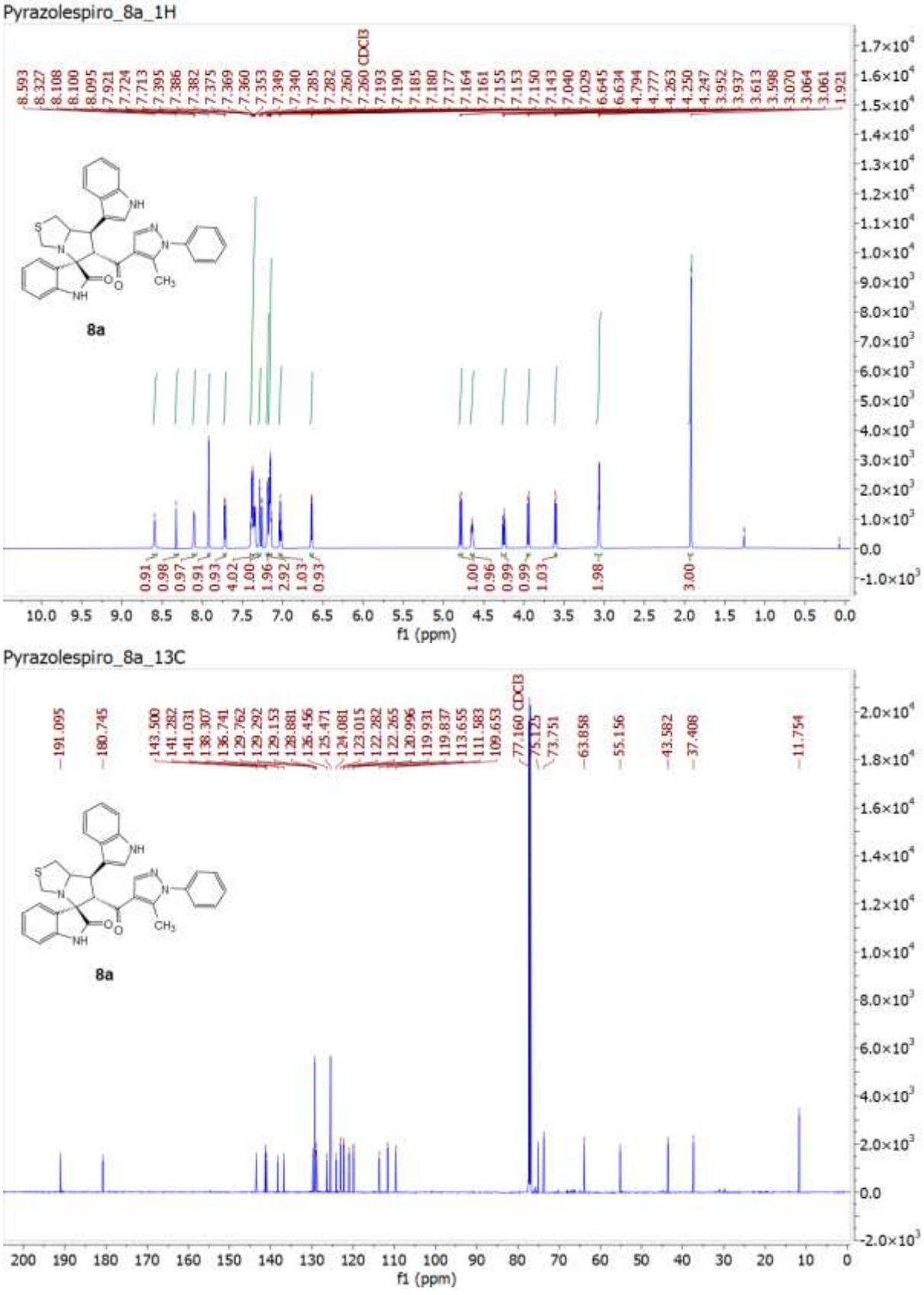

Figure S7. ^{1}H-NMR and ^{13}C-NMR for compound-**8b**

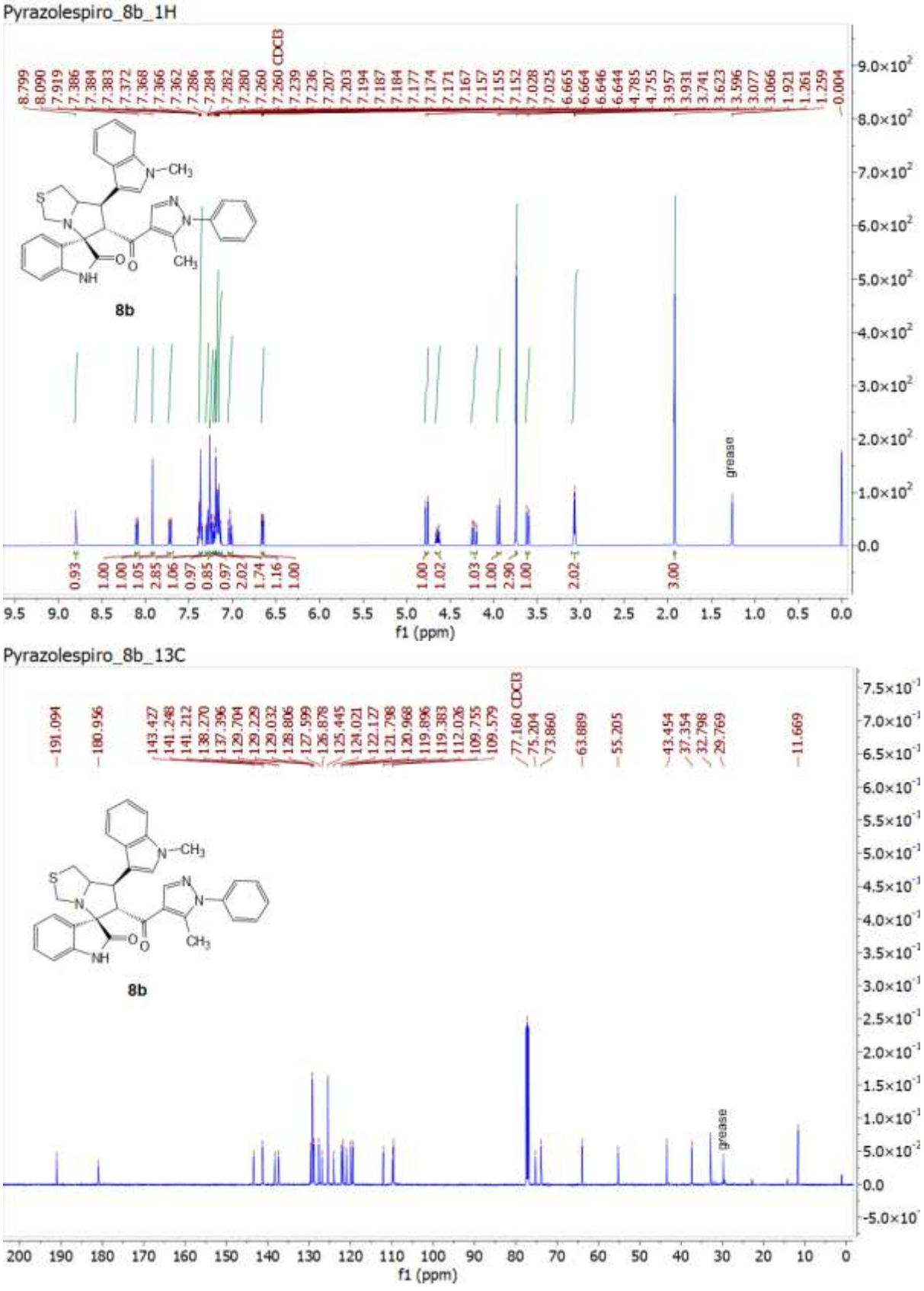

Figure S8. ^{1}H-NMR and ^{13}C-NMR for compound-**8c**

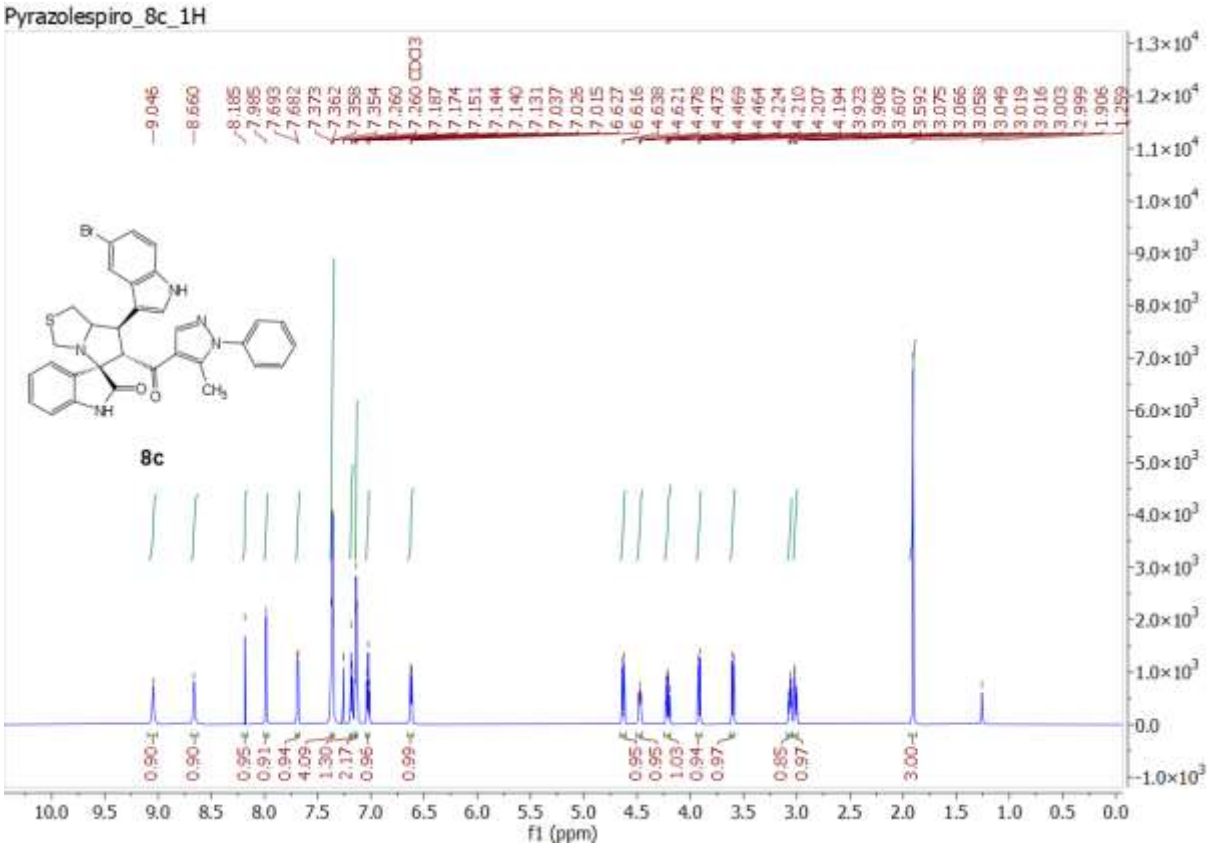

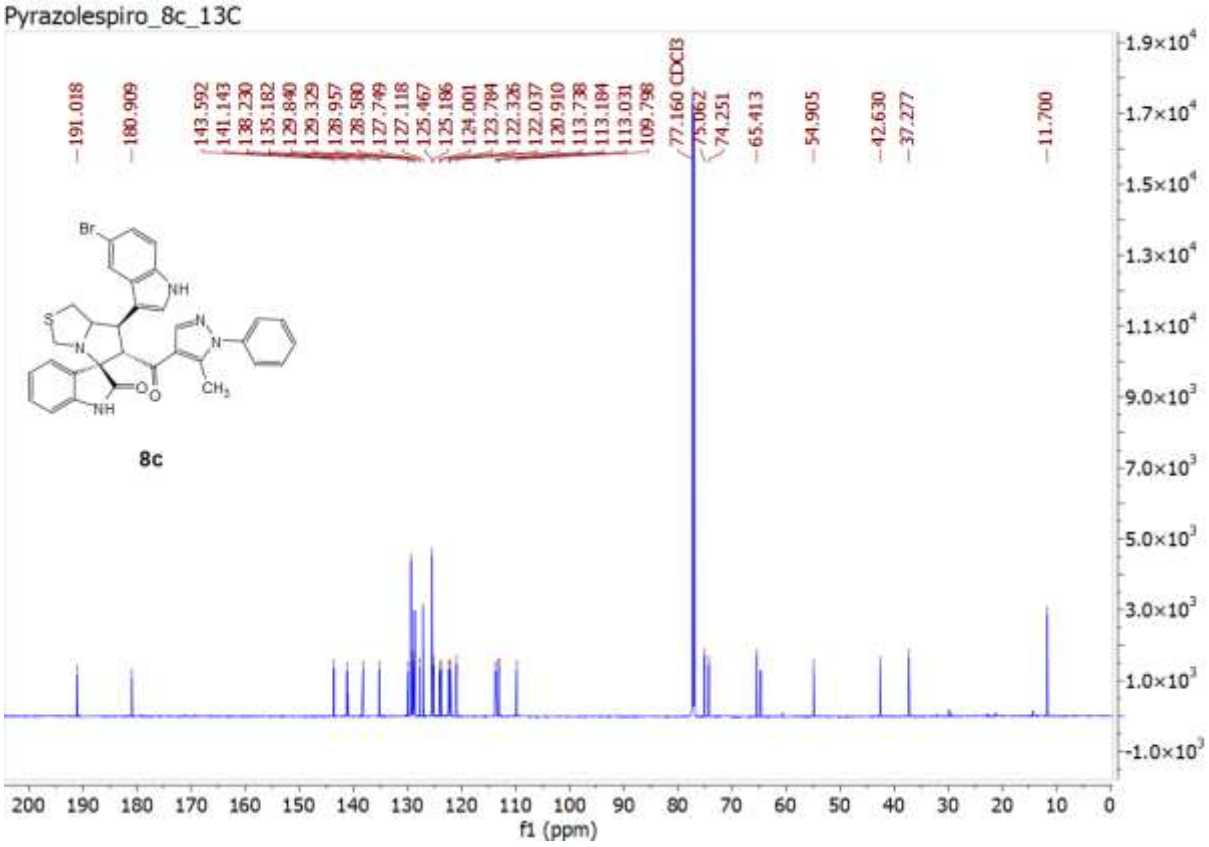

Figure S9. ^{1}H-NMR and ^{13}C-NMR for compound-**8d**

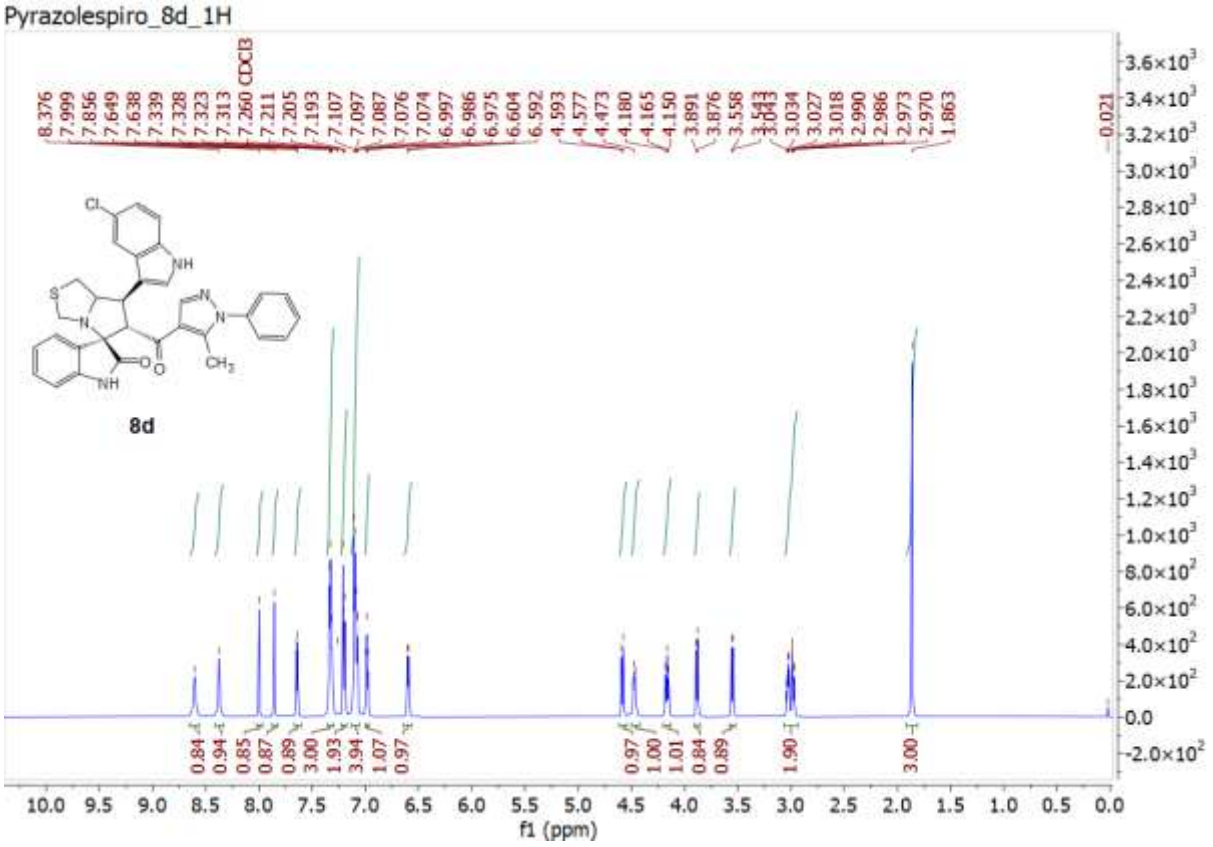

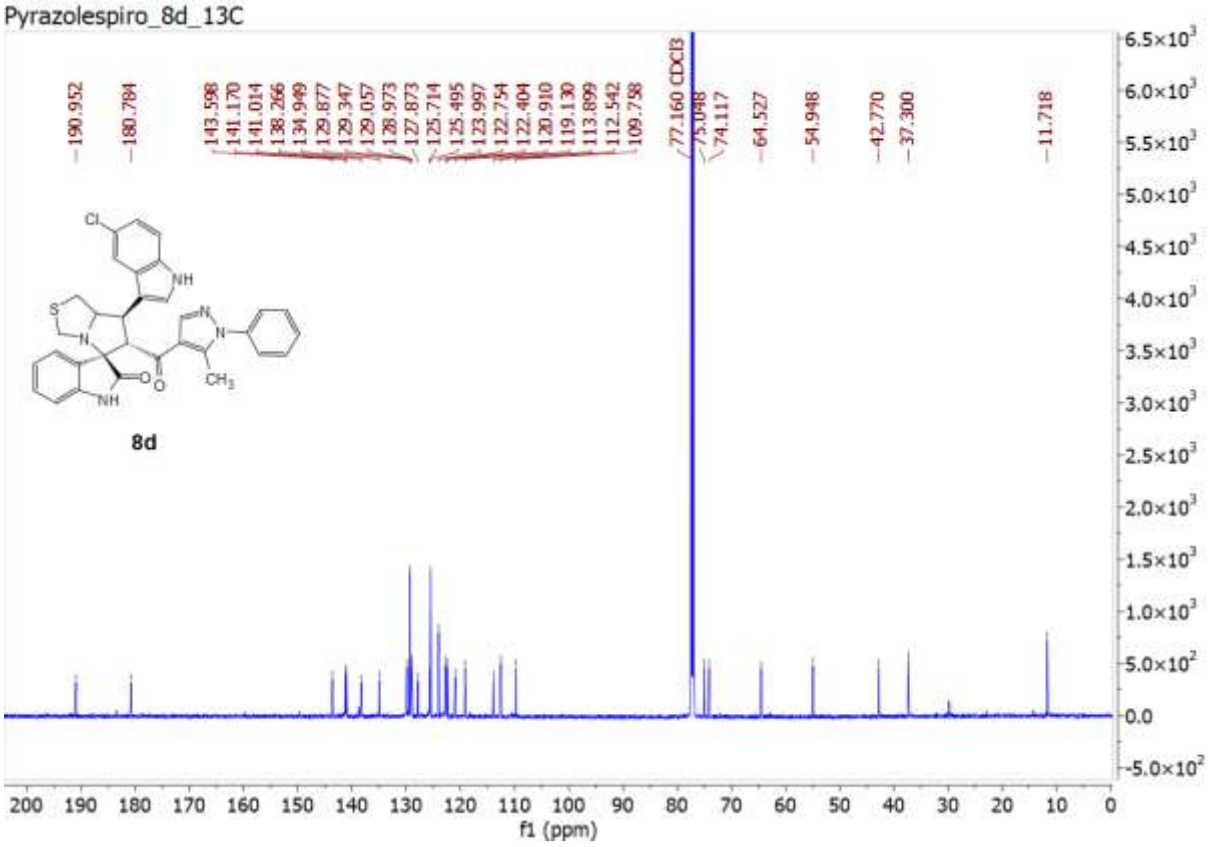

Figure S10. ^{1}H-NMR and ^{13}C-NMR for compound-**8e**

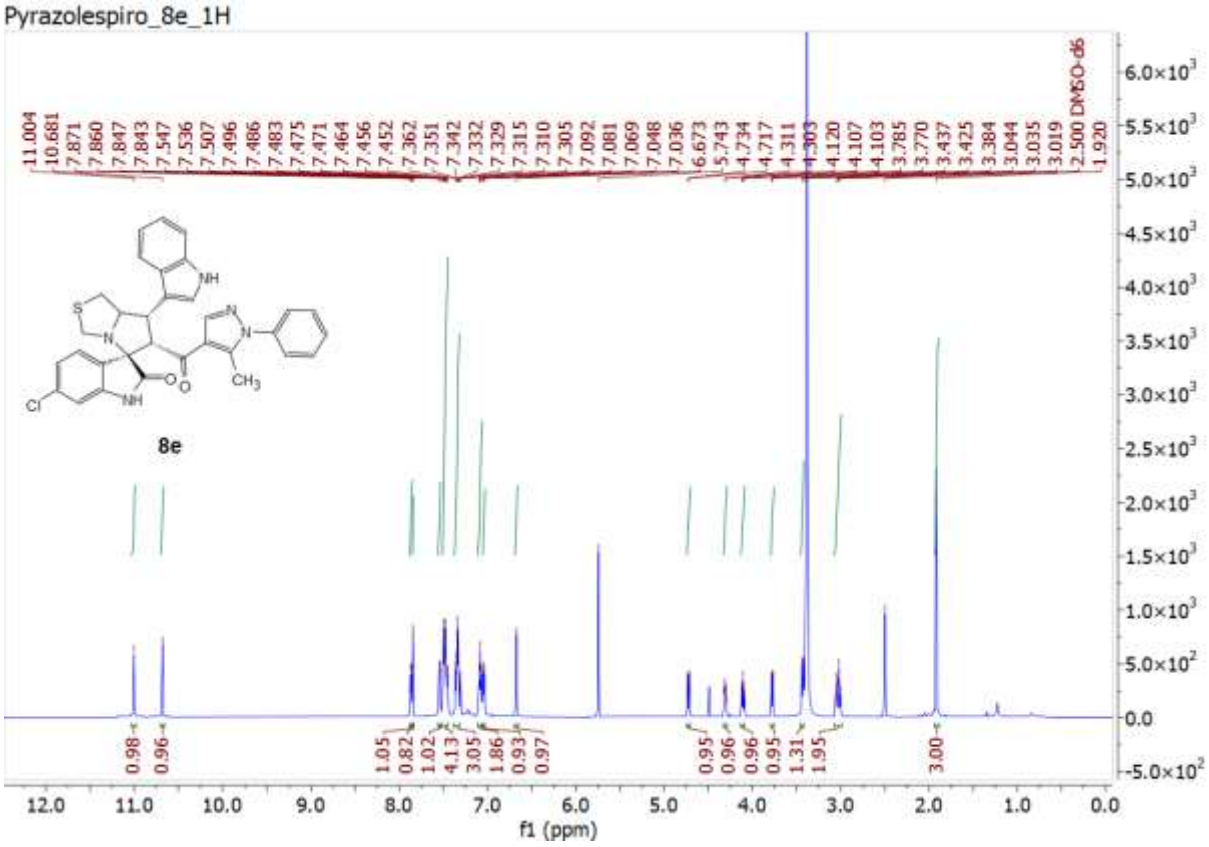

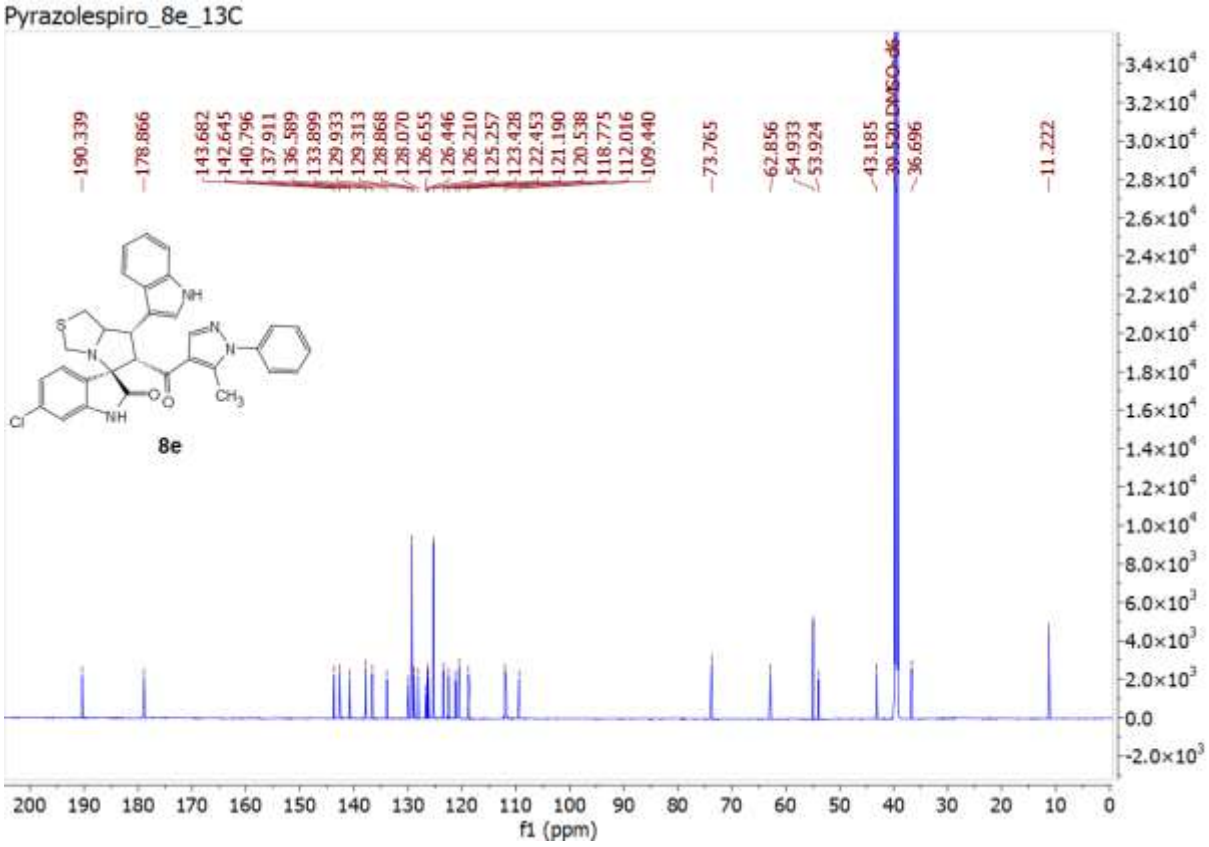

Figure S11. ^{1}H-NMR and ^{13}C-NMR for compound-**8f**

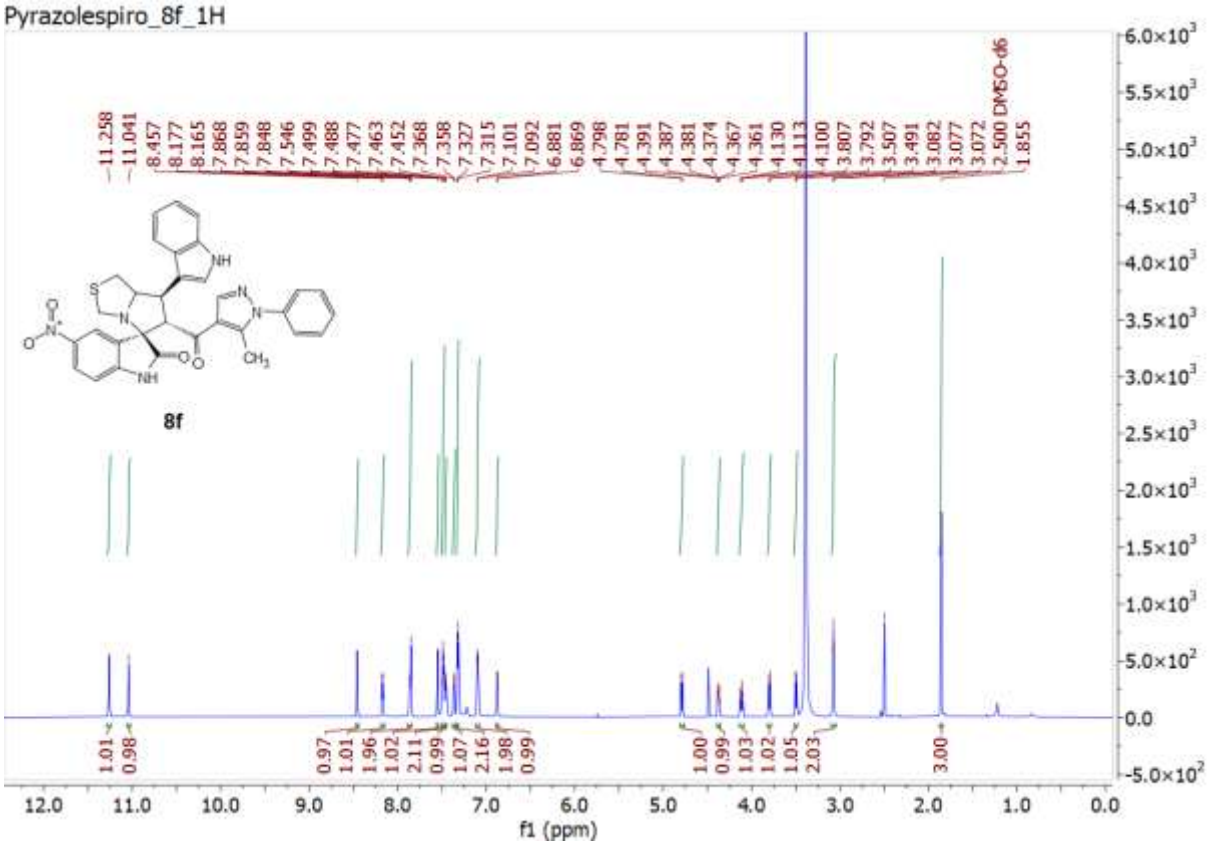

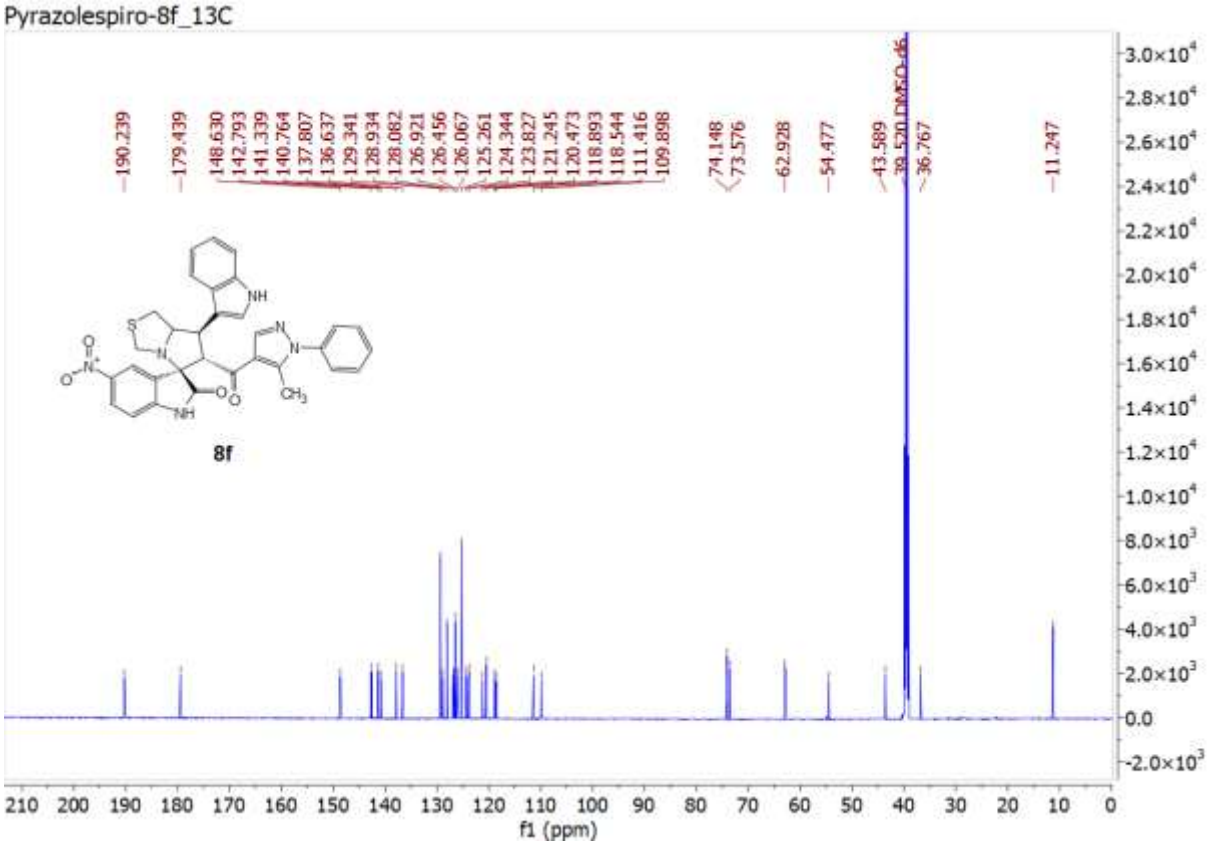

Figure S12. ^{1}H-NMR and ^{13}C-NMR for compound-**8g**

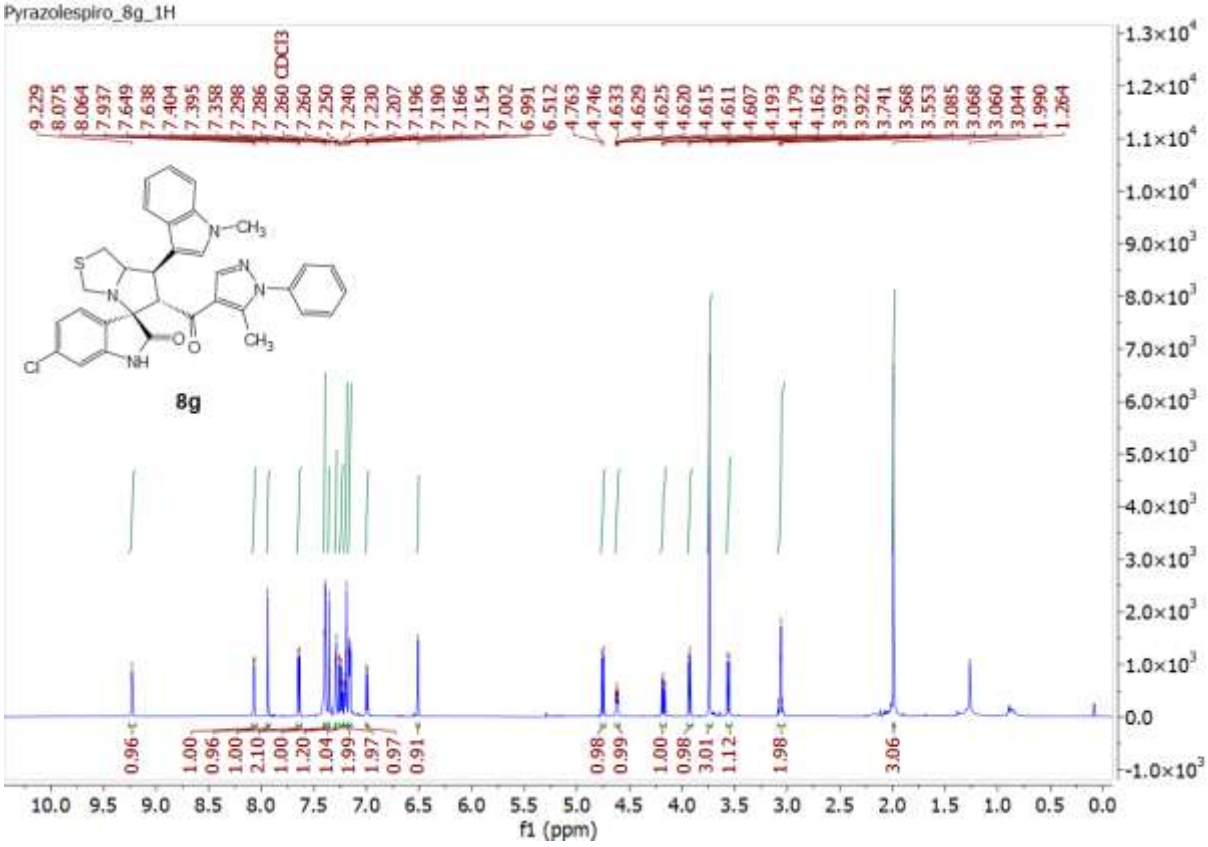

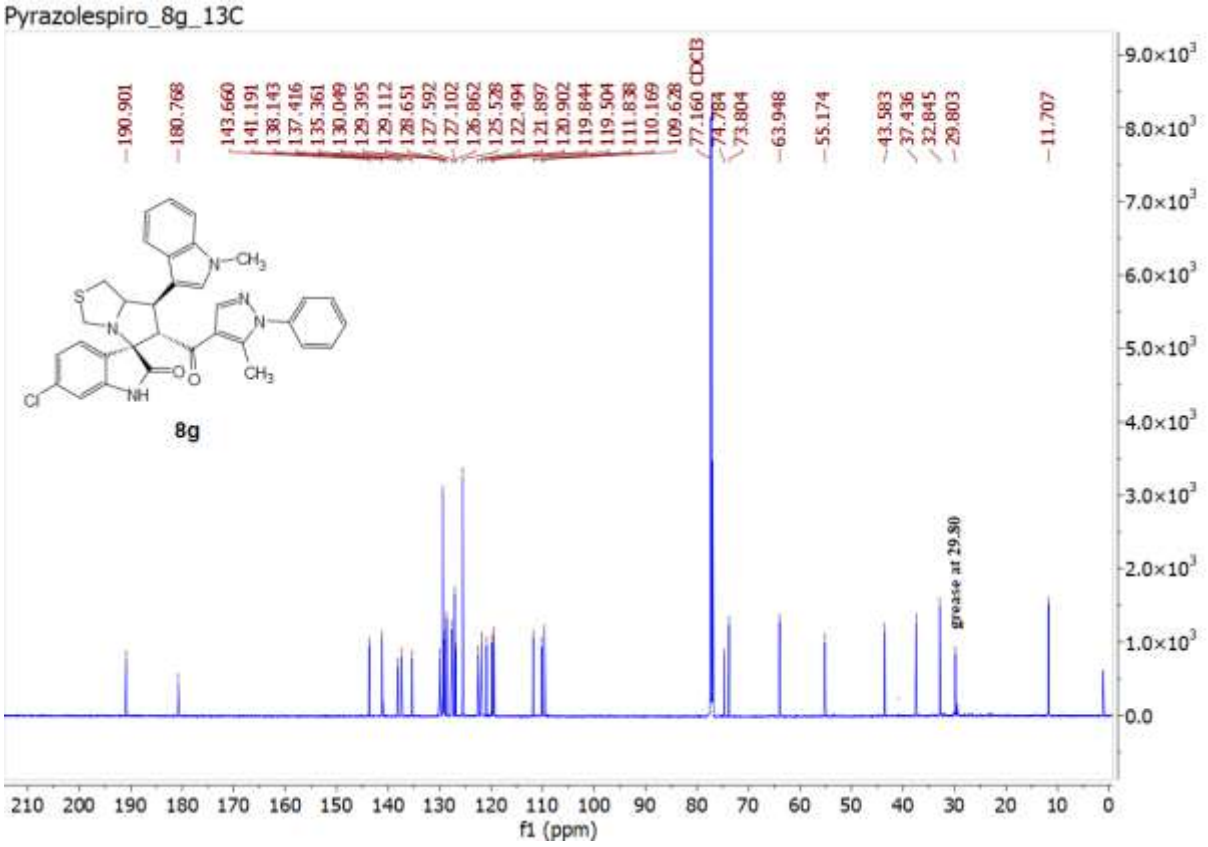

Figure S13. ^{1}H-NMR and ^{13}C-NMR for compound-**8h**

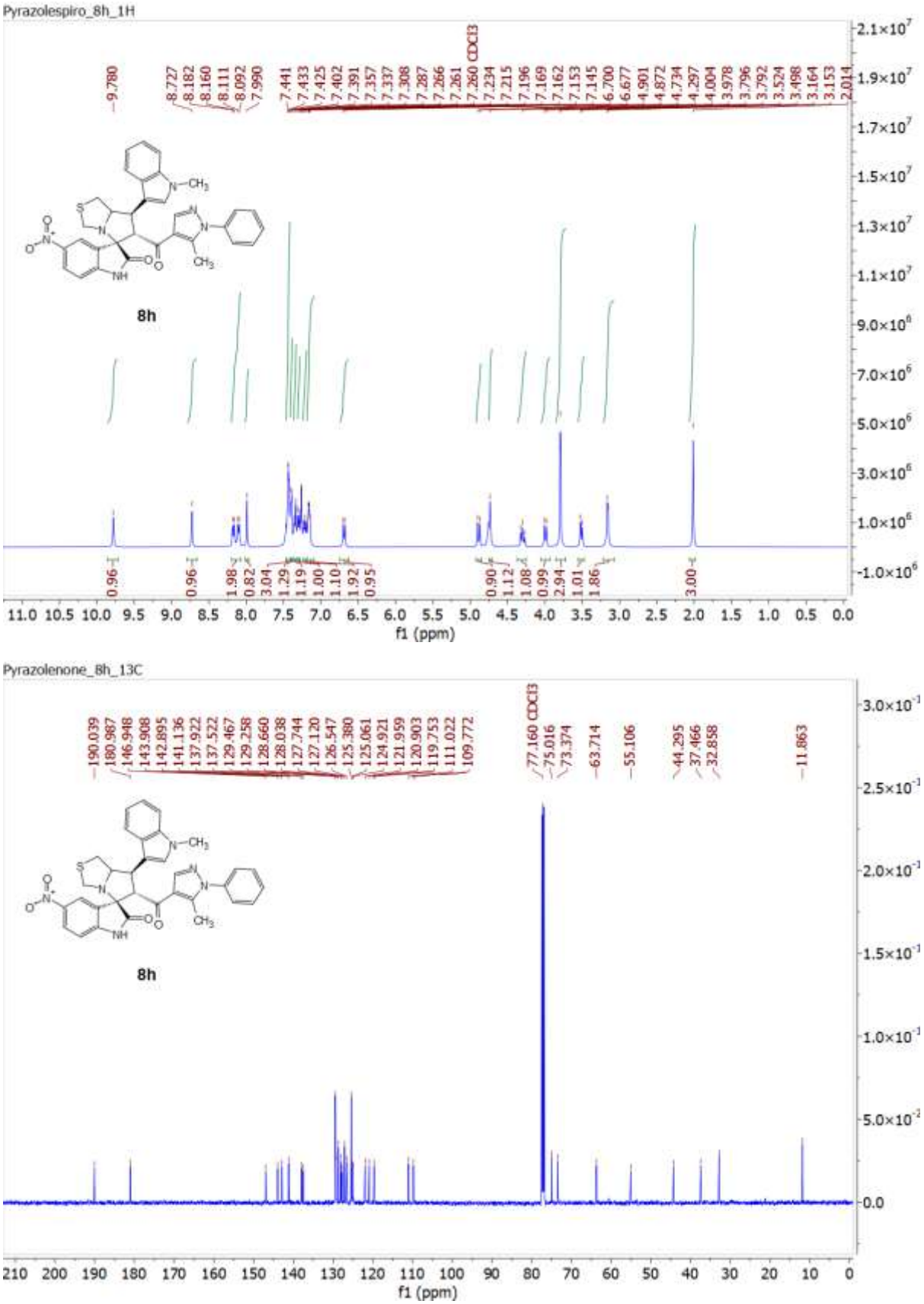

Figure S14. ^{1}H-NMR and ^{13}C-NMR for compound-**8i**

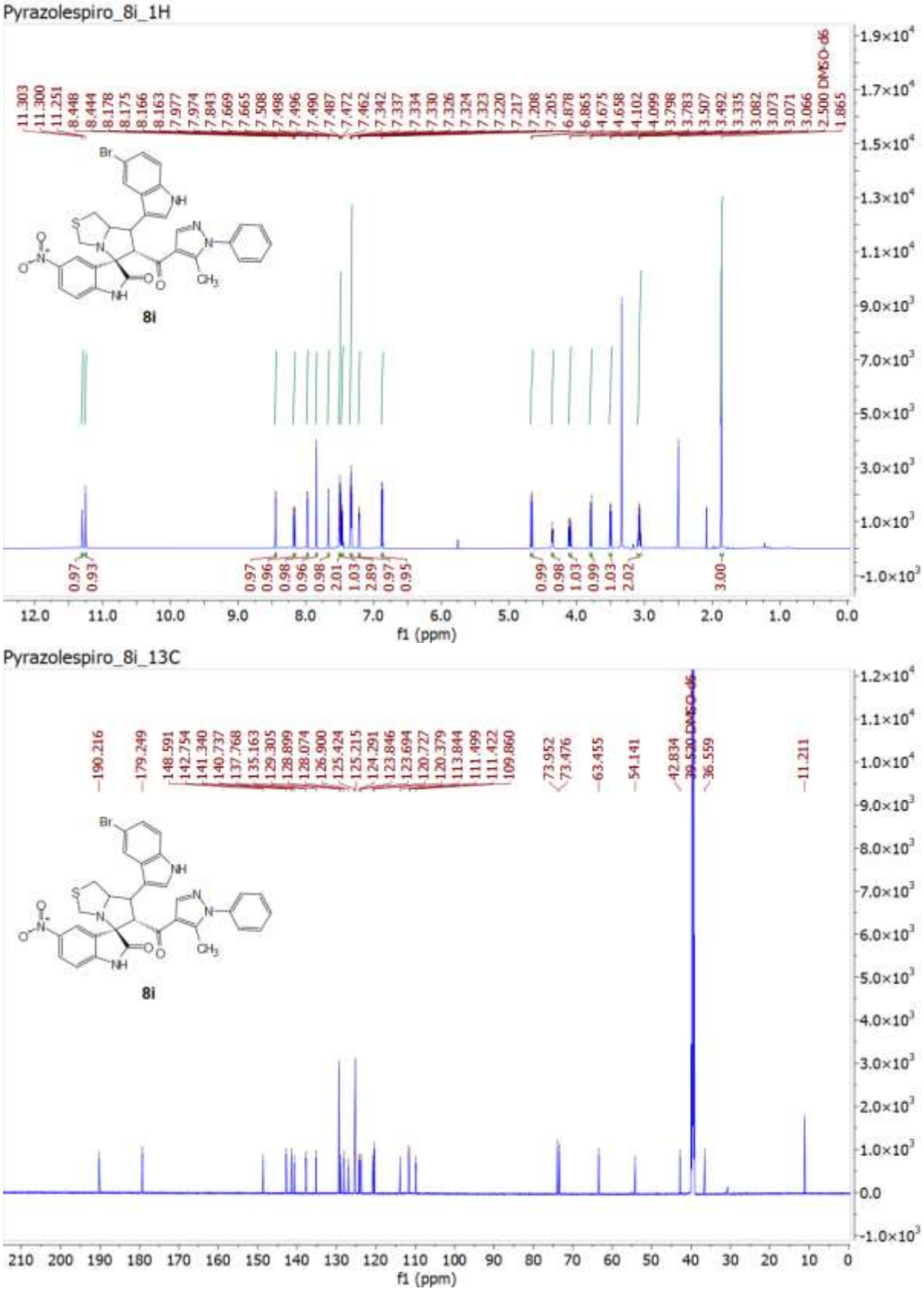

Figure S15. ^{1}H-NMR and ^{13}C-NMR for compound-**8j**

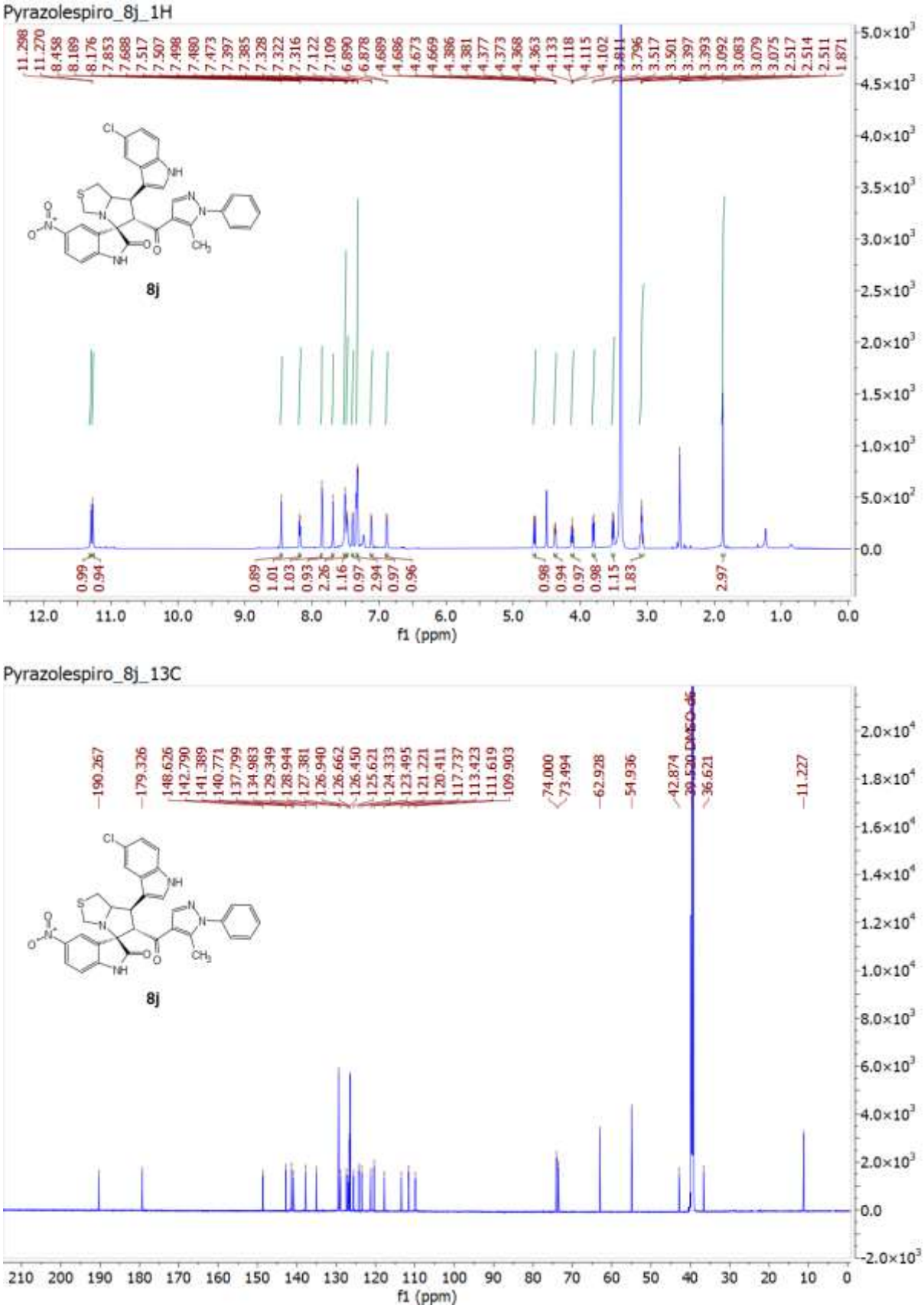

Figure S16. ^{1}H-NMR and ^{13}C-NMR for compound-**8k**

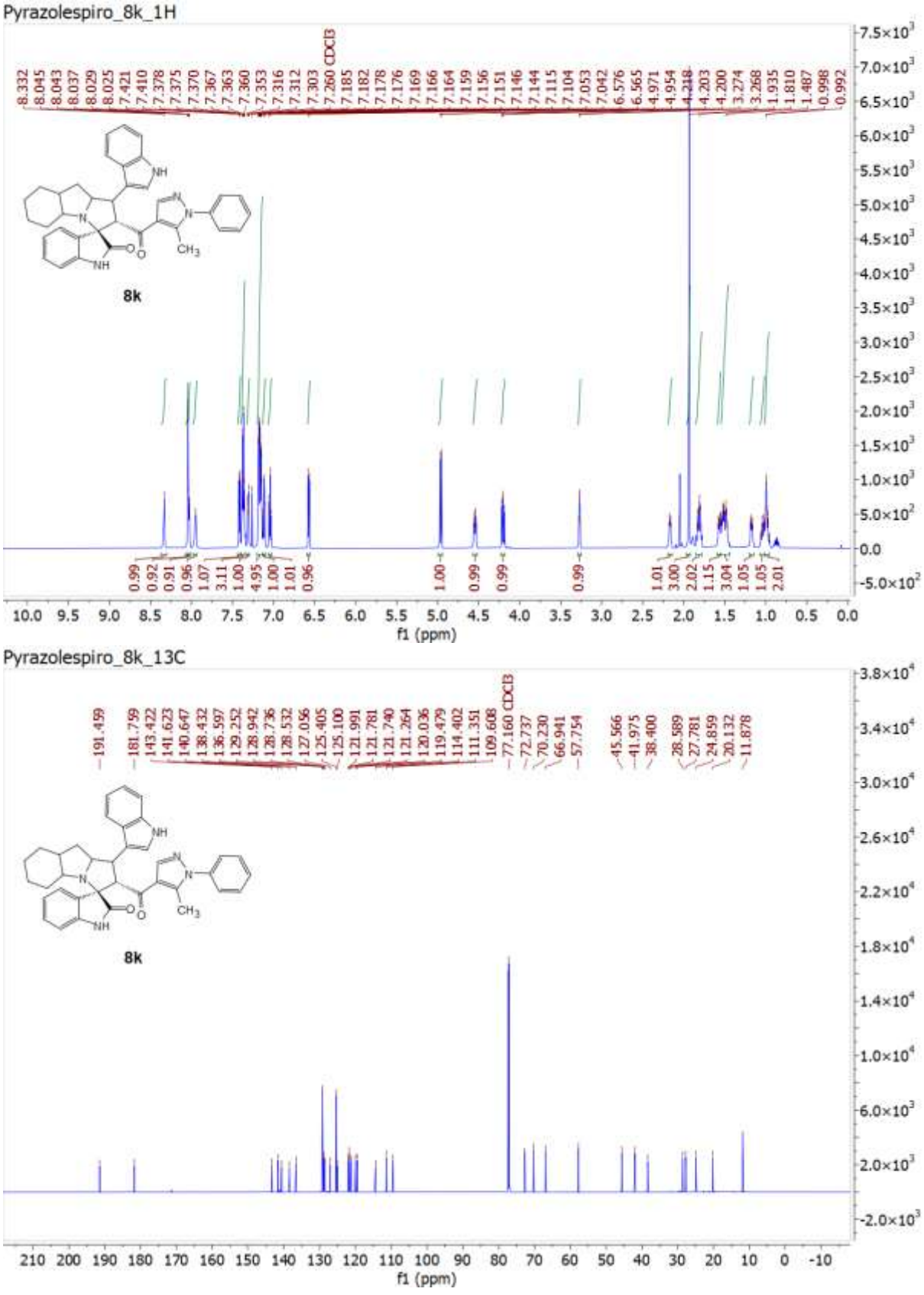

Figure S17. ^{1}H-NMR and ^{13}C-NMR for compound-**8l**

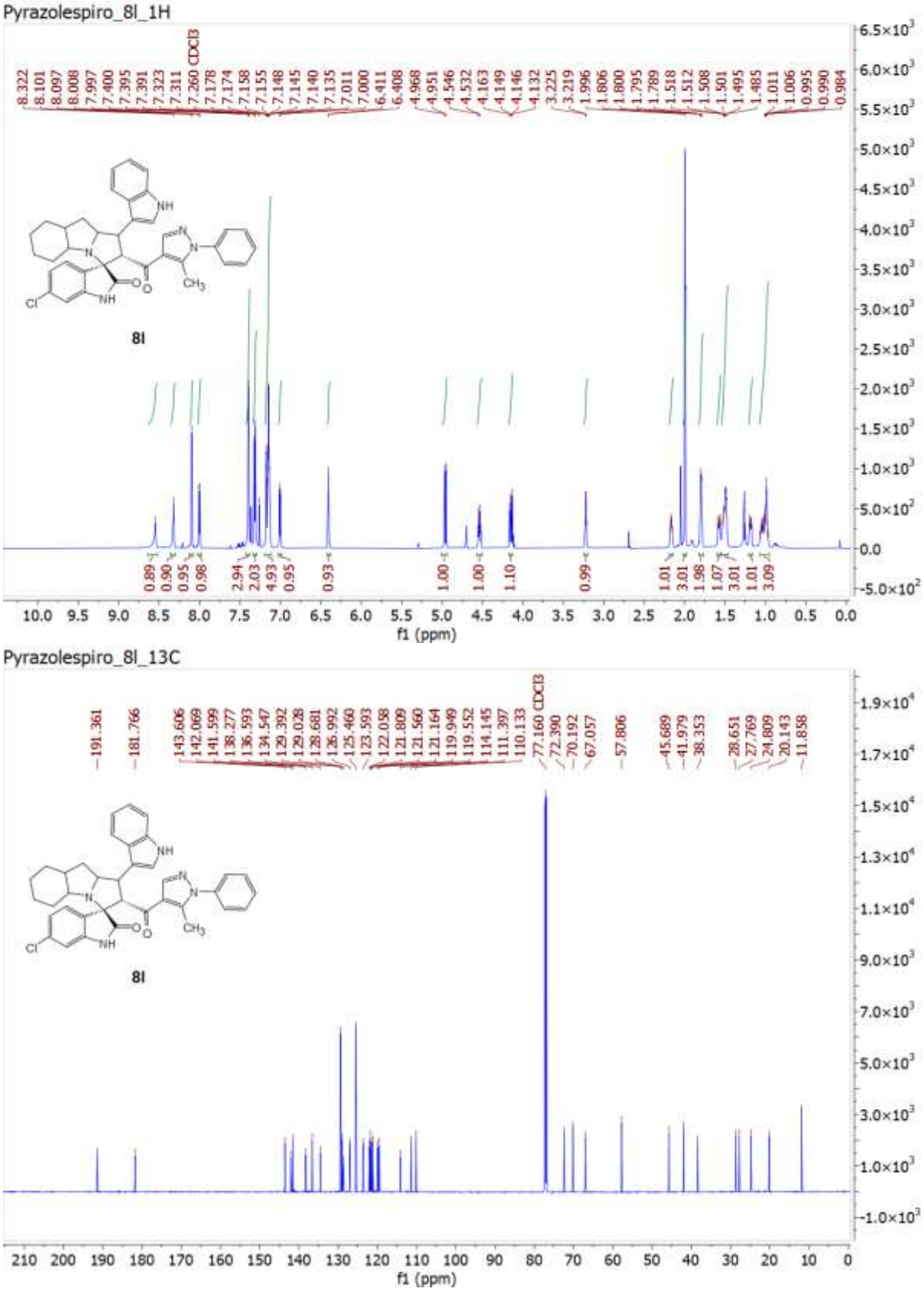

Figure S18. ^{1}H-NMR and ^{13}C-NMR for compound-**8m**

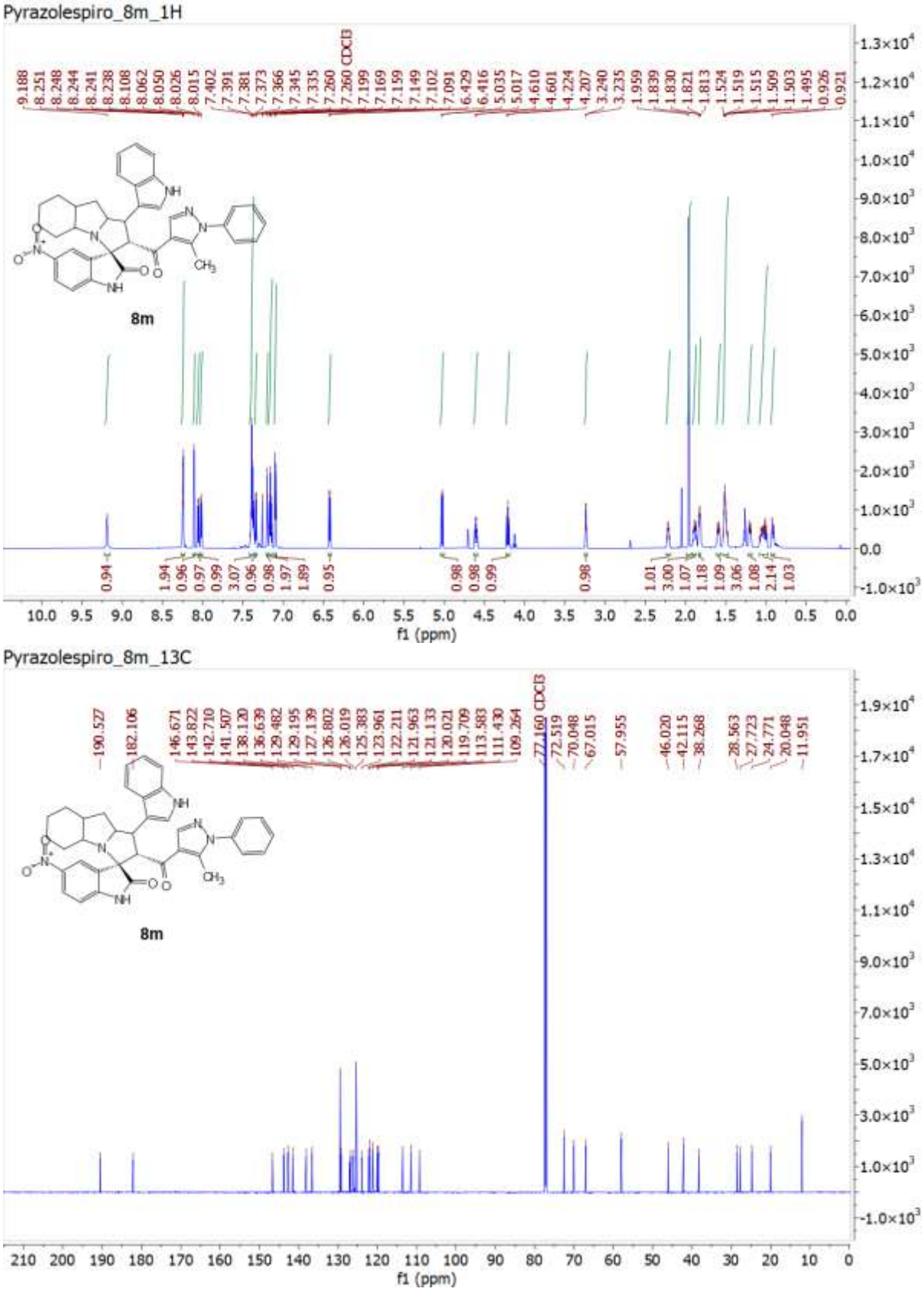

Figure S19. ^{1}H-NMR and ^{13}C-NMR for compound-**8n**

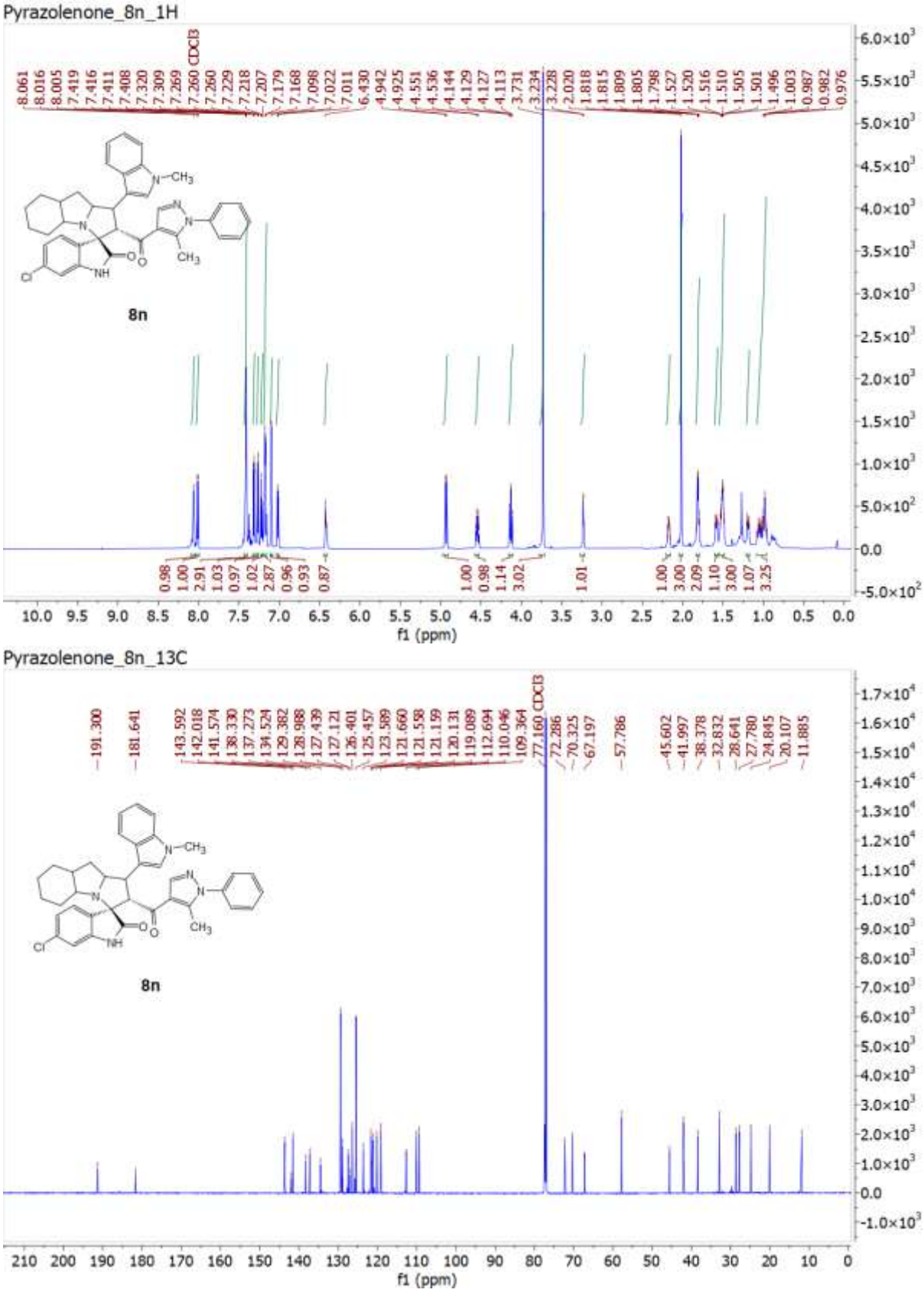

Figure S20. ^{1}H-NMR and ^{13}C-NMR for compound-**8o**

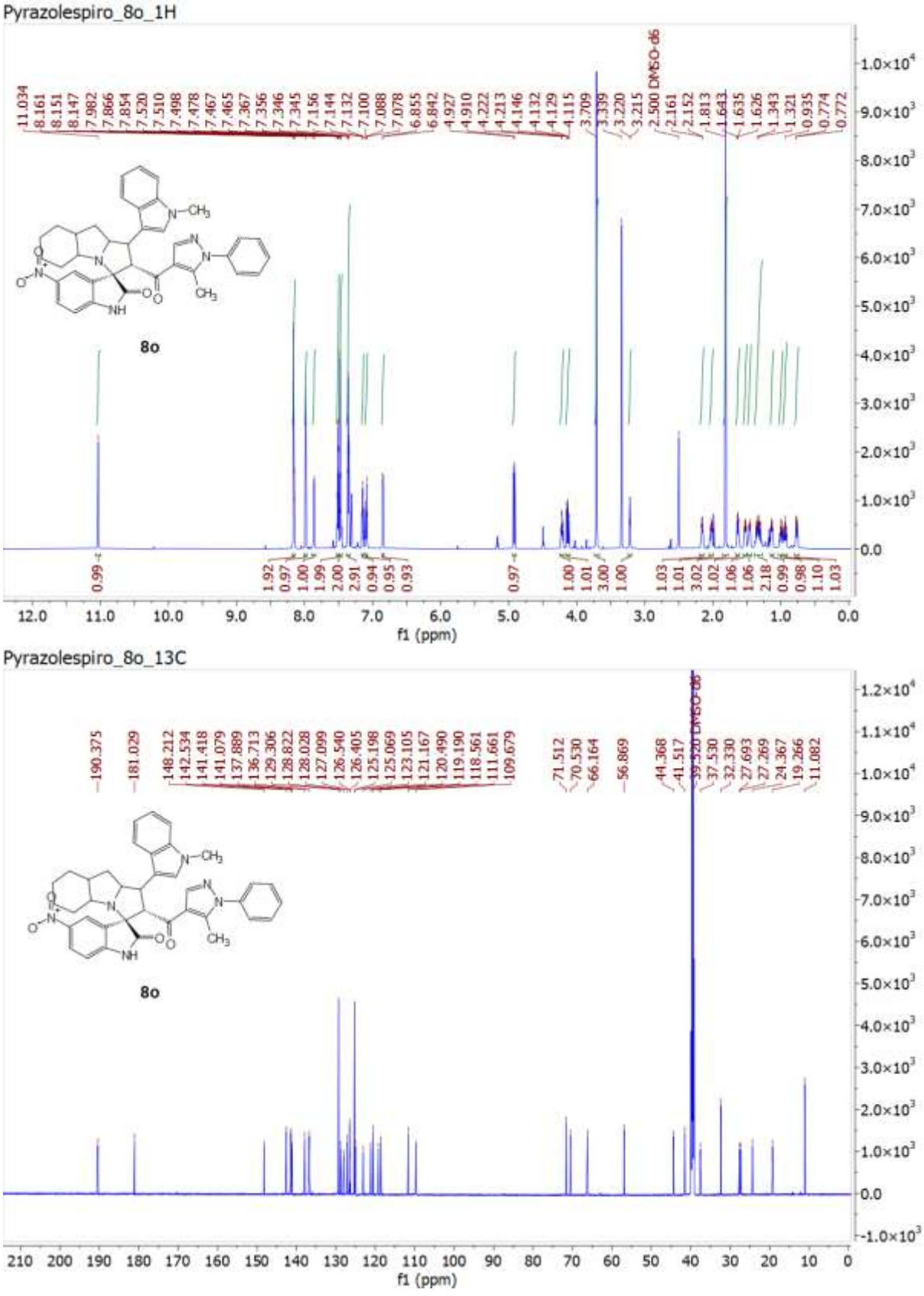

Figure S21. ^{1}H-NMR and ^{13}C-NMR for compound-**8p**

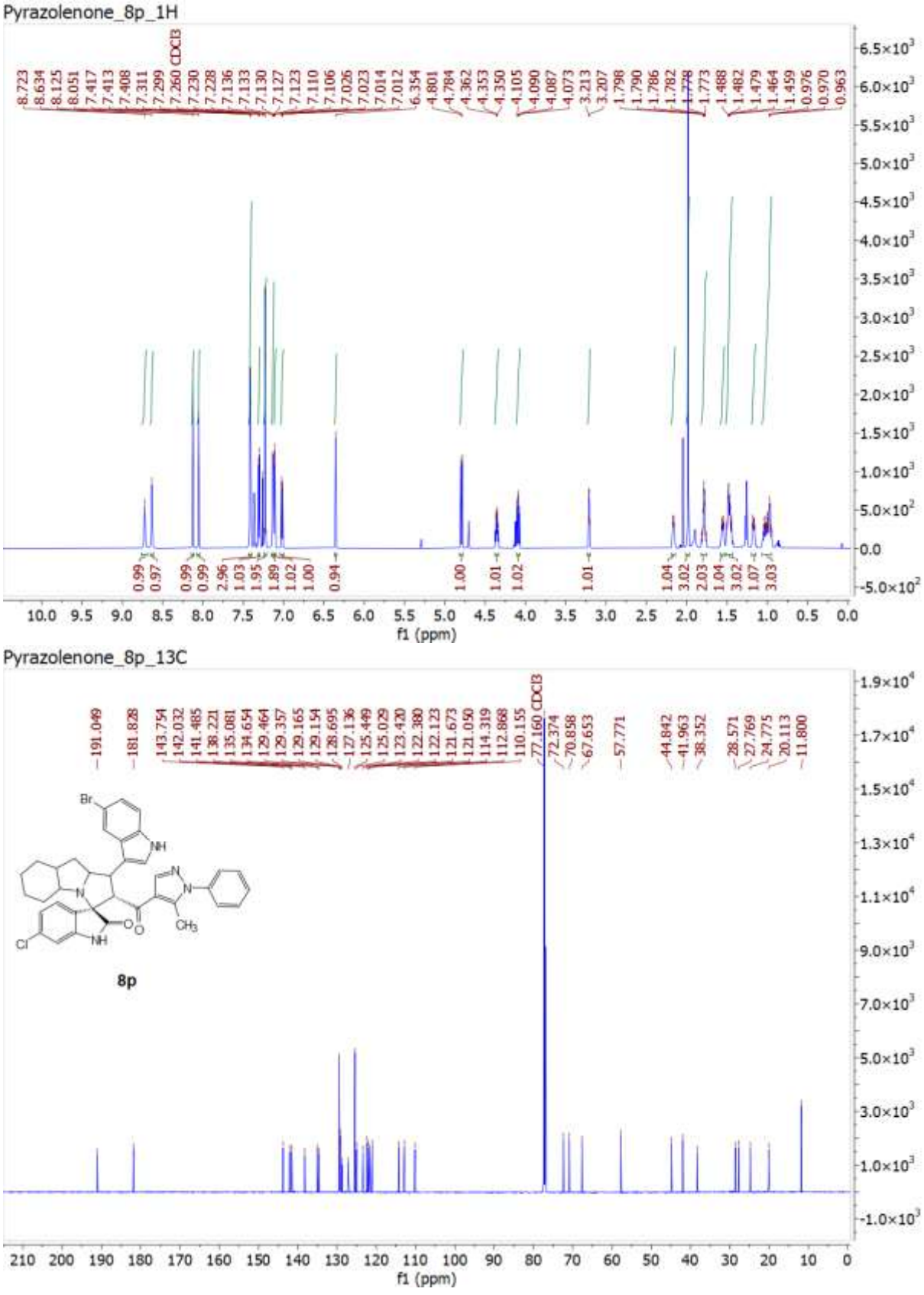

Figure S22. ^{1}H-NMR and ^{13}C-NMR for compound-**8q**

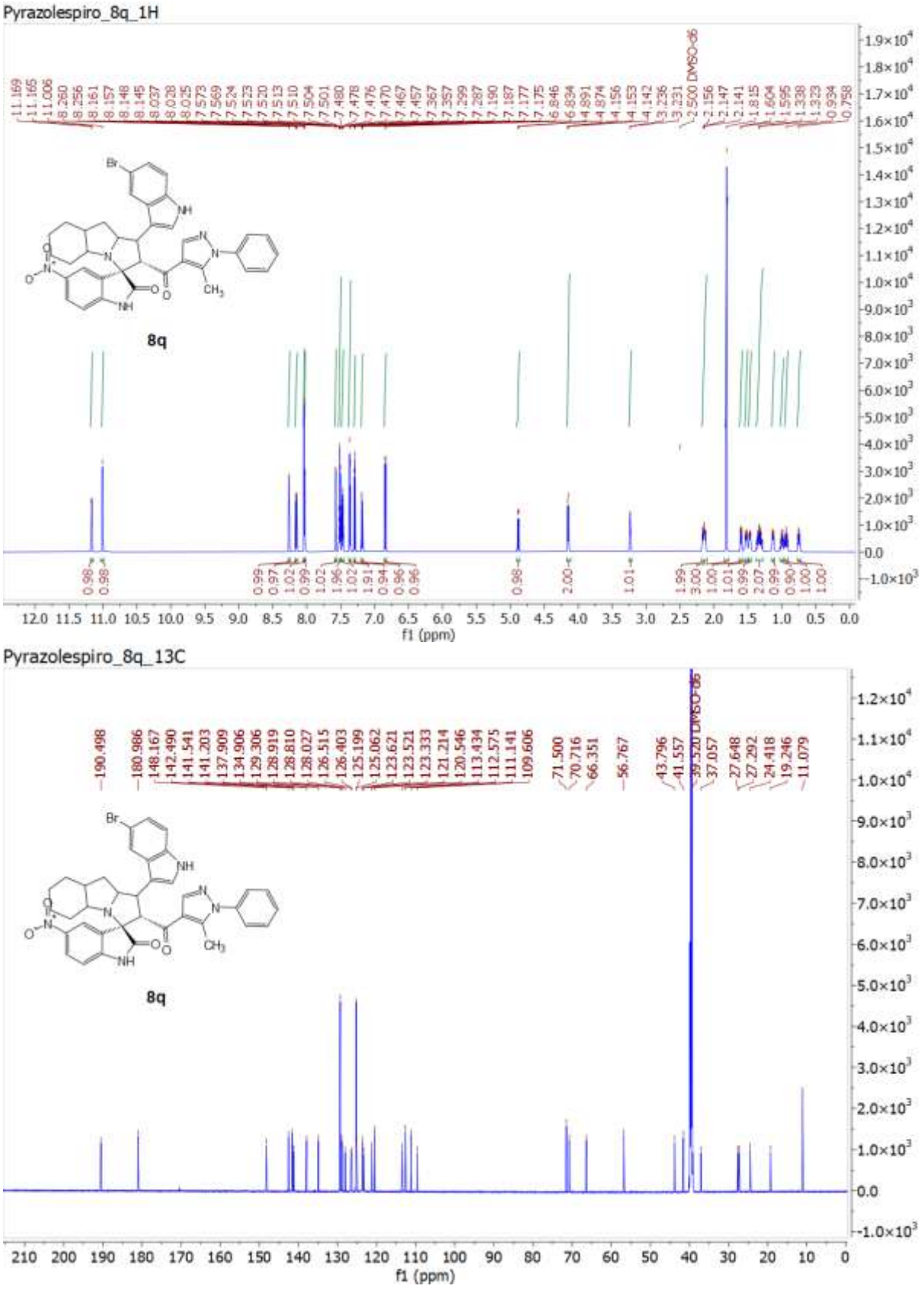

Figure S23. ^{1}H-NMR and ^{13}C-NMR for compound-**8r**

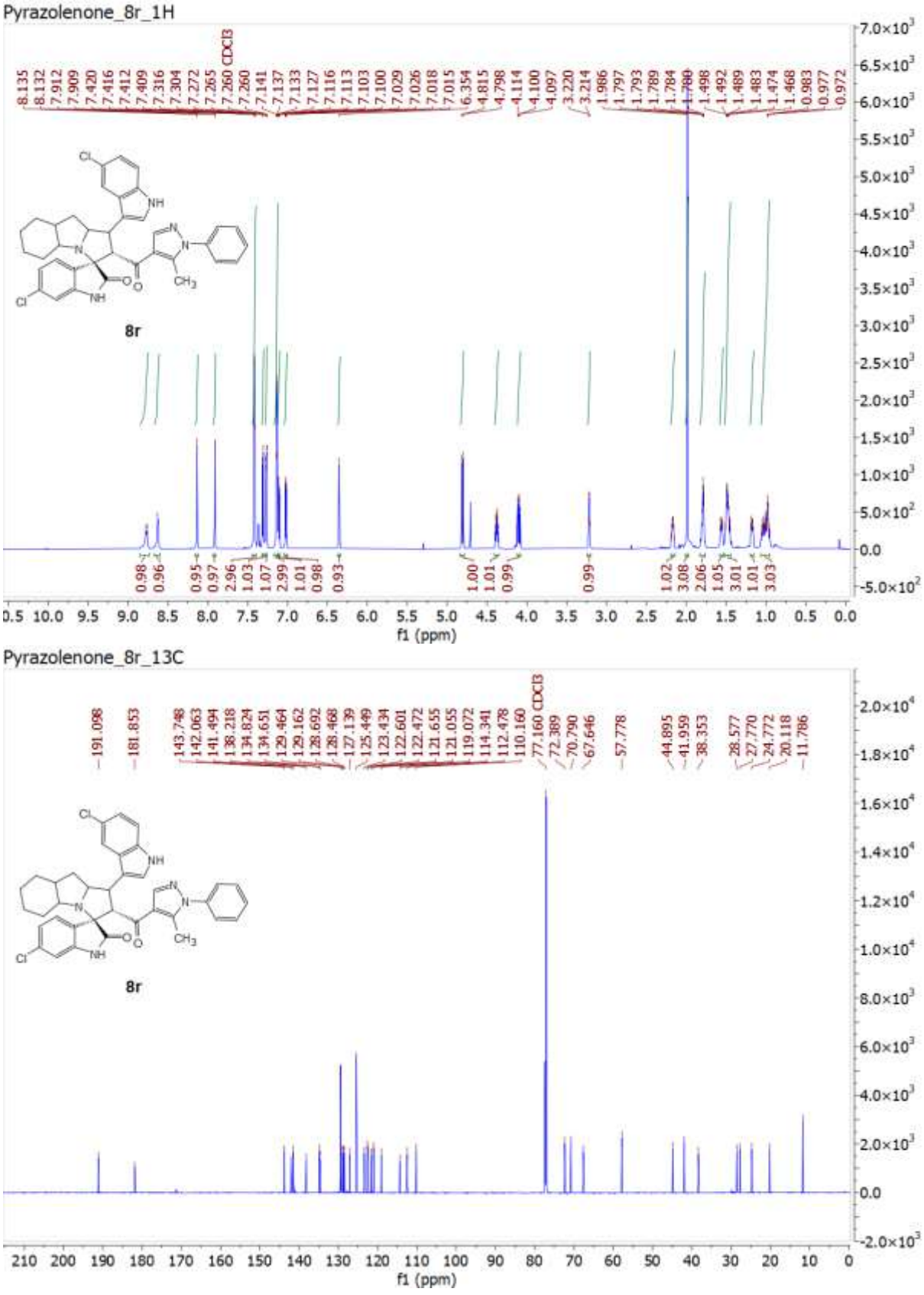

Figure S24. ^{1}H-NMR and ^{13}C-NMR for compound-**8s**

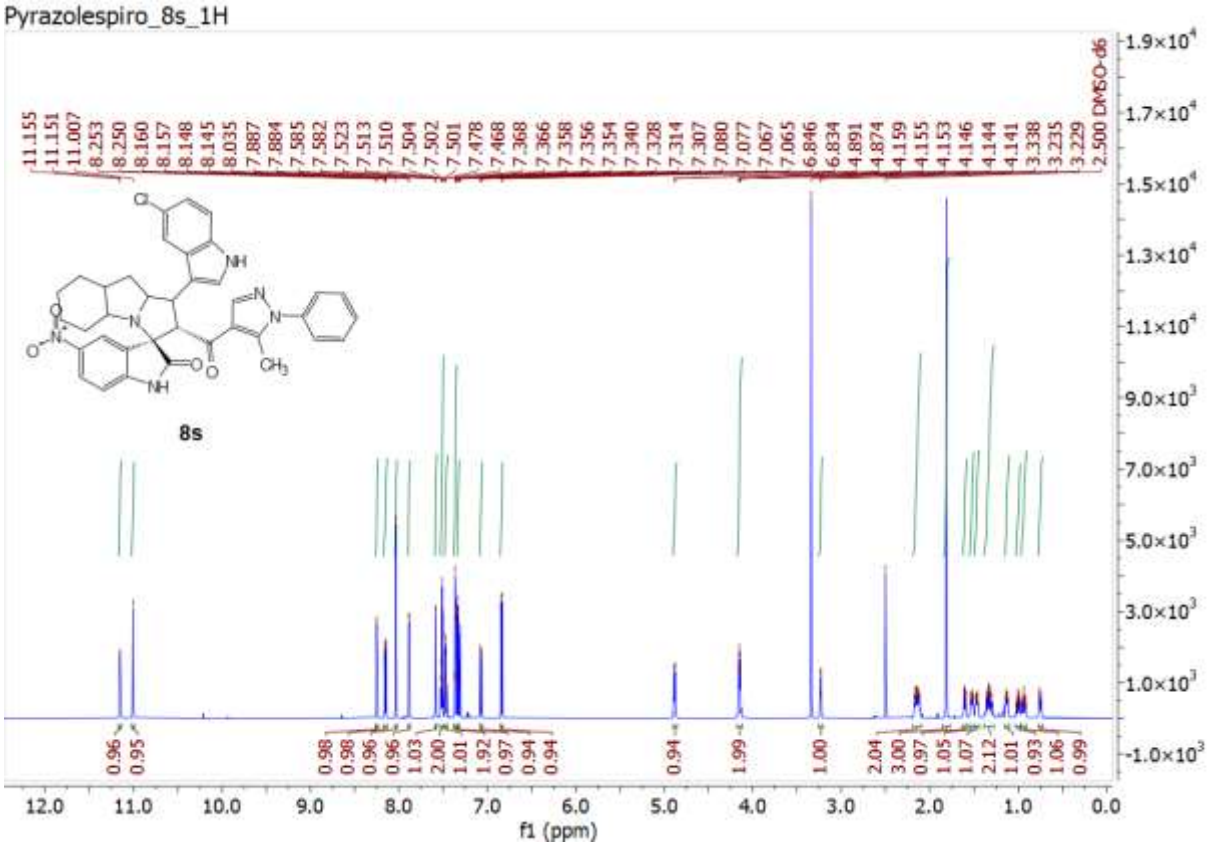

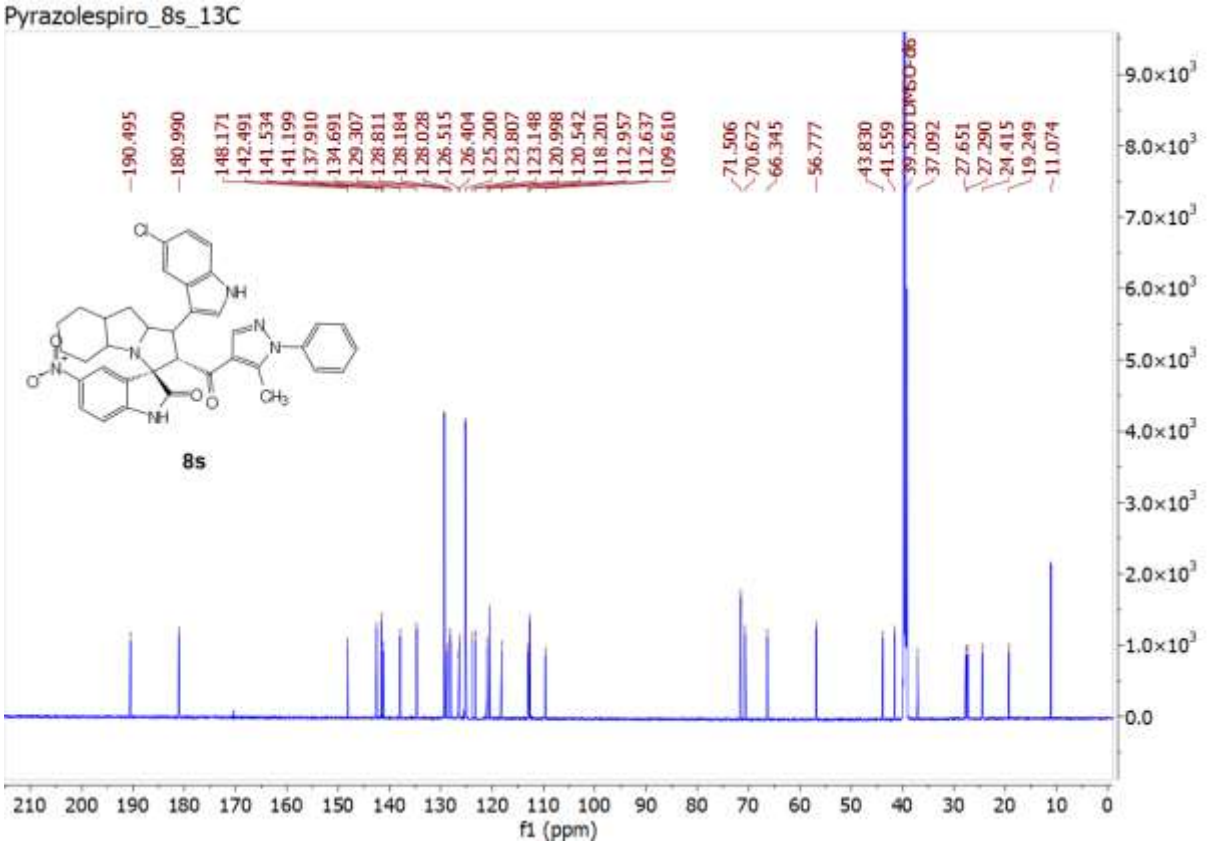

Figure S25. ^{1}H-NMR and ^{13}C-NMR for compound-**8t**

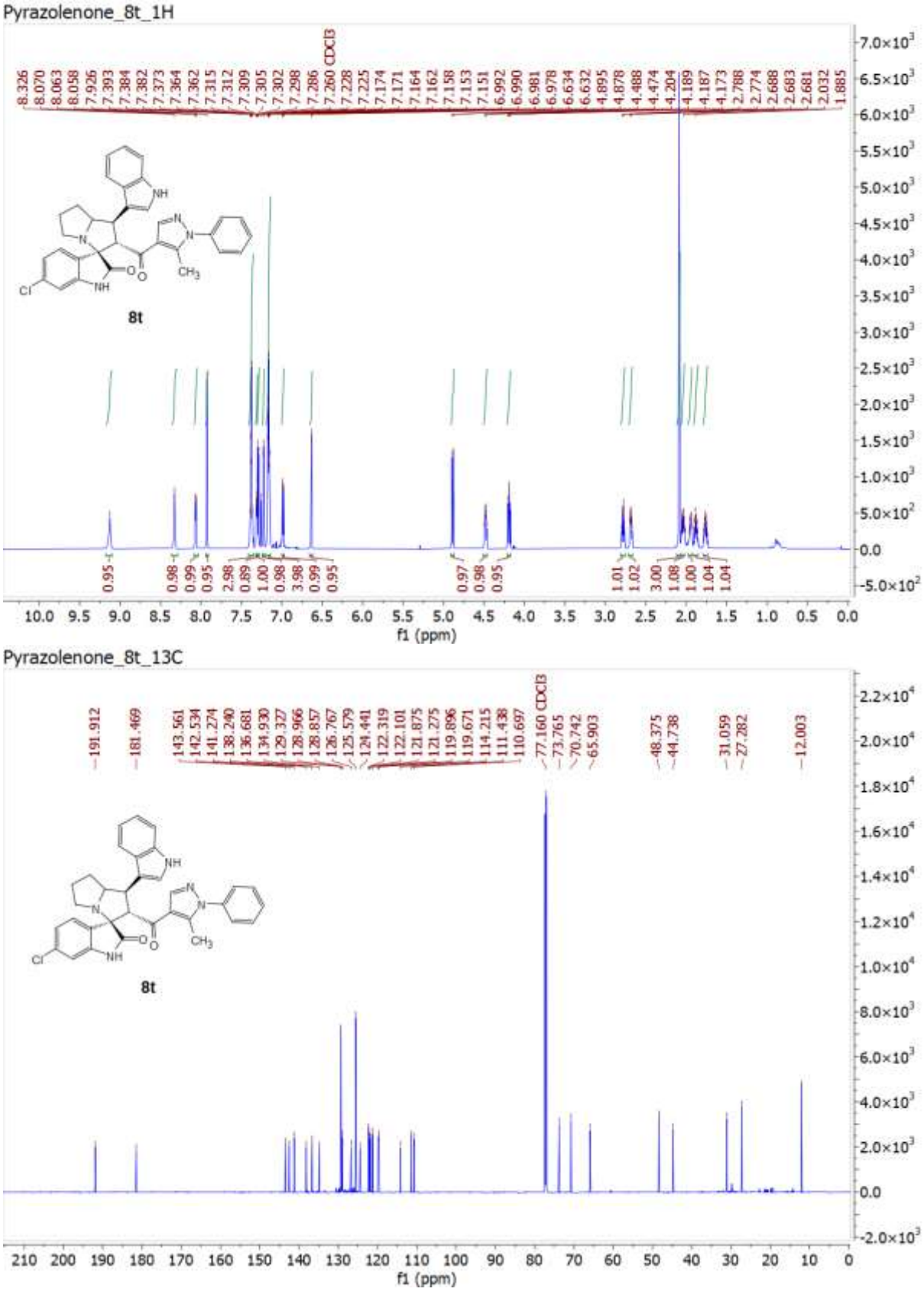

Figure S26. ^{1}H-NMR and ^{13}C-NMR for compound-**8u**

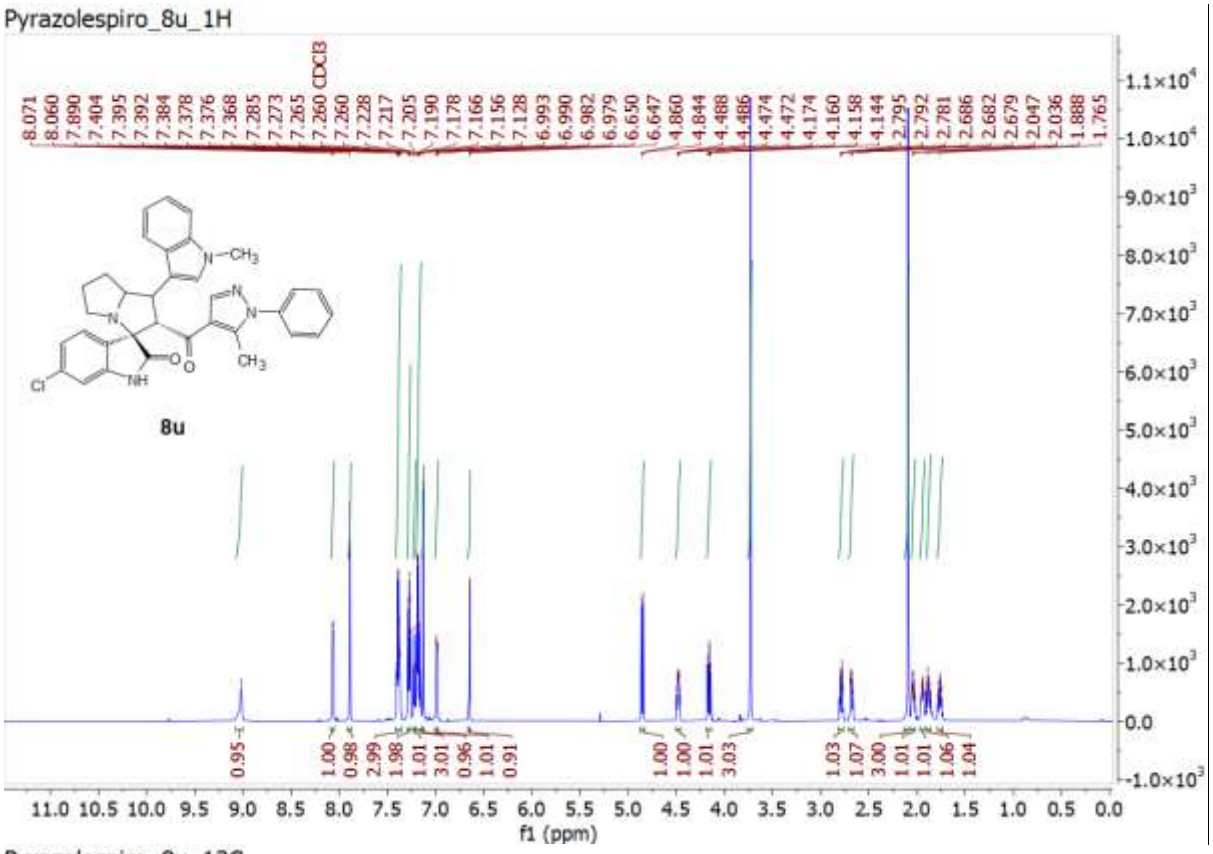

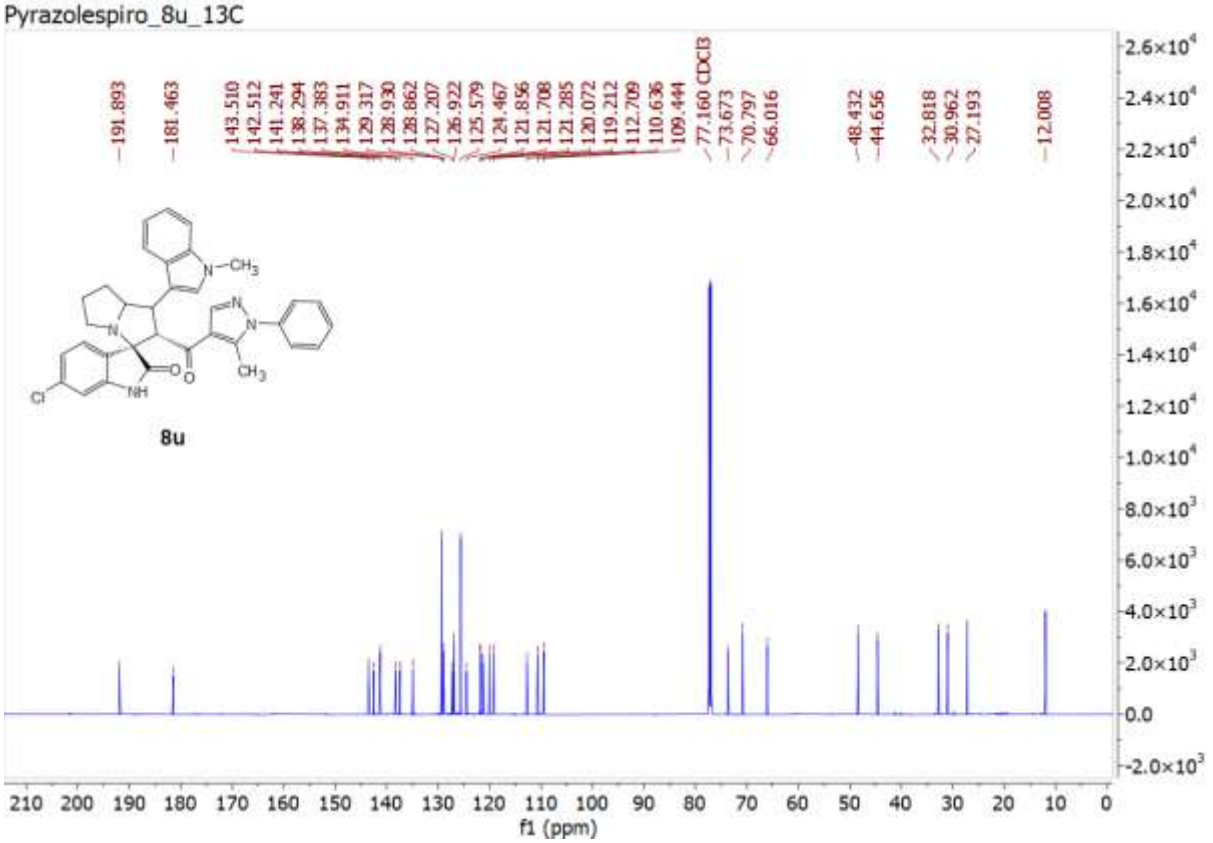

Figure S27. ^{1}H-NMR and ^{13}C-NMR for compound-**8v**

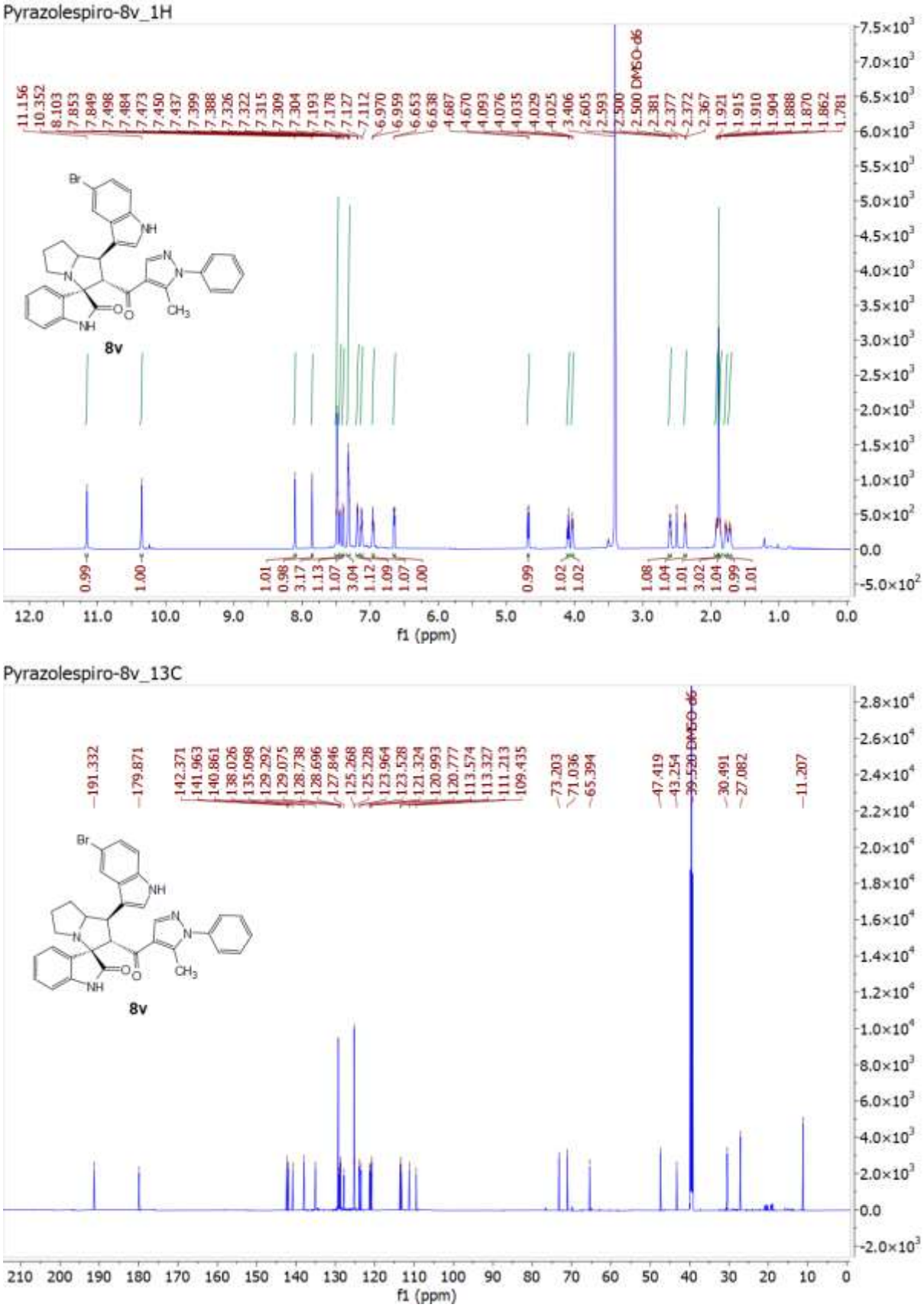

Figure S28. ^{1}H-NMR and ^{13}C-NMR for compound-**8w**

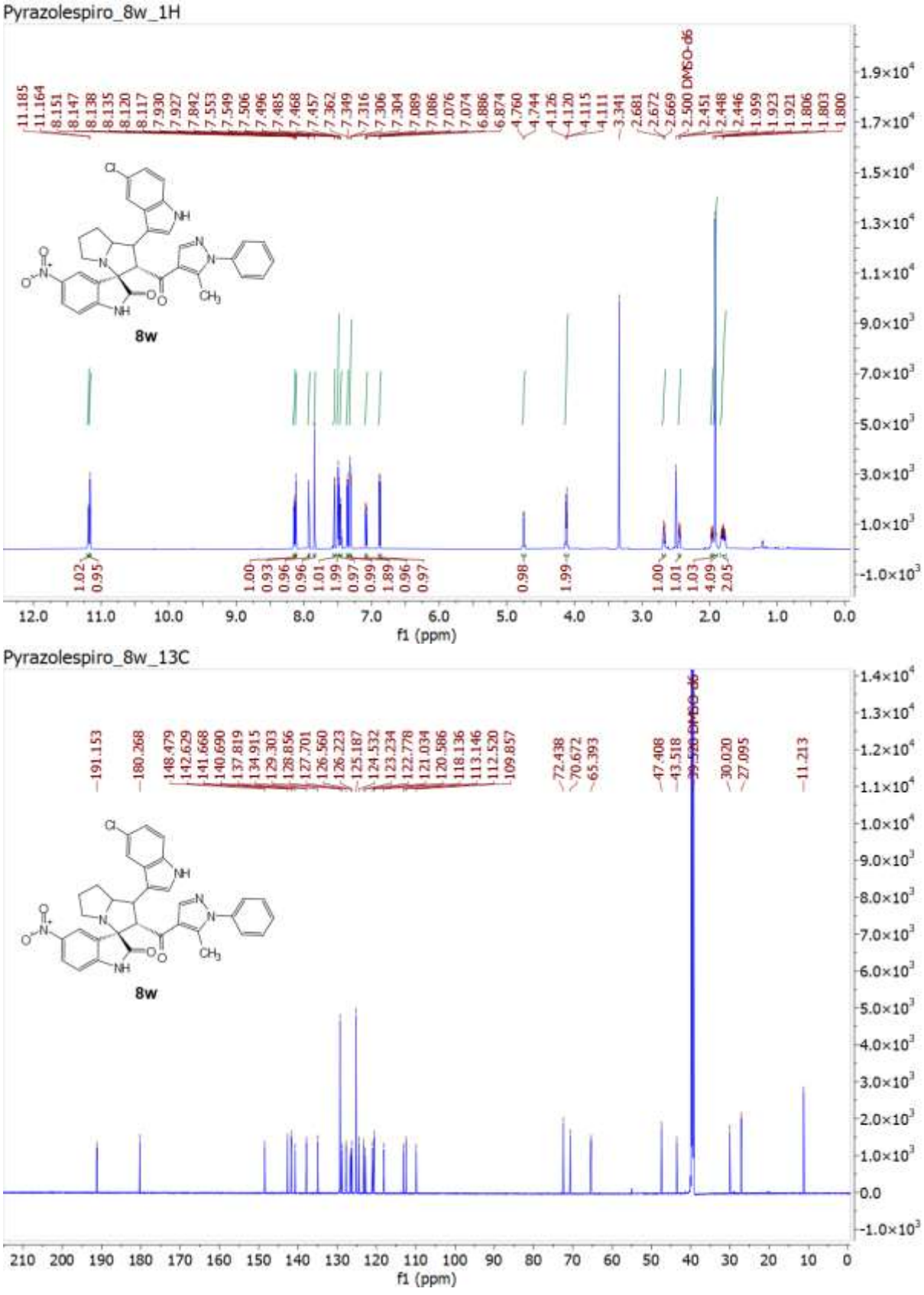

Figure S29. ^{1}H-NMR and ^{13}C-NMR for compound-**8x**

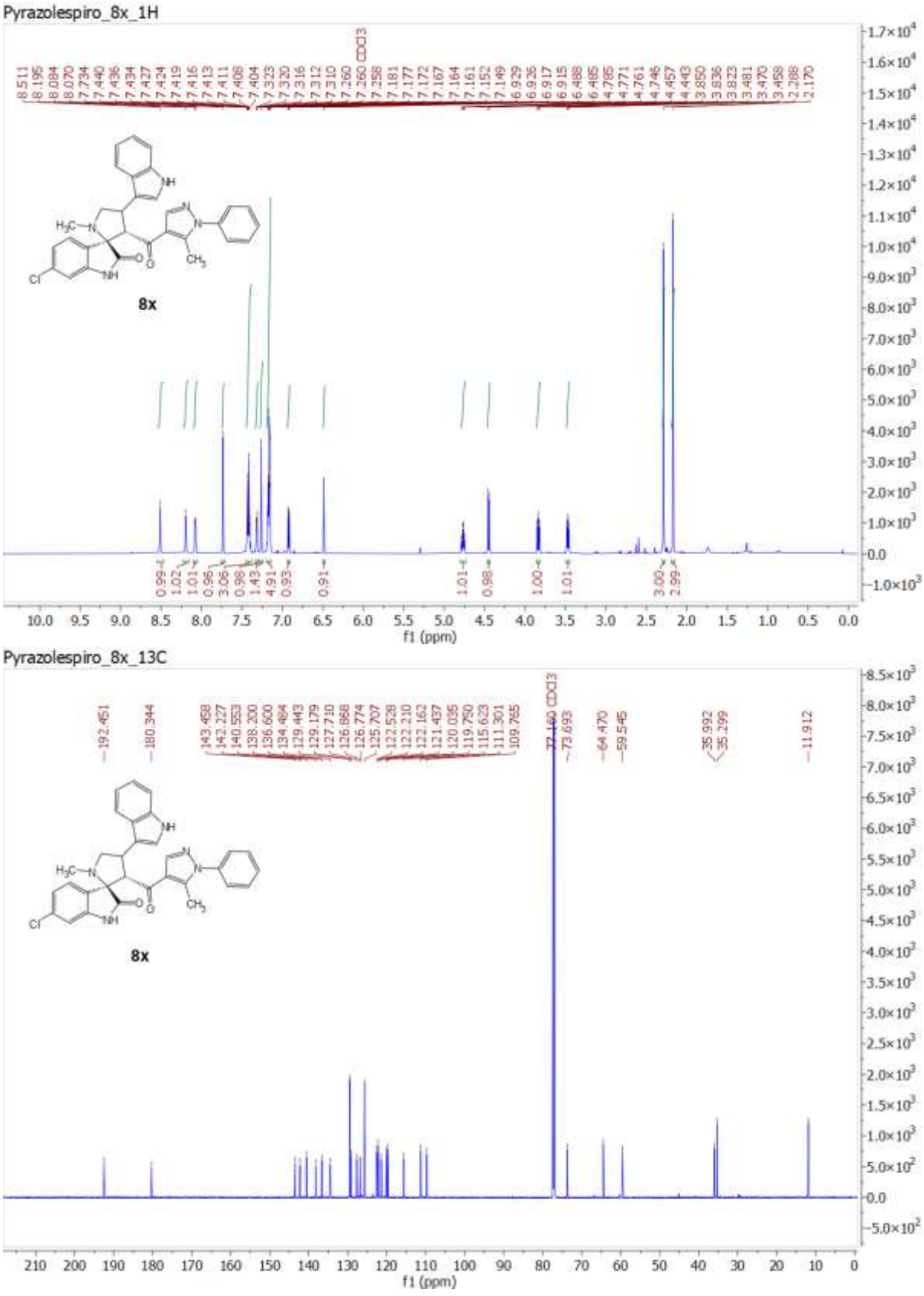

Figure S30. ^{1}H-NMR and ^{13}C-NMR for compound-**8y**

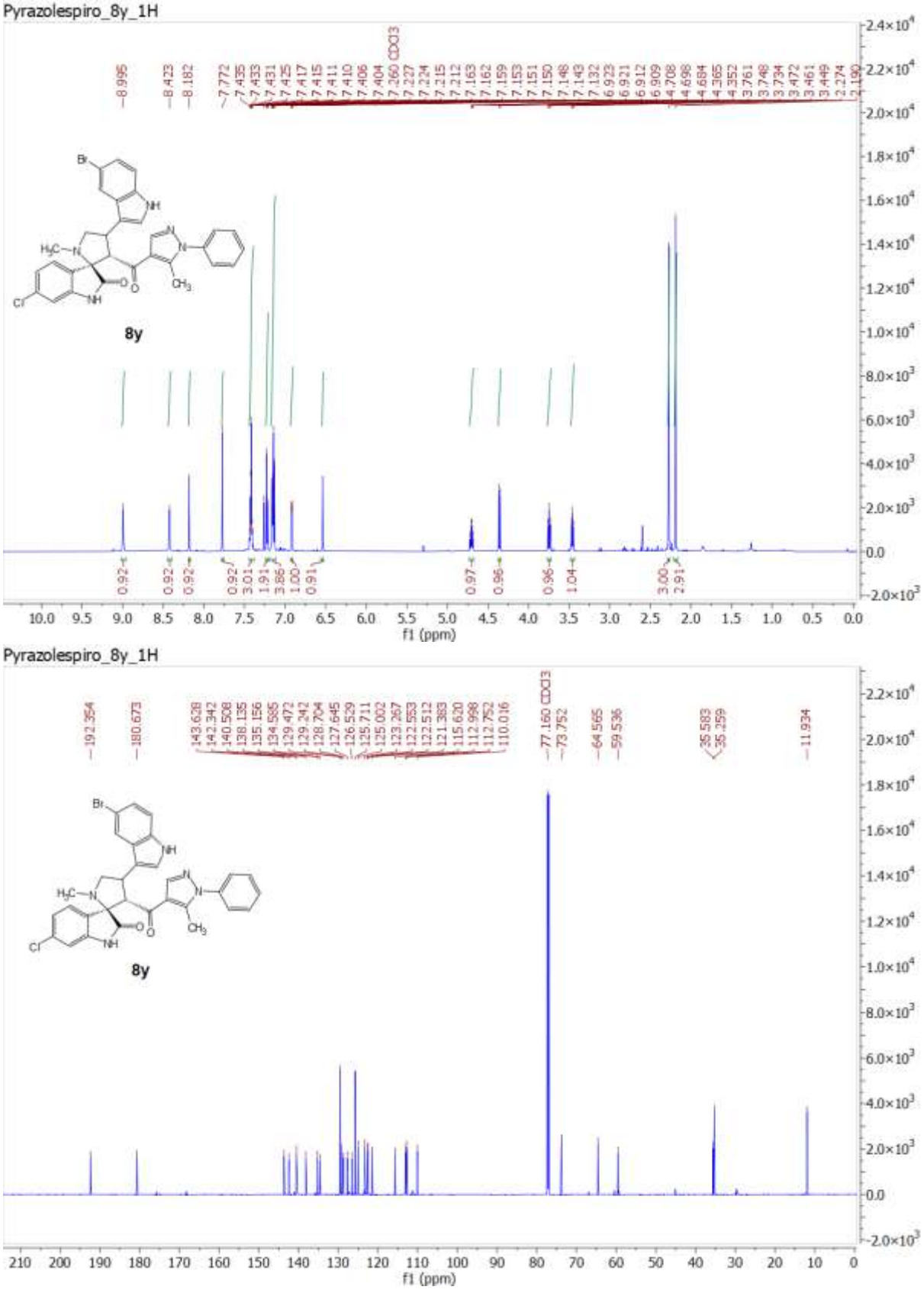

Figure S31. LCMS for compound-**5a**

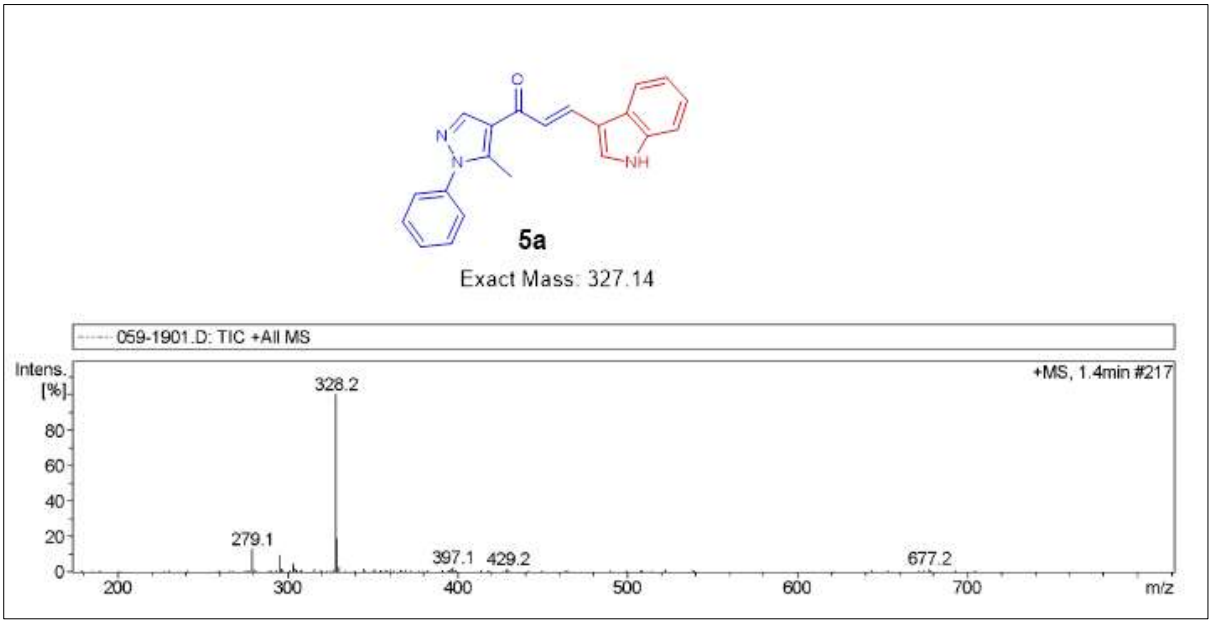

Figure S32. LCMS for compound-**5b**

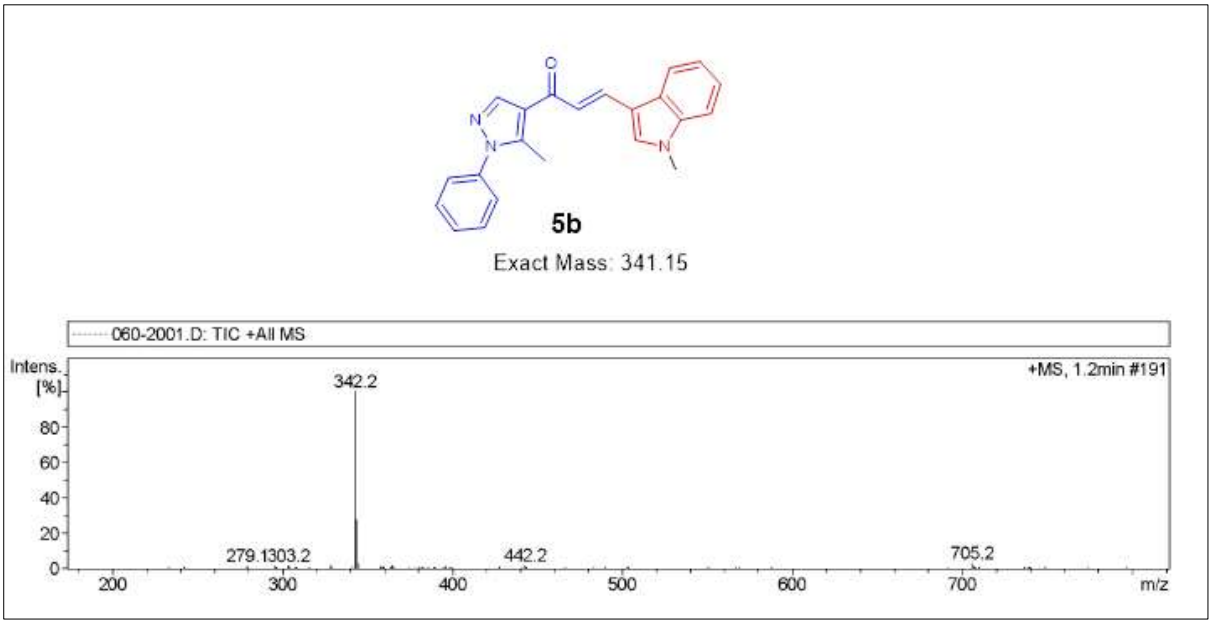

Figure S33. LCMS for compound-**5c**

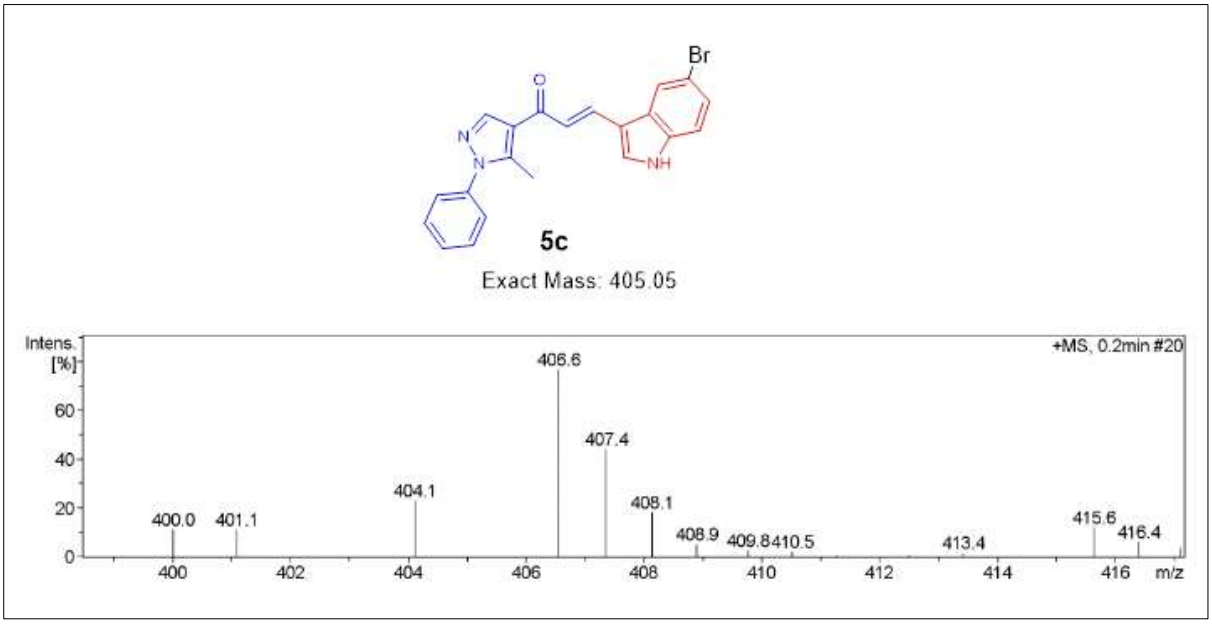

Figure S34. LCMS for compound-**5d**

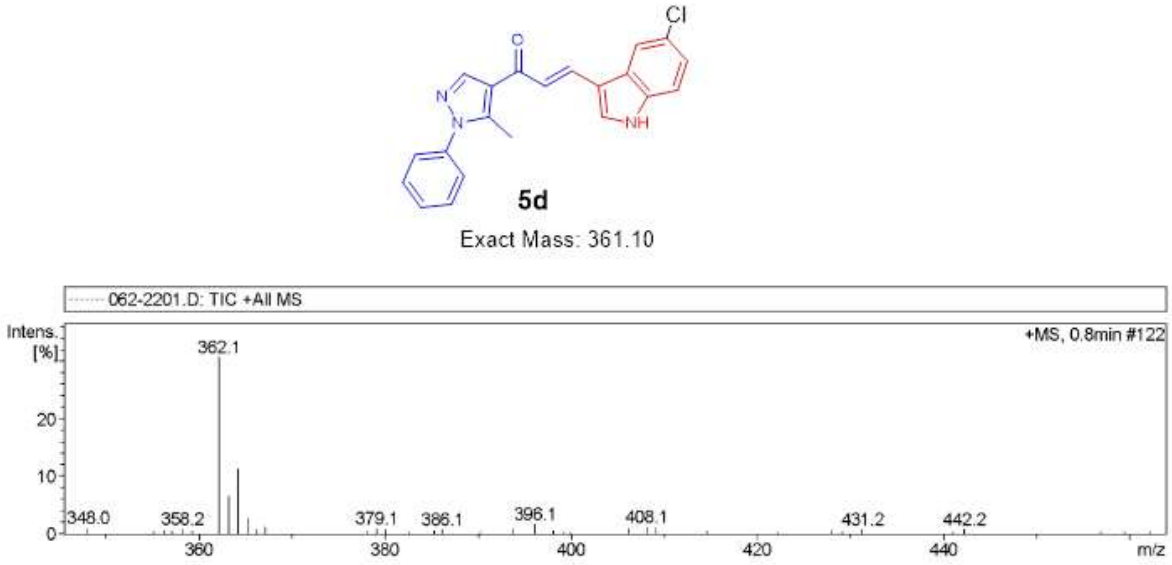

Figure S35. LCMS for compound-**8a**

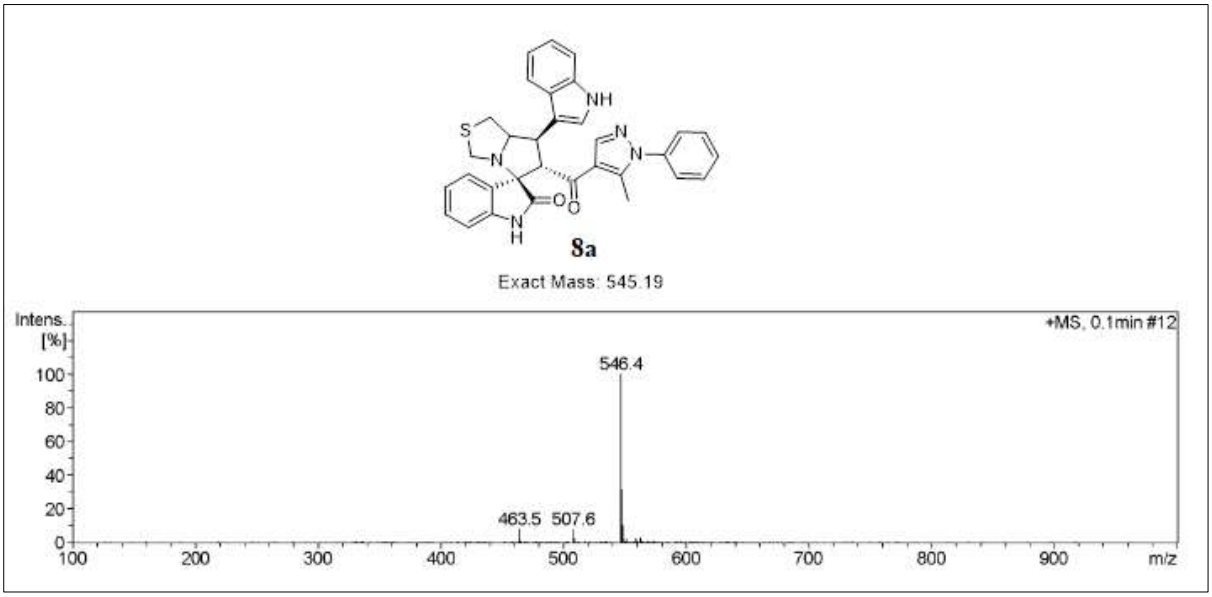

Figure S36. LCMS for compound-**8b**

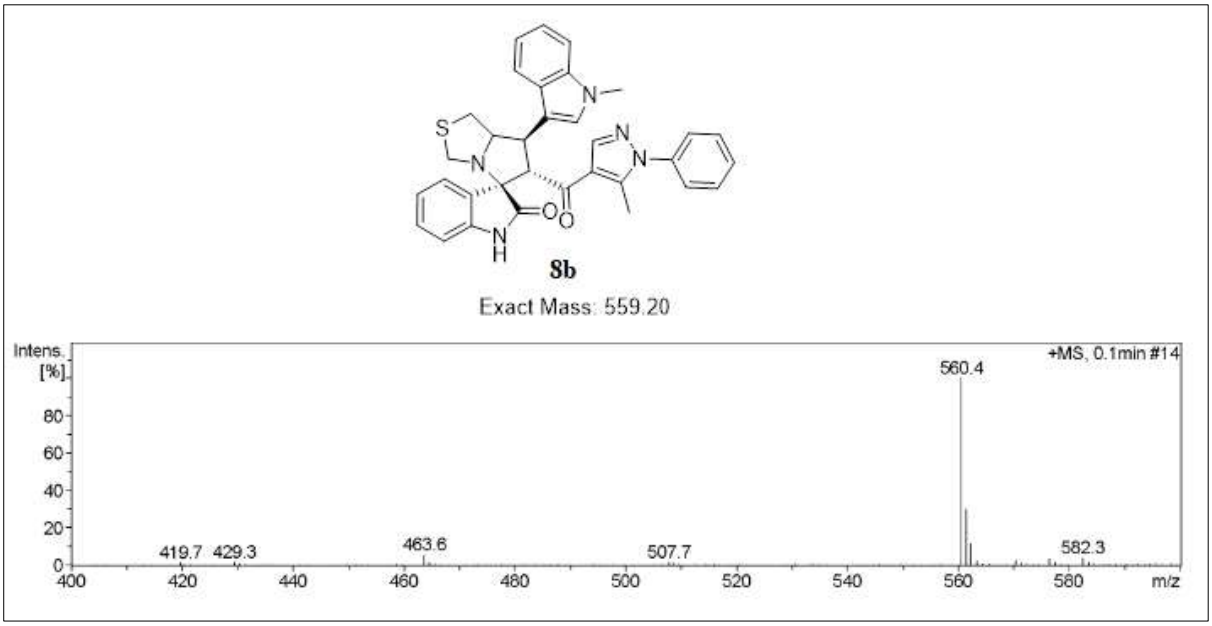

Figure S37. LCMS for compound-**8c**

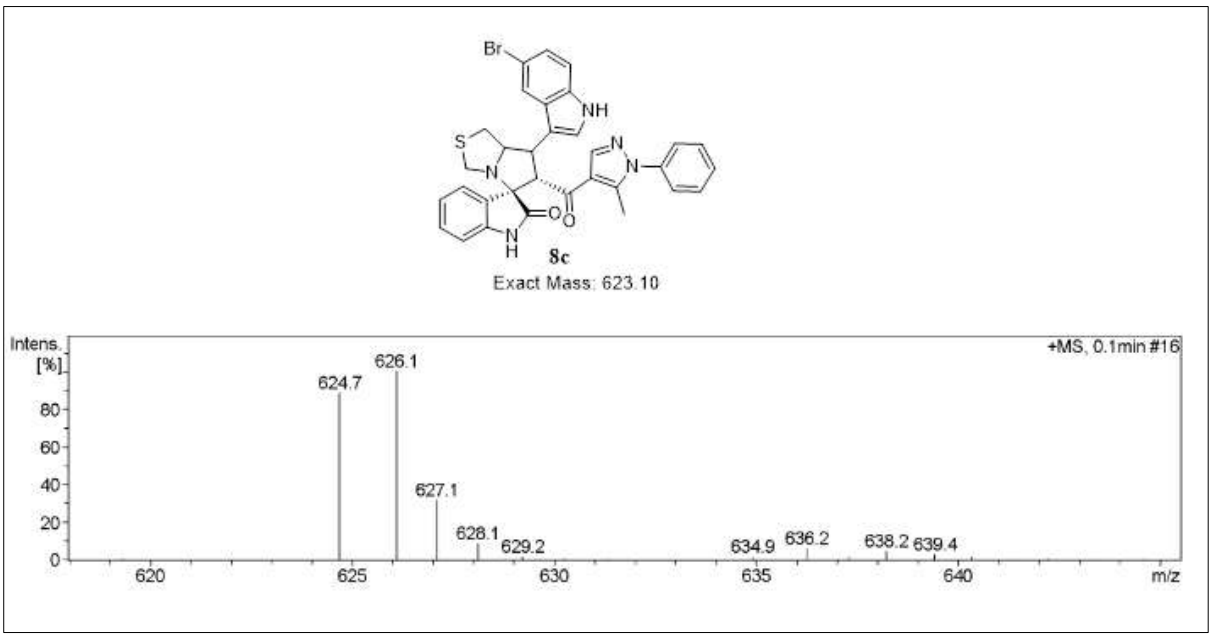

Figure S38. LCMS for compound-**8d**

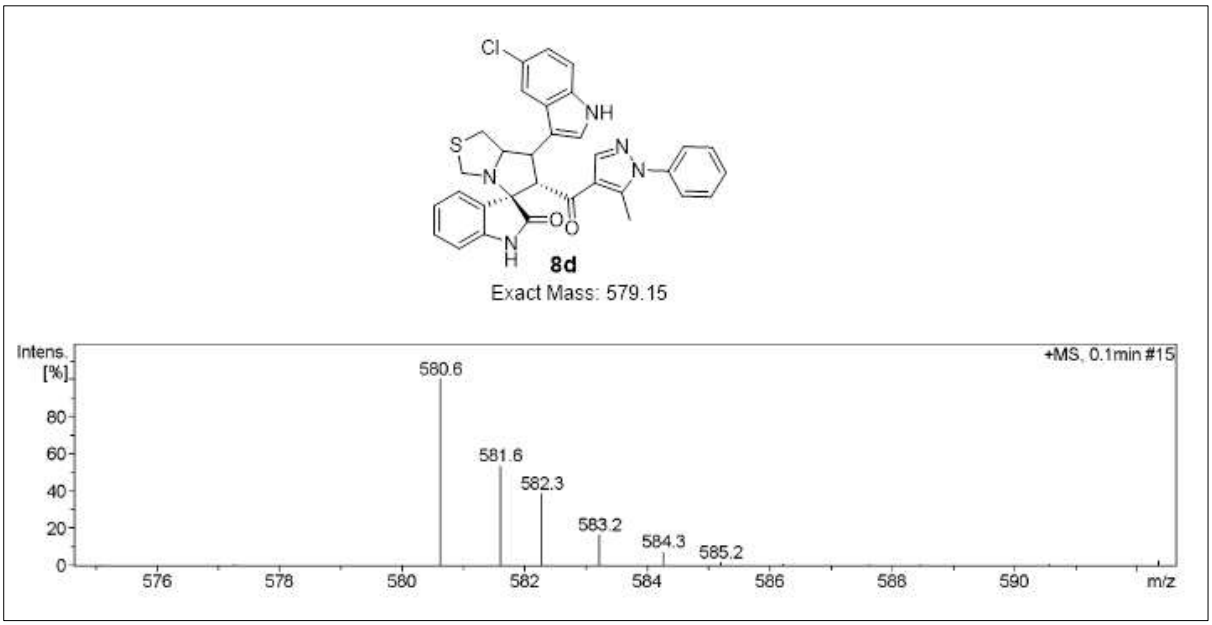

Figure S39. LCMS for compound-**8e**

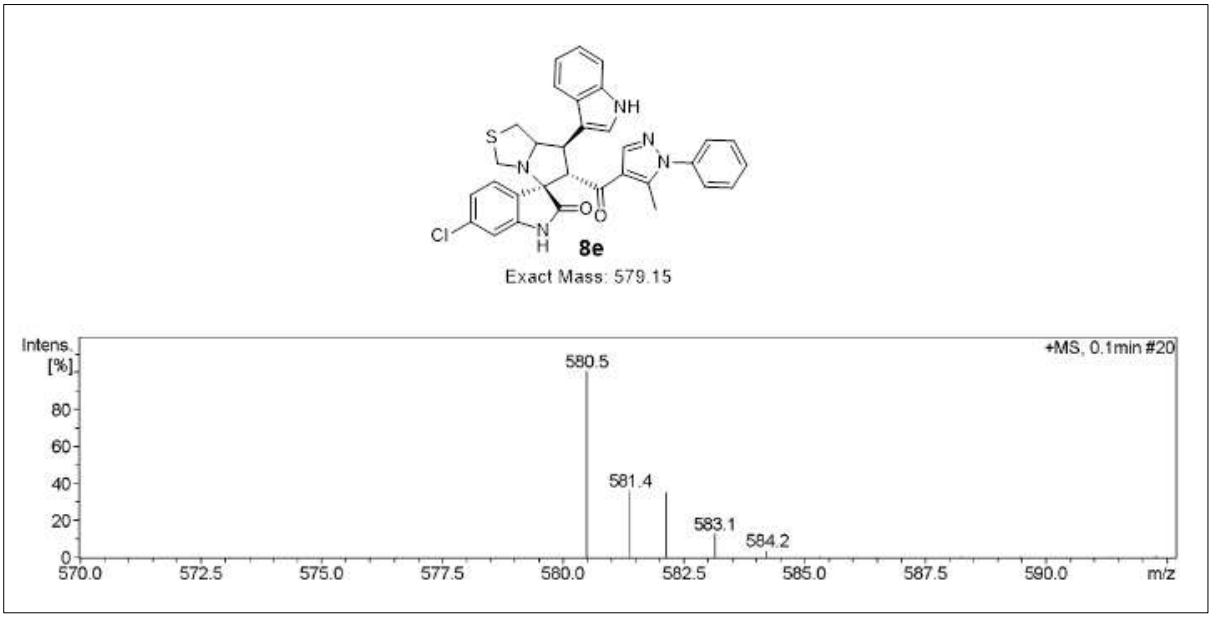

Figure S40. LCMS for compound-**8f**

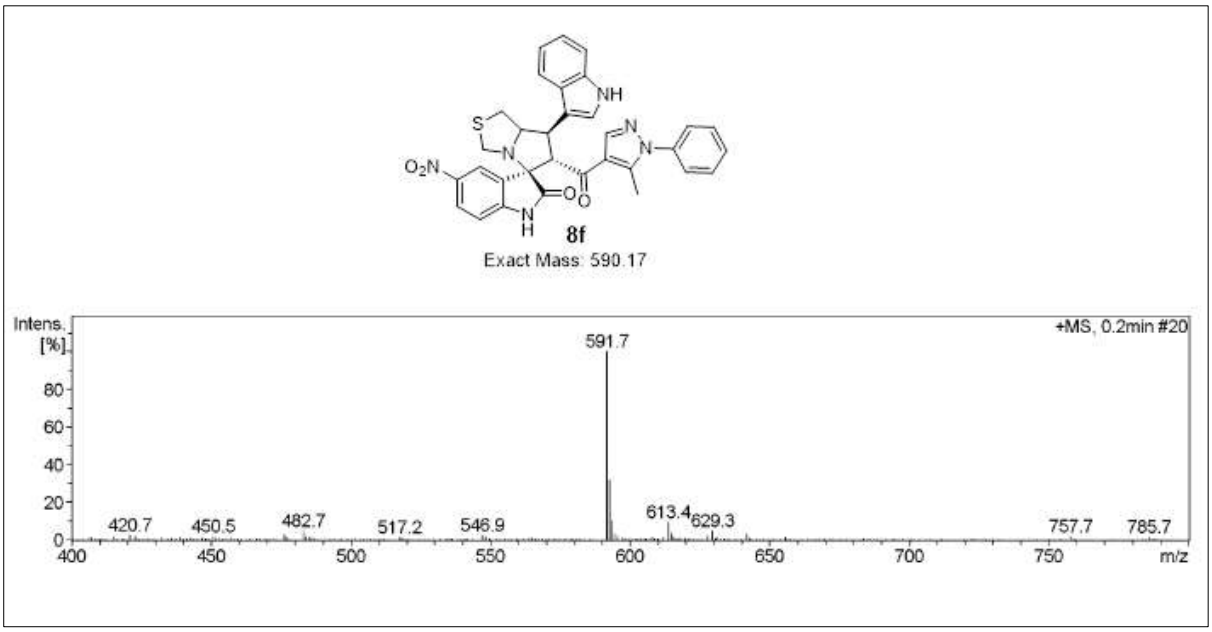

Figure S41. LCMS for compound-**8g**

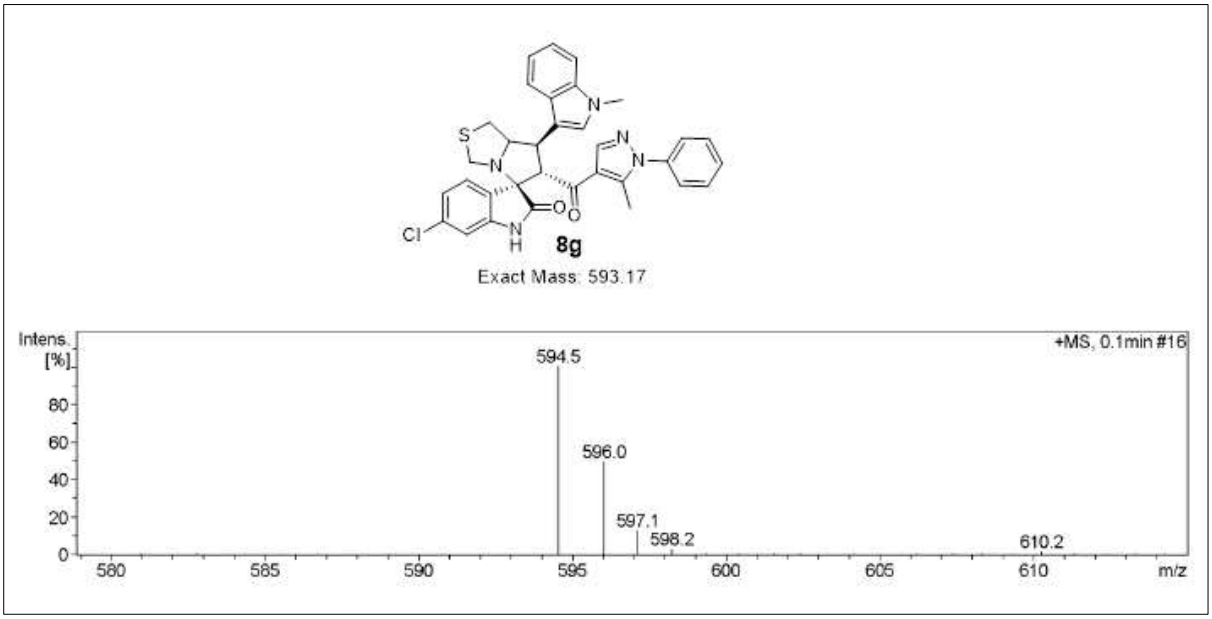

Figure S42. LCMS for compound-**8h**

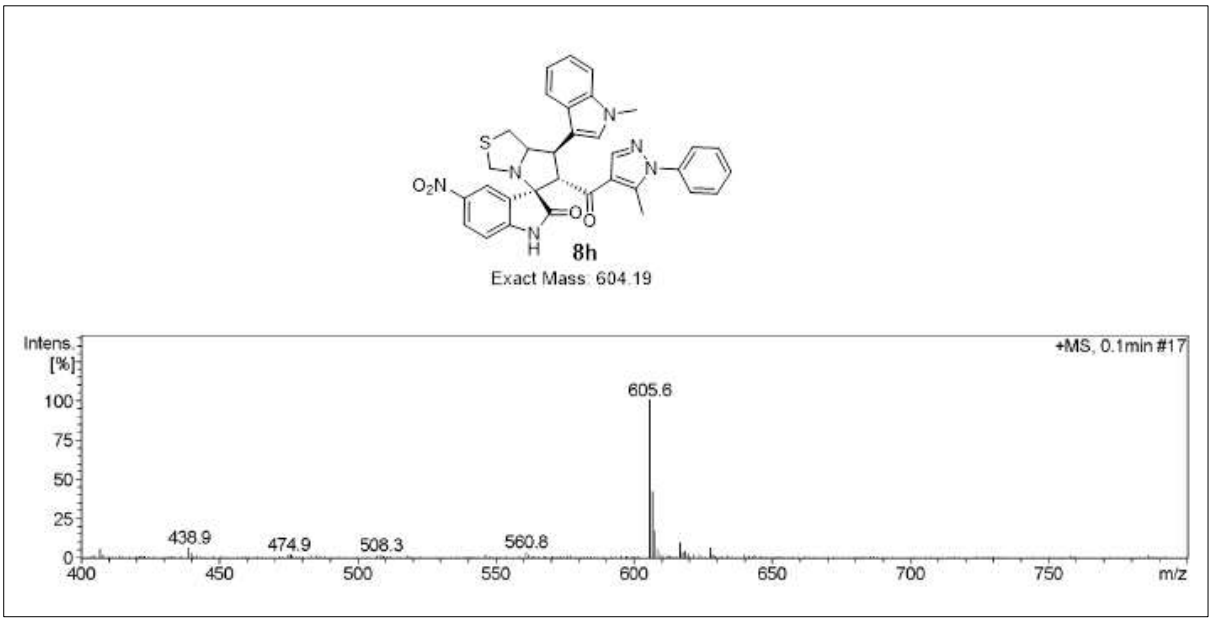

Figure S43. LCMS for compound-**8i**

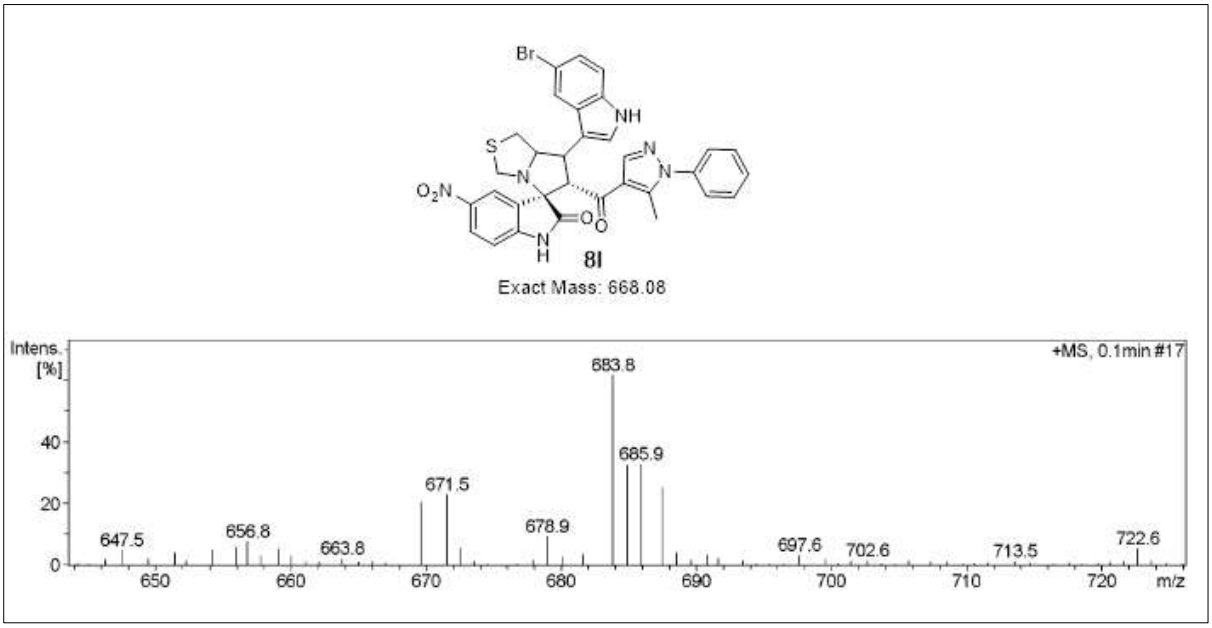

Figure S44. LCMS for compound-**8j**

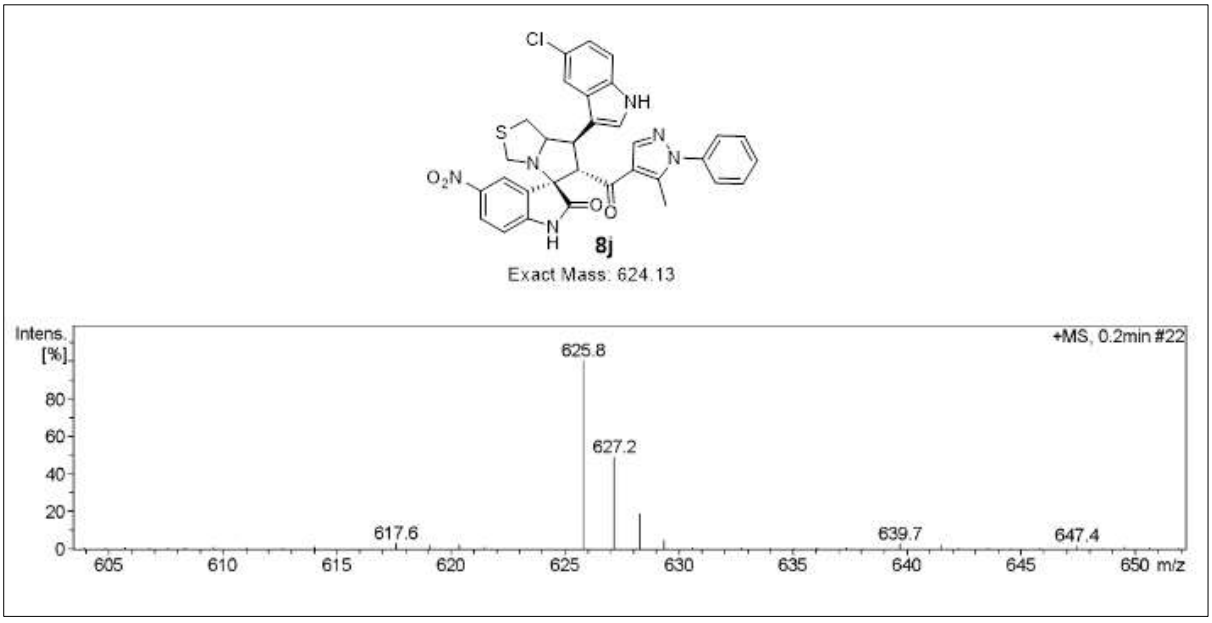

Figure S45. LCMS for compound-**8k**

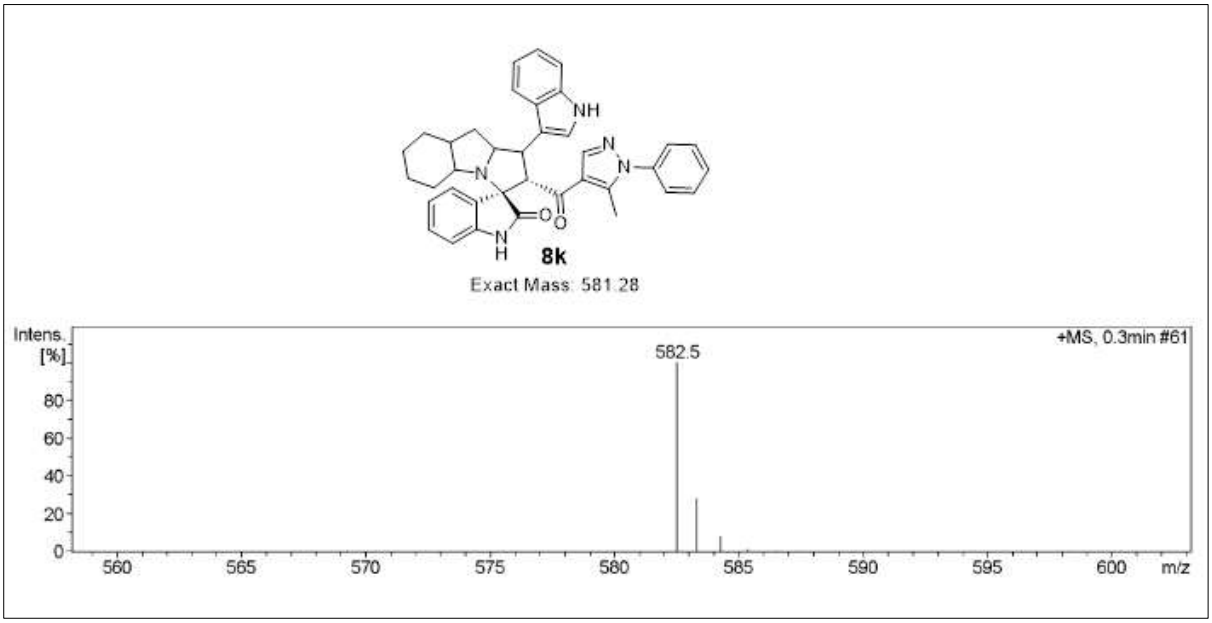

Figure S46. LCMS for compound-**8l**

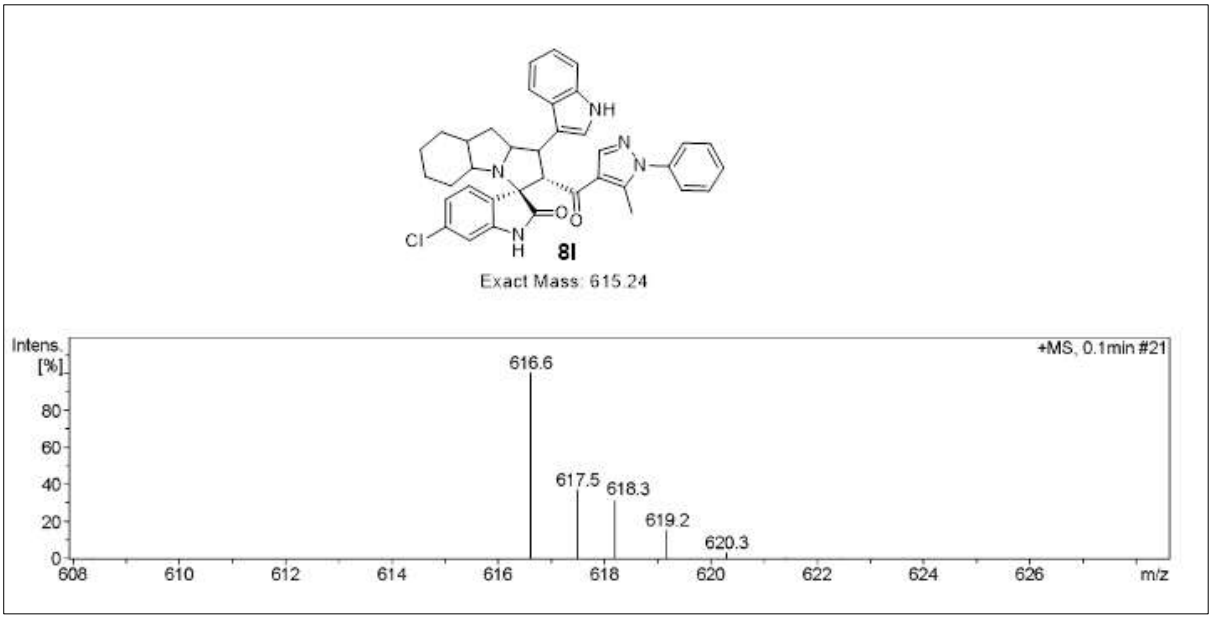

Figure S47. LCMS for compound-**8m**

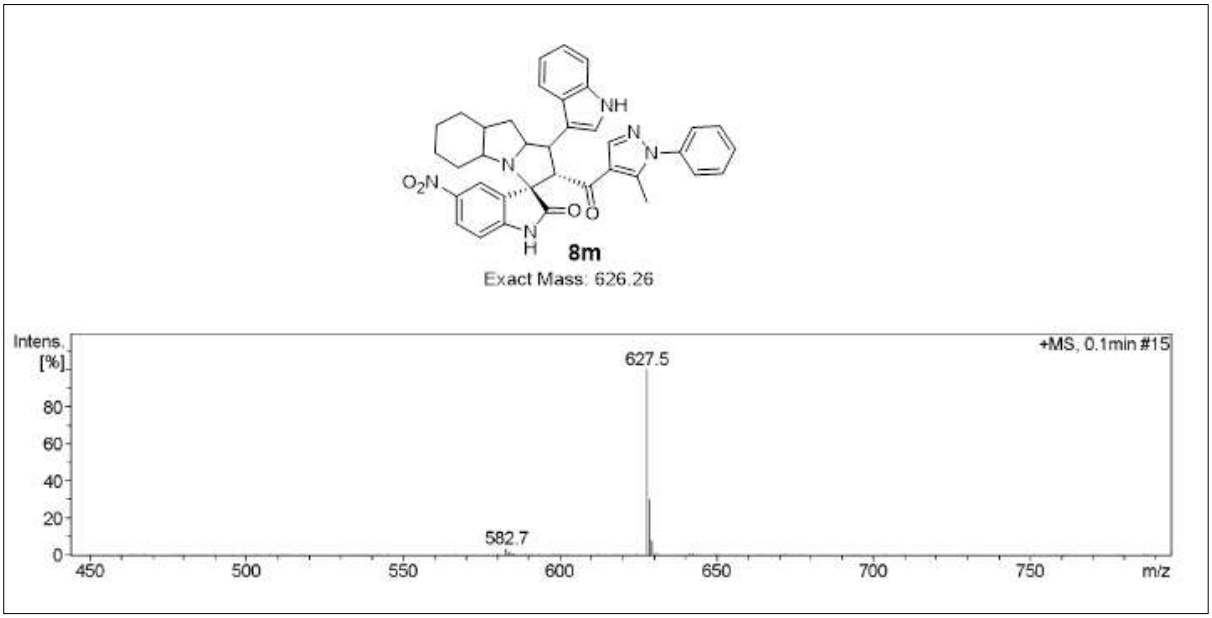

Figure S48. LCMS for compound-**8n**

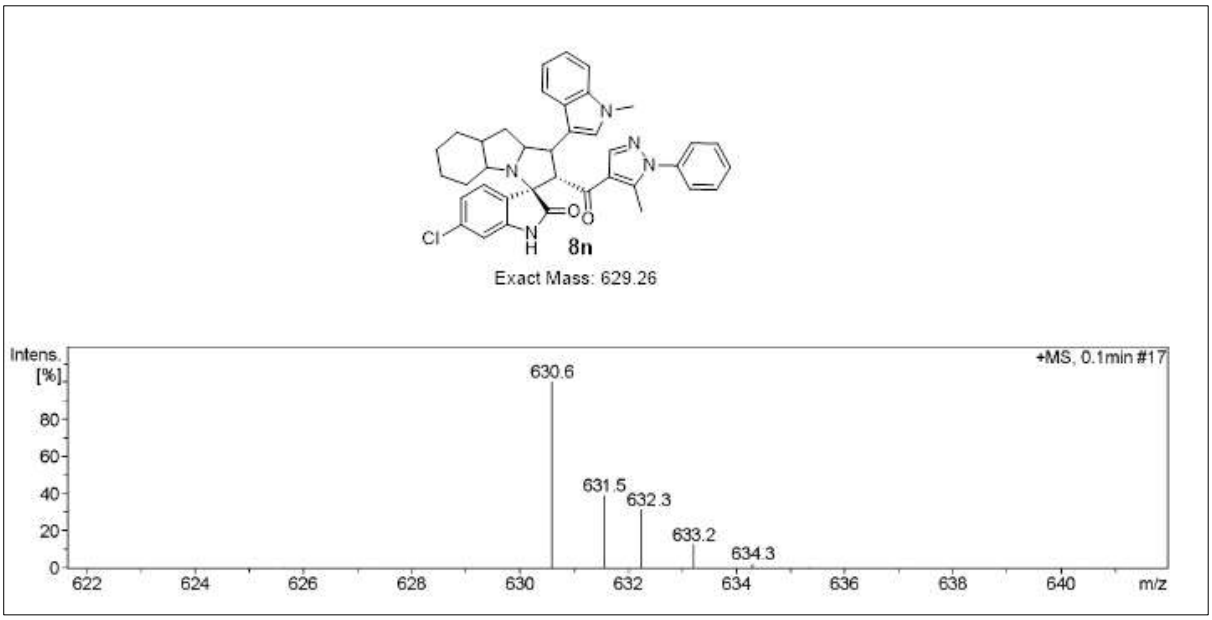

Figure S49. LCMS for compound-**8o**

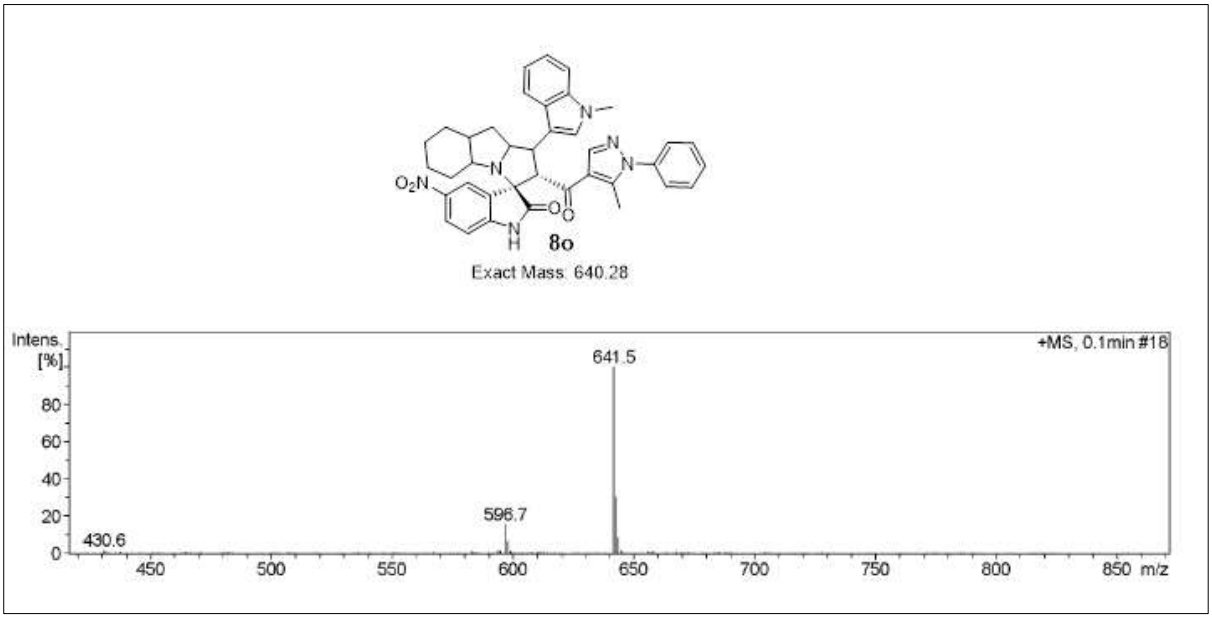

Figure S50. LCMS for compound-**8p**

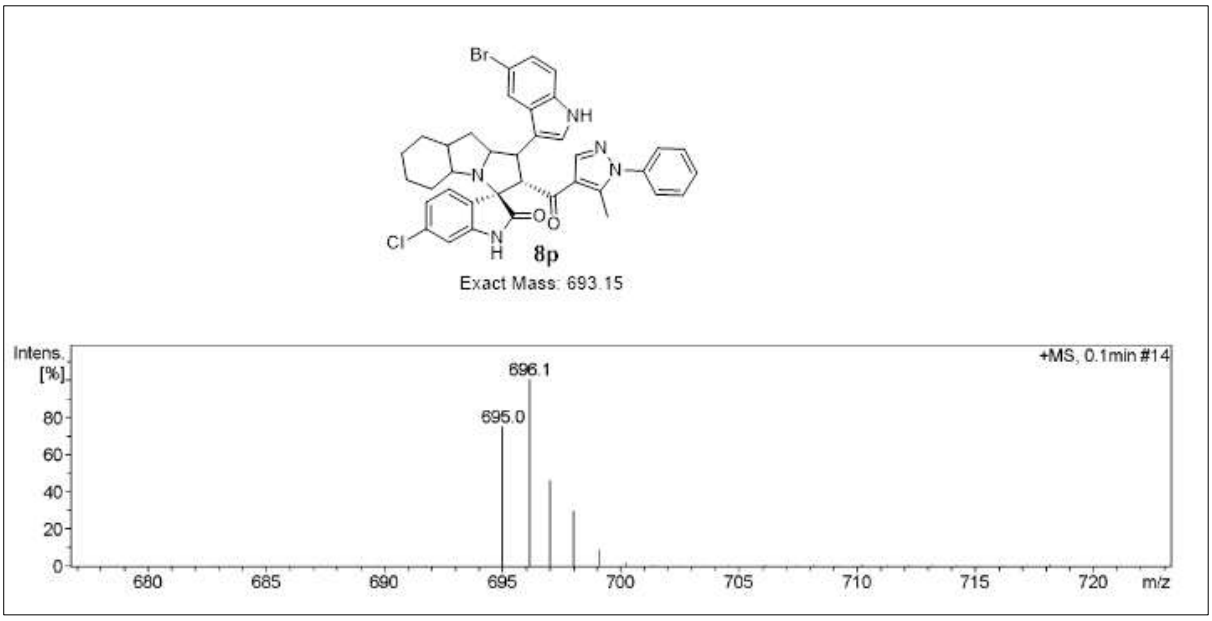

Figure S51. LCMS for compound-**8q**

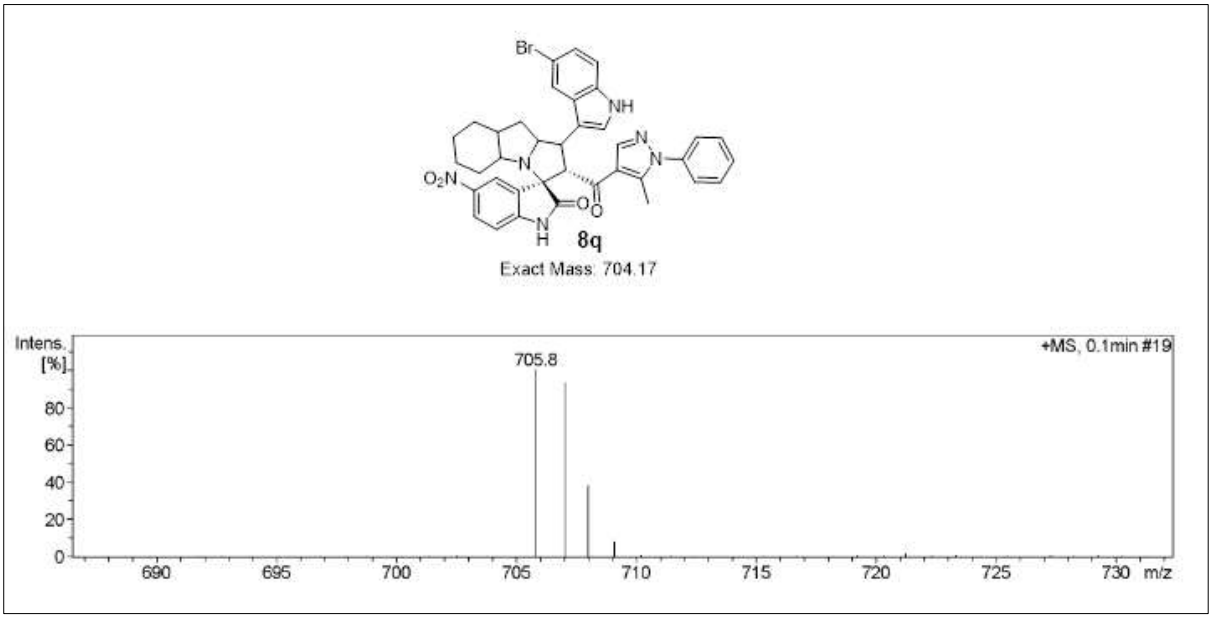

Figure S52. LCMS for compound-**8r**

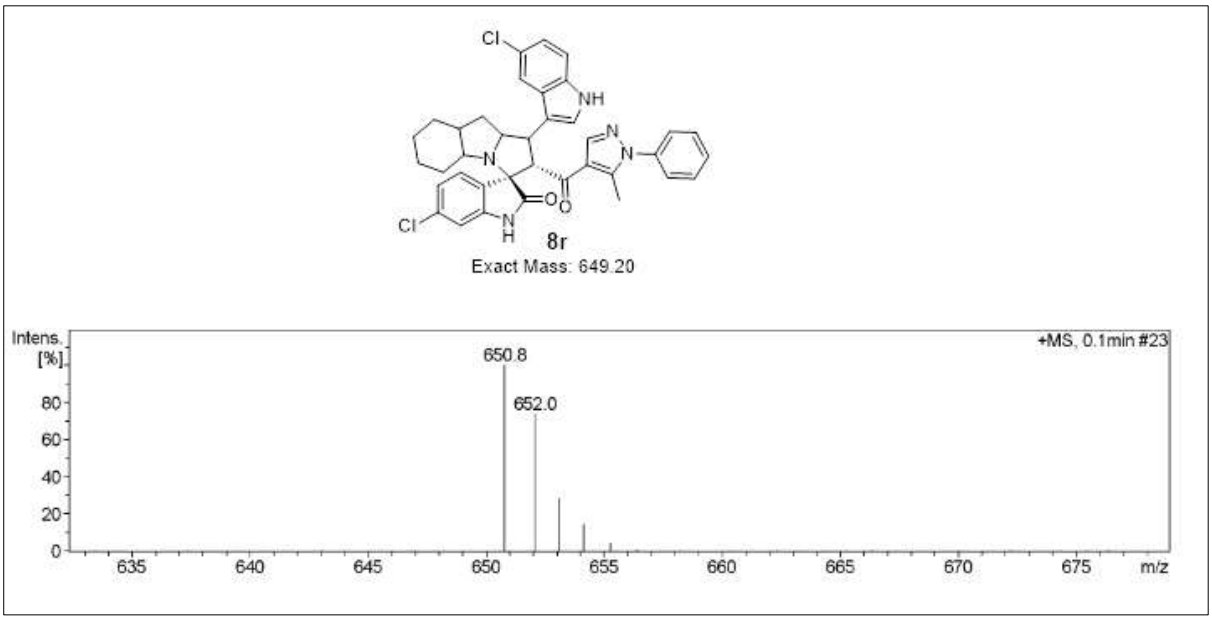

Figure S53. LCMS for compound-**8s**

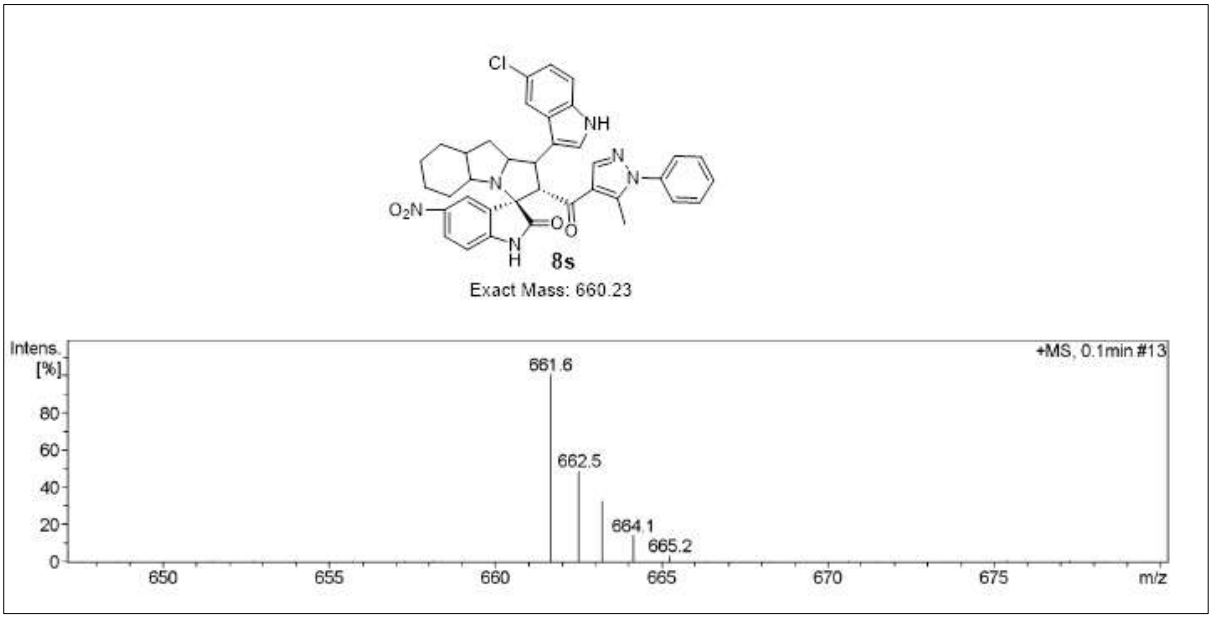

Figure S54. LCMS for compound-**8t**

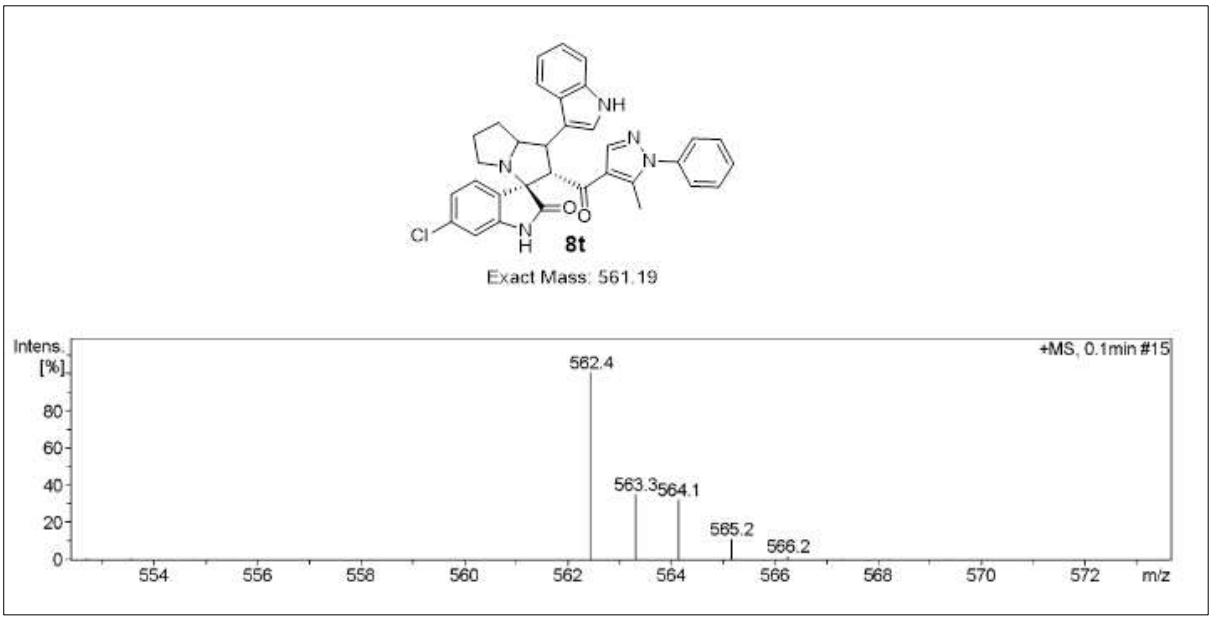

Figure S55. LCMS for compound-**8u**

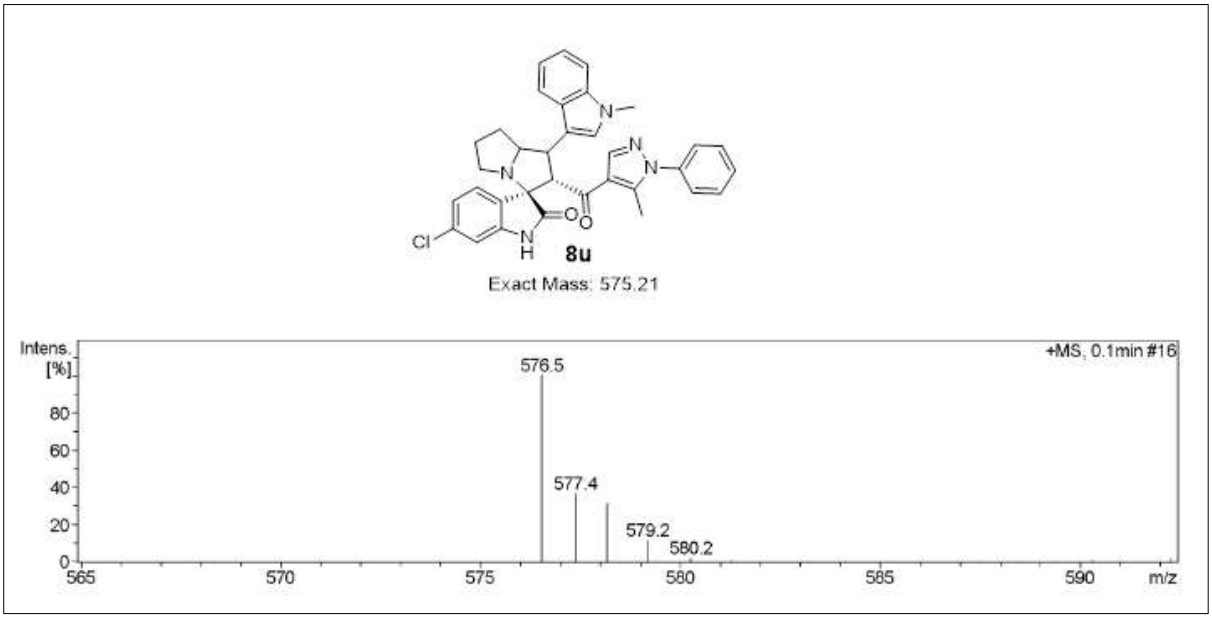

Figure S56. LCMS for compound-**8v**

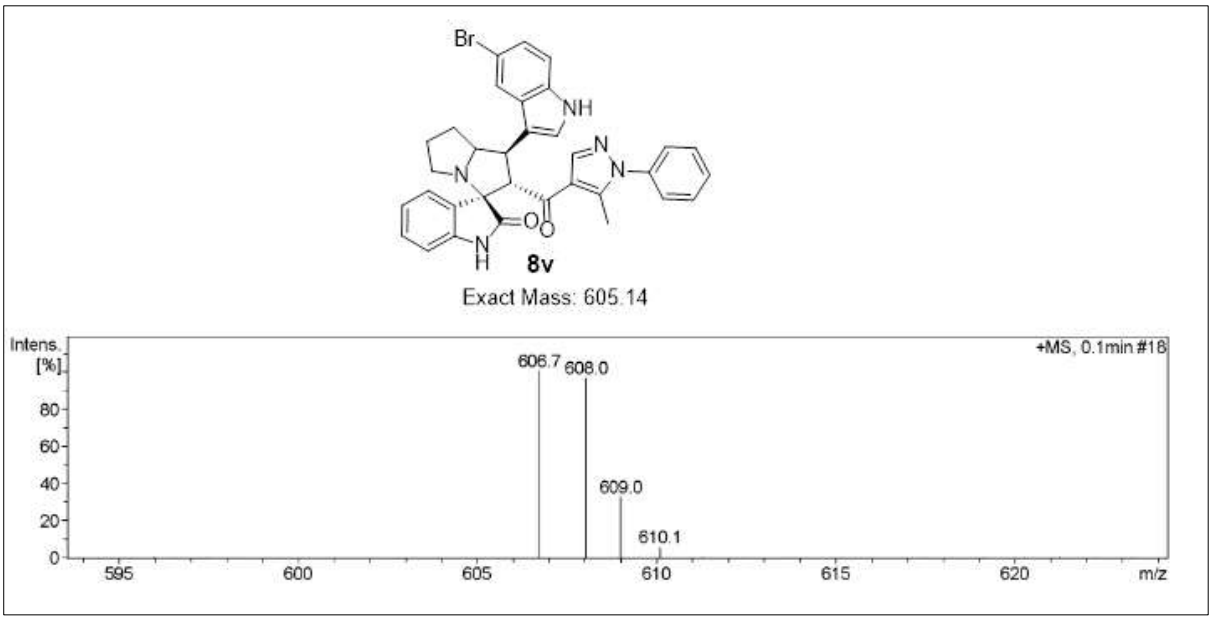

Figure S57. LCMS for compound-**8w**

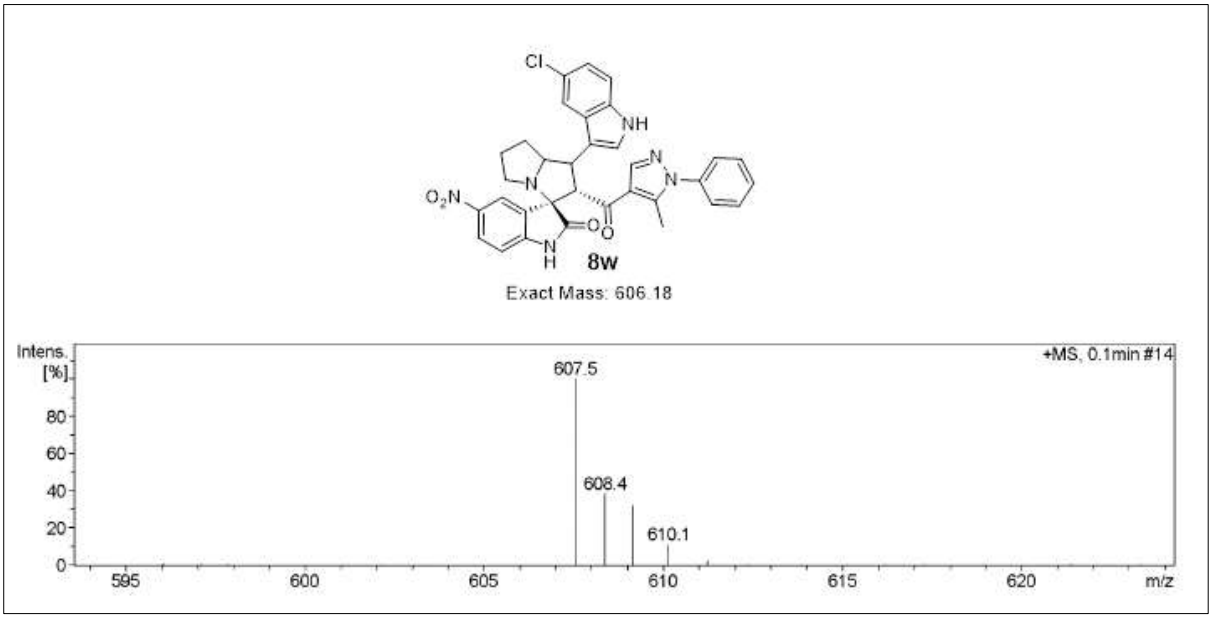

Figure S58. LCMS for compound-**8x**

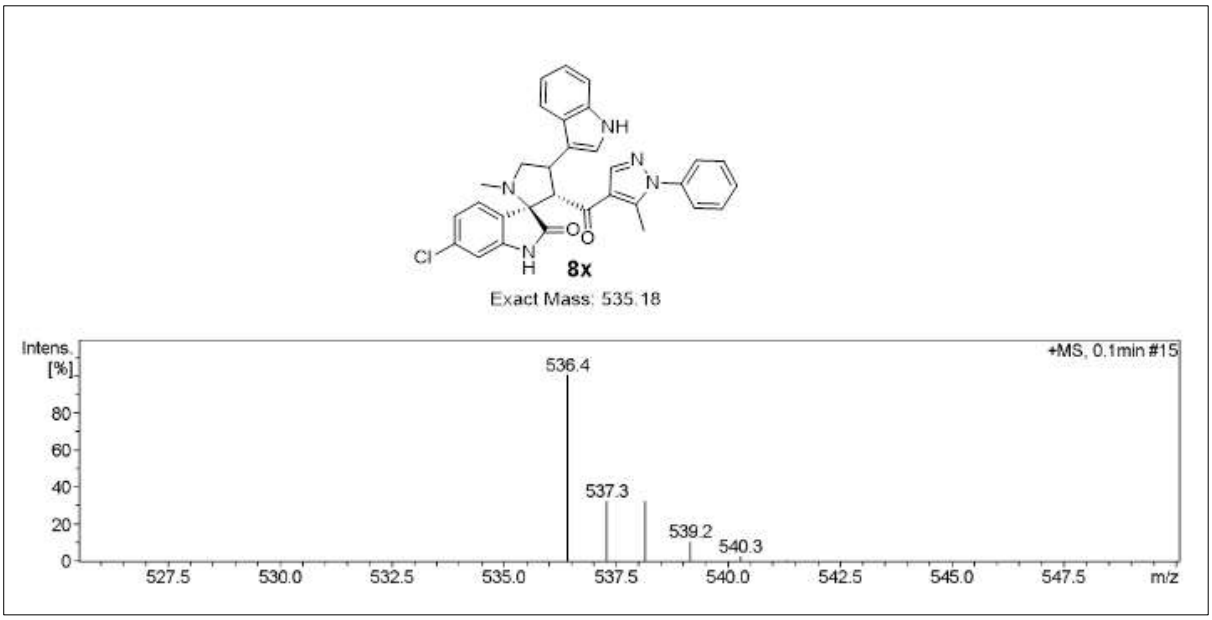

Figure S59. LCMS for compound-**8y**

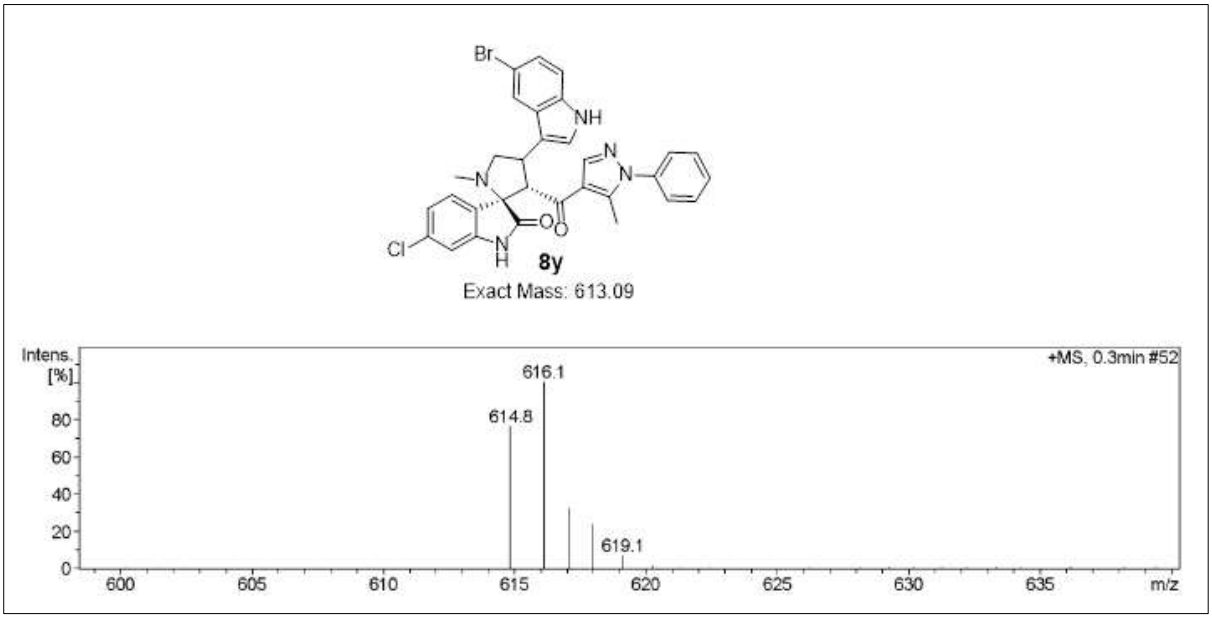

1. X-Ray structure determinations

The crystal of **8c** was immersed in cryo-oil, mounted in a loop, and measured at a temperature of 120 K. The X-ray diffraction data was collected on a Rigaku Oxford Diffraction Supernova diffractometer using Cu Kα radiation. The *CrysAlisPro*[8] software package was used for cell refinement and data reduction. A multi-scan absorption correction (*CrysAlisPro*[8]) was applied to the intensities before structure solution. The structure was solved by intrinsic phasing (*SHELXT*[9]) method. Structural refinement was carried out using *SHELXL*[10] software with *SHELXLE*[11] graphical user interface. The NH hydrogen atoms were located from the difference Fourier map and refined isotropically. All other hydrogen atoms were positioned geometrically and constrained to ride on their parent atoms, with C-H = 0.95-1.00 Å and U_{iso} = 1.2-1.5· U_{eq}(parent atom).

Table S1: Selected bond lengths [Å] and angles [°] for **8c**.

Atoms	**Distance**	**Atoms**	**Distance**
Br(1)-C(3)	1.910(2)	N(2)-C(13)	1.478(2)
S(1)-C(11)	1.811(2)	N(2)-C(10)	1.480(2)
S(1)-C(12)	1.820(2)	N(3)-C(14)	1.347(2)
O(1)-C(14)	1.230(2)	N(4)-C(24)	1.329(2)
O(2)-C(22)	1.219(2)	N(4)-N(5)	1.375(2)
N(1)-C(6)	1.368(3)	N(5)-C(25)	1.352(2)
N(1)-C(7)	1.374(3)	N(5)-C(27)	1.437(2)
N(2)-C(12)	1.458(2)		
Atoms	**Angle**	**Atoms**	**Angle**
C(11)-S(1)-C(12)	88.76(9)	C(25)-N(5)-N(4)	112.95(15)
C(6)-N(1)-C(7)	108.60(17)	C(25)-N(5)-C(27)	127.82(17)
C(12)-N(2)-C(13)	117.44(15)	N(4)-N(5)-C(27)	119.13(16)
C(12)-N(2)-C(10)	112.14(14)	C(2)-C(1)-C(6)	119.03(18)
C(13)-N(2)-C(10)	110.43(14)	C(2)-C(1)-C(8)	134.46(17)

C(14)-N(3)-C(15)	111.52(15)	C(6)-C(1)-C(8)	106.49(17)
C(24)-N(4)-N(5)	104.34(15)	C(3)-C(2)-C(1)	117.86(18)

Table S2: Hydrogen bonds for **8c** [Å and °].

D-H...A	d(D-H)	d(H...A)	d(D...A)	<(DHA)
C(12)-H(12B)...Cl(1)#1	0.99	2.76	3.611(2)	144.2
C(16)-H(16)...Cl(3)#2	0.95	2.82	3.389(2)	119
C(24)-H(24)...O(1)	0.95	2.53	3.321(2)	140.3
C(28)-H(28)...Cl(3)#2	0.95	2.83	3.749(2)	162.2
C(33)-H(33)...O(1)#3	1	2.34	3.164(3)	138.7
C(33)-H(33)...N(2)#3	1	2.49	3.367(3)	146.8
C(34)-H(34)...Br(1)	1	2.8	3.636(3)	141.2
N(1)-H(1)...N(4)#4	0.89(3)	2.16(3)	3.045(2)	175(3)
N(3)-H(3)...O(1)#5	0.83(3)	2.03(3)	2.846(2)	169(3)

#1 -x+1/2,y+1/2,-z+1/2; #2 x+1/2,-y+1/2,z+1/2; #3 -x+1/2,y-1/2,-z+1/2; #4 x-1/2,-y+1/2,z-1/2; #5 -x+1,-y+1,-z+1

References

1. Ellman, G. L.; Courtney, K. D.; Andres Jr, V.; Featherstone, R. M., A new and rapid colorimetric determination of acetylcholinesterase activity. *Biochem. Pharmacol.* **1961,** *7* (2), 88-95.
2. Mira, A.; Yamashita, S.; Katakura, Y.; Shimizu, K., In vitro neuroprotective activities of compounds from Angelica shikokiana Makino. *Molecules* **2015,** *20* (3), 4813-4832.
3. Abdel Bar, F. M.; Elimam, D. M.; Mira, A. S.; El-Senduny, F. F.; Badria, F. A., Derivatization, molecular docking and in vitro acetylcholinesterase inhibitory activity of glycyrrhizin as a selective anti-Alzheimer agent. *Nat. Prod. Res.* **2019,** *33* (18), 2591-2599.
4. ChemOffice, C. J. C. C. S. C. I. M., USA.
5. C.C.G.C.M.O.E.M.S.S.W. Inc., Suite #910, Montreal, QC, Canada, H3A 2R7.
6. Hsu, K.-C.; Chen, Y.-F.; Lin, S.-R.; Yang, J.-M., iGEMDOCK: a graphical environment of enhancing GEMDOCK using pharmacological interactions and post-screening analysis. *BMC Bioinformatics* **2011,** *12* (1), 1-11.
7. D.J.A.I.S.D. Studio, CA, USA (2009). "version 2.5.
8. Rikagu Oxford Diffraction, CrysAlisPro, Agilent Technologies inc., 2018, Yarnton, Oxfordshire, England.
9. Sheldrick, G. M., SHELXT-Integrated space-group and crystals-structure determination. *Acta Cryst. A* **2015,** *71*, 3-8.
10. Sheldrick, G. M., Crystal structure refinement with SHELXL. *Acta Cryst. C* **2015,** *71*, 3-8.
11. Hübschle, C. B.; Sheldrick, G. M.; Dittrich, B., ShelXle: a Qt graphical user interface for SHELXL. *J. Appl. Crystallogr.* **2011,** *44* (6), 1281-1284.